

Tatiana Marisa Andrade Burrinha

Licenciada em Biologia Celular e Molecular

Bridging Integrator 1 (BIN1) controls beta-amyloid accumulation in Alzheimer's disease

Dissertação para obtenção do Grau de Mestre em Genética Molecular e Biomedicina

Orientador: Cláudia Guimas de Almeida Gomes Investigadora Principal no Centro de Estudos de Doenças Crónicas (CEDOC)

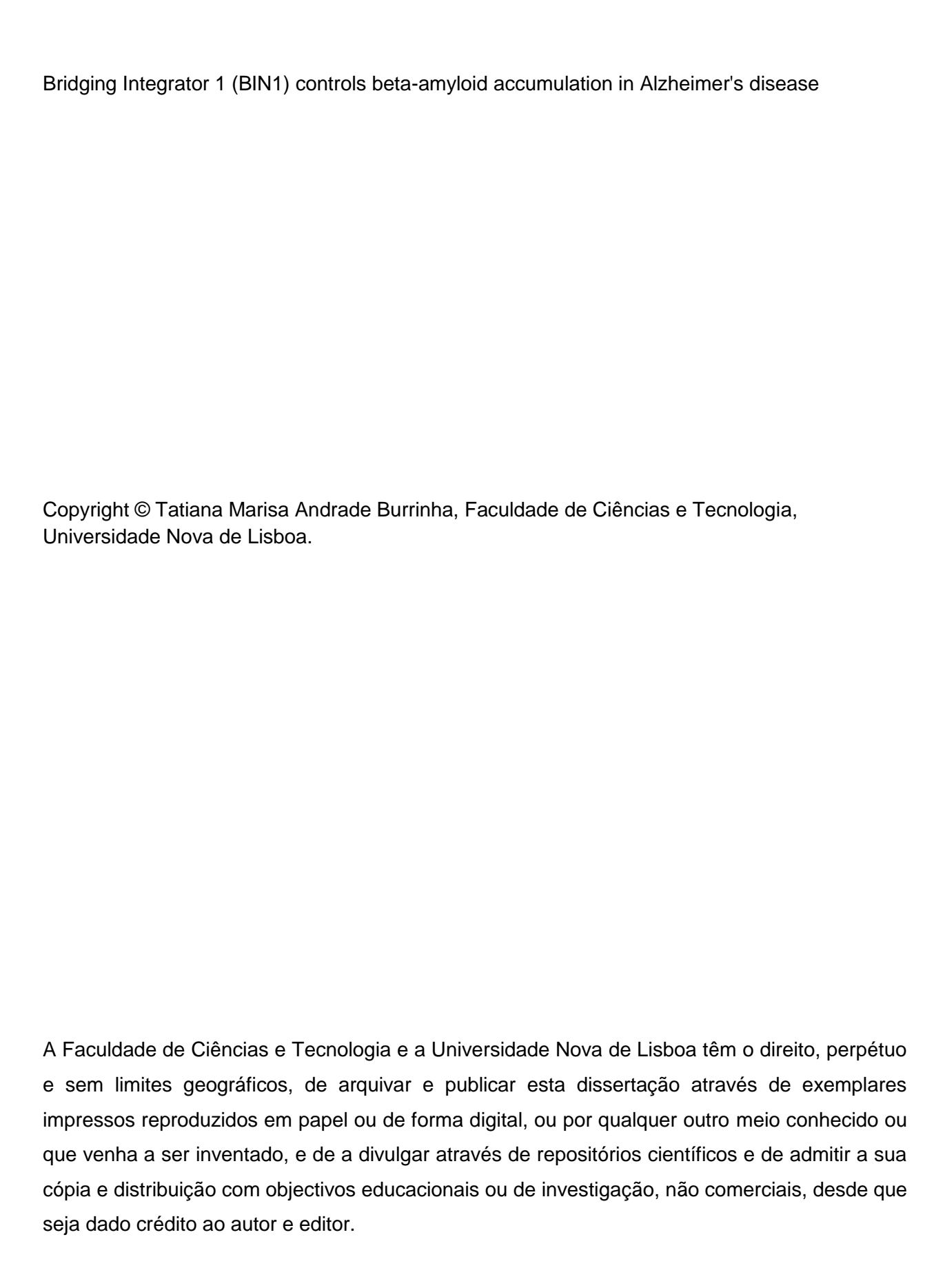
Júri:

Presidente: Dra. Paula Maria Theriaga Mendes Bernardo Gonçalves

Arguente: Dra. Maria João Lopes Gonçalves de Brito Amorim

Vogal: Dra. Cláudia Guimas de Almeida Gomes





Para os meus Pais

Acknowledgements

Começo por agradecer à Cláudia, orientadora desta dissertação, por me ter aceite neste grupo e pela confiança que depositou em mim. Agradeço a oportunidade de aprender um pouco mais sobre o mundo das Neurociências e por me ter recebido de braços abertos. Estou muito grata por trabalhar com alguém com um tão vasto conhecimento científico e espírito critico. Além disso, a capacidade nata de liderança, de comunicação de forma aberta e transparente com quem trabalha, a humildade na aceitação de erros, o positivismo e entusiasmo face aos obstáculos diários, e a capacidade de encorajar e enaltecer sempre o melhor que há em cada um de nós é, sem dúvida alguma, uma inspiração para mim e para o meu desenvolvimento como investigadora. Obrigada por toda a paciência e interesse depositado neste trabalho. Trabalhar contigo foi um privilégio.

Florent, un merci pour le support, pour la patience que vous aviez à m'expliquer toutes les choses et pour la volonté de répondre à toutes mes questions, même avec l'énorme quantité de travail que vous aviez tous les jours. Merci de me faire apprendre comment résoudre les problèmes quotidiens de travail dans le laboratoire. Merci pour vos suggestions, pour votre dévouement et toute la passion que vous déposez dans ce que vous faites. Vous êtes un exemple pour moi, non seulement par vos compétences scientifiques, mais aussi pour votre intelligence. Vous étiez essentiel à la réalisation de mon travail. Je remercie aussi votre manière chaleureuse et conviviale d'etre avec moi, et je remercie aussi tout ce que vous m'avez appris.

Ao Ricardo Gomes, muito obrigado por toda a paciência e boa vontade em me explicar sempre tudo, por todas as discussões para tentar solucionar problemas e por me ensinares tudo acerca de Western Blot. Obrigado também por todos os conselhos, pela motivação e encorajamento, por toda a prontidão no esclarecimento de dúvidas a qualquer hora e sempre com um sorriso na cara. És um óptimo investigador e, acima de tudo, uma excelente pessoa. Obrigada por tudo.

Agradeço também ao orientador interno da minha dissertação, Professor Doutor José Paulo Sampaio e à Professora Doutora Paula Gonçalves pela prontidão e eficiência que sempre demonstraram no esclarecimento de dúvidas.

Aos meus colegas de laboratório, à Andreia, à Noelia, ao Cláudio, ao André, à Fabiana, à Ângela,

e à Laura agradeço a vossa alegria, o vosso apoio, a transmissão dos vossos conhecimentos, o vosso companheirismo e todos os momentos de convívio, descontracção e gargalhadas.

À minha Mafalda, um muito obrigado é pouco para demonstrar o quão grata me sinto por tudo o que fizeste por mim. És um exemplo a seguir, um exemplo de força, inteligência, garra e amor pela Vida. Obrigada por conseguires pôr-me sempre um sorriso na cara. És muito especial.

À Dona Isabel, um muito obrigado por todos os pequenos momentos onde me ensina tanto sobre a escola da Vida.

À Mariana, à Joana e à Sara agradeço o apoio, amizade e disponibilidade para ouvir os meus desabafos. Obrigada pela vossa boa disposição e alegria.

Às minhas meninas, Lucy, Maria João, Marisa, Ana e Isabel, obrigada por me apoiarem, por amenizarem as minhas "tempestades", por tornarem os meus problemas mais simples de resolver, por me darem a força necessária no momento exacto, por todas as tolices e momentos de grande felicidade. Muito obrigada por me fazerem rir. São as maiores. Gosto muito de vocês.

À minha madrinha Marta, muito obrigada por estares sempre presente e disponível para me ajudares. Obrigada por todos os bons conselhos e pela tua constante simpatia.

À minha Inês, a minha companheira de sempre, agradeço a tua constante preocupação, motivação e o apoio em todos os momentos mais difíceis. Obrigado pelo teu ombro amigo que sei que vai estar sempre ai. Foste e és fundamental para o meu bem-estar, para a minha alegria. Aprendo muito contigo, e tenho um orgulho enorme em ti. Gosto muito de ti.

Aos meus amigos Miguel e Eduardo, agradeço a boa disposição, o apoio, o companheirismo e as gargalhadas. Com vocês o tempo passa a correr e é sempre muito divertido. Obrigada por tudo.

A toda a minha família, agradeço o apoio, a motivação e a constante preocupação. Aos meus avós, Tonica, Burrinha, Júlia, Andrade e à bisávo Antónia muito obrigado por tomarem conta de mim, por se preocuparem com o meu bem-estar e por me darem força para ultrapassar todos os problemas, assim como sábios conselhos para tomar as minhas decisões. Sinto muito orgulho por vos ter na minha Vida. Gosto muito de vocês.

À minha tia Ivete muito obrigada pela motivação, apoio e vontade de aprender um pouco mais sobre o meu trabalho. Obrigada também à pequenina Diana por me fazer rir e por me dar abracinhos tão bons. Gosto muito de vocês.

Às minha manas, Jéssica e Cíntia, e ao meu futuro cunhado, João, obrigada por me alegrarem, por me fazerem rir muito, por me apoiarem sempre apesar do meu mau feitio. Obrigada por serem chatos e por se preocuparem comigo. Gosto muito de vocês.

Ao meu Luís, o homem que me dá todos os dias sem excepção a força e o ânimo para não desistir. Obrigada pelo teu apoio incondicional, pelo conforto que me dás, pela tua eterna amizade, pela tua compreensão, pelo teu carinho constante, pela tua interminável paciência, e principalmente pelo teu amor. És o melhor companheiro que eu podia desejar, aquele com quem posso partilhar todos os bons e maus momentos. És o meu orgulho. Tornas a minha Vida muito mais feliz. Obrigado por me fazeres sorrir e sentir que sou especial para ti. Agradeço também à dona Dulce e ao senhor António por ouvirem os meus desabafos depois de um dia de trabalho e por terem um filho tão maravilhoso.

Aos meus pais, Mena e Fernando, para vocês vai o meu maior obrigado. Sem vocês não teria sido possível chegar até aqui. Vocês fazem parte da pessoa que me tornei. Tenho muito orgulho em vocês. Obrigada por me apoiarem e acreditarem sempre nas minhas escolhas. Obrigada por estarem sempre presentes quando mais precisei, por me ouvirem e por me aconselharem. Gosto muito de vocês. Obrigada por tudo.

"O sucesso é ter quem fique feliz com o meu sucesso (...) vale-me quem me abrace quando estou feliz, e no final das contas é mais por isso que estou feliz (...). Todas as vitórias são colectivas, sobretudo as individuais."

Pedro Chagas Freitas

Abstract

Alzheimer's disease (AD), the most common cause of dementia, is an aging-related progressive neurodegenerative disease. The major neuropathological features are the neurofibrillary tangles of hyperphosphorylated tau protein and the amyloid plaques, extracellular deposits composed of amyloid β peptides (A β). A β peptide accumulation plays a central role in the pathogenesis of AD. Prior to plaques and tangles formation there is progressive accumulation of A β 42 extra- and intracellularly with aging. This accumulation leads to A β 42 oligomerization and to compromised synaptic function, correlated with cognitive decline. Eventually damage spreads and leads to the loss of synapses, neurodegeneration, neuronal death and severe dementia. In early-onset AD, autosomal dominant mutations in amyloid precursor protein (APP) and in the secretases that cleave APP cause A β 42 accumulation. However, in the majority of AD cases (late-onset sporadic AD) it remains to be elucidated what begins the cascade of events underlying A β accumulation.

A strong candidate for causing AD is Bridging Integrator 1 (BIN1; a.k.a. amphiphysin 2) identified as an AD risk locus by Genome Wide Association Studies (GWAS). Since Bin1 is a regulator of the endocytic trafficking and A β generation depends on APP and β -site APP-cleaving enzyme 1 (BACE-1) trafficking, we hypothesized that BIN1 may have an impact in A β 42 accumulation and thus contribute to the development of AD.

Our data demonstrate that Bin1 controls A β 42 production and APP processing. We found evidences that Bin1 may control A β 42 accumulation by regulating the APP and/or BACE-1 trafficking. However, the specific intracellular trafficking mechanisms whereby Bin1 is involved in the A β 42 production require further investigation.

Keywords: Alzheimer's disease, Bridging Integrator 1 (BIN1), Amyloid β (A β), amyloid precursor protein (APP), BACE-1, intracellular trafficking.

Resumo

A doença de Alzheimer (DA), causa mais comum de demência, é uma doença neurodegenerativa progressiva associada à idade. As principais características neuropatológicas são as tranças neurofibrilares da proteína tau hiperfosforilada e as placas amilóides, depósitos extracelulares compostos pelo péptido β-amilóide (βA). A acumulação do péptido βA tem um papel central na patogénese da DA. Antes da formação das placas e tranças, há uma acumulação progressiva do βA42 extra- e intracelularmente com o envelhecimento. Esta acumulação leva à oligomerização de βA42 e uma função sináptica comprometida, relacionada com o declínio cognitivo. Eventualmente o dano propaga-se e leva à perda de sinapses, neurodegeneração, morte neuronal e demência severa. Na DA de início precoce, mutações autossómicas dominantes na proteína precursora amilóide (PPA) e nas secretases que clivam PPA causam a acumulação de βA42, contudo na maioria da DA (DA esporádica de início tardio) permanece por elucidar a questão central acerca do que inícia a cascata de eventos na base da acumulação de βA.

A DA de início tardio poderá ser causada pelo "Bridging integrator 1" (BIN1; "amphiphysin 2"), identificado como um *locus* de risco para a DA por "Genome Wide Association Studies" (GWAS). Uma vez que o Bin1 é um regulador do tráfego endocítico e que a produção de βA depende do transporte da PPA e "β-site APP-cleaving enzyme 1" (BACE-1), a nossa hipótese é que Bin1 poderá ter impacto na acumulação de βA42 e assim contribuir para o desenvolvimento da DA.

Os nossos dados demonstraram que Bin1 controla a produção de β A42 e o processamento da PPA. Descobrimos que o Bin1 poderá controlar a acumulação de β A42 através da regulação da reciclagem intracelular de PPA e/ou da BACE-1. Contudo, os mecanismos específicos de tráfego intracelular nos quais Bin1 está envolvido na produção de β A42 requerem uma maior investigação.

Palavras-chave: Doença de Alzheimer, Bridging Integrator 1 (BIN1), β amilóide (βA), proteína precursora amilóide (PPA), BACE-1, tráfego intracelular.

Index

| Acknowledgements | V |
|--|-----|
| Abstract | ix |
| Resumo | xi |
| Abbreviations | xix |
| I. Introduction | 1 |
| The Nervous System and Neuron biology | 1 |
| 2. Alzheimer's disease | 2 |
| 2.1. Brief History of Alzheimer's Disease | 2 |
| 2.2. Alzheimer's Disease Pathogenesis | 3 |
| 2.3. Early-onset AD vs Late-onset AD | 5 |
| 2.4. Amyloid precursor protein (APP) | 5 |
| 2.4.1. APP trafficking in neurons | 6 |
| 2.4.2. APP processing | 7 |
| 2.4.3. The role of APP endocytosis for AD development | 9 |
| 2.5. β-site APP-cleaving enzyme 1 (BACE-1) | 10 |
| 2.5.1. The role of BACE-1 endocytosis for AD development | 11 |
| 3. Bridging integrator 1 (BIN1) or amphiphysin 2 (AMPH2) | 11 |
| 3.1. BIN1 gene and domain organization | 12 |
| 3.2. Bin1 cellular functions | 13 |
| 3.2.1. The role of Bin1 in endocytosis and trafficking | 13 |
| 3.2.2. Endocytic trafficking and AD | 15 |
| 4. Aims of the current work | 17 |
| II. Materials and methods | 18 |
| 1. Reagents | 18 |
| 2. DNA amplification | 19 |
| 3. Tissue Culture | 20 |
| 4. Fluorescence microscopy | 23 |
| 5. Immunobloting | 25 |
| 6. Statistical analysis | 26 |
| III. Results | 27 |

| 1. Characterization of Bin1 localization in cell lines and primary neurons | 27 |
|--|----|
| 1.1. Distribution of endogenous Bin1 in HeLa cells, N2a cells and primary neurons | 27 |
| 1.2. Distribution of exogenous Bin1 in HeLa cells, N2a cells and primary neurons | 28 |
| 1.3. Subcellular distribution of exogenous Bin1 in HeLa cells | 29 |
| 1.4. Subcellular distribution of endogenous Bin1 in primary neurons | 37 |
| 2. Role of Bin1 in APP processing and Aβ42 accumulation | 40 |
| 2.1. Effect of Bin1 overexpression on Aβ42 accumulation and APP processing in N2a cells | |
| 2.2. Bin1 overexpression, APP processing and A β 42 accumulation in primary neurons4 | 42 |
| 2.3. The effect of Bin1 downregulation on Aβ42 accumulation in N2a cells | 44 |
| 2.4. Bin1 downregulation, APP processing and A β 42 accumulation in primary neurons4 | 46 |
| 3. Role of Bin1 in APP and BACE-1 distribution | 48 |
| 3.1. Bin1 overexpression effect on APP distribution | 48 |
| 3.2. Effect of Bin1 overexpression on BACE-1 distribution | 51 |
| IV. Discussion | 54 |
| V. Future perspectives | 57 |
| VI. References | 58 |

Index of Figures

| I. Introduction1 |
|--|
| Figure I.1. Representation of a neuron with all its componentes: dendrites, cell body, axon and axon terminals2 |
| Figure I.2. Comparison between the normal brain and the neuropathological features of the brain with AD: neurofibrillary tangles of hyperphosphorylated tau protein and the extracellular deposits of Aβ peptides (amyloid plaques)3 |
| Figure I.3. APP trafficking in neurons7 |
| Figure I.4. Processing of APP through the non-amyloidogenic and amyloidogenic pathway8 |
| Figure I.5. Sites of APP cleavage by the different secretases9 |
| Figure I.6. Alternative splicing isoform of BIN1/Amphiphysin 2, with the different functional domains for each tissue specific isoform13 |
| Figure I.7. Molecular mechanisms involved in clathrin-mediated endocytosis14 |
| III. Results |
| Figure III.1. Intracellular distribution of endogenous Bin127 |
| Figure III.2. Intracellular distribution of exogenous Bin1 and of Bin1 c-terminal domain28 |
| Figure III.3. Subcellular distribution of exogenous Bin1 |
| Figure III.4. A pool of Bin1 can be found associated with APP and BACE-1 in early endossomes |
| Figure III.5. Subcellular endogenous Bin1 distribution and colocalization with organelle markers in primary neurons40 |
| Figure III.6. Bin1 overexpression impacts Aβ42 accumulation and APP processing in N2a cells41 |
| Figure III.7. Myc-Bin1 and myc-Bin1 c-ter overexpression increase Aβ42 accumulation and alter APP processing in primary neurons43 |
| Figure III.8. Bin1 downregulation increases Aβ42 accumulation in N2a cells45 |
| Figure III.9. Bin1 downregulation increases Aβ42 accumulation and alter APP processing in primary neurons48 |
| Figure III.10. Myc-Bin1 and myc-Bin1 c-ter overexpression has an effect on APP |
| distribution51 |
| Figure III.11. Myc-Bin1 and myc-Bin1 c-ter overexpression has an effect on BACE-1 distribution |

Index of Tables

| II. Materials and methods | 18 |
|--|----|
| Table II.1. Antibodies and probes | 18 |
| Table II.2. Number of cells per mL that were plated to perform each type of method | 21 |

Abbreviations

AD Alzheimer's Disease

AICD APP intracellular domain

AMPH2 Amphiphysin 2

AnkG AnkyrinG

ANOVA Analysis of Variance
AP-2 Adaptor Protein-2

APP Amyloid precursor protein

APP₆₉₅ APP isoform (695 amino acids)
APP₇₅₁ APP isoform (751 amino acids)
APP₇₇₀ APP isoform (770 amino acids)

APP-mRFP APP-monomeric Red Fluorescence Protein

Aβ Amyloid β

Aβ40Amyloid β (40 amino acids)Aβ42Amyloid β (42 amino acids)BACE-1β-site APP-cleaving enzyme 1

BAR BIN-Amphiphysin-RvsBIN1 Bridging Integrator 1BSA Bovine serum albumin

C83 α-carboxyl-terminal fragment containing 83 amino acids
 C99 β-carboxyl-terminal fragment containing 99 amino acids

cDNA
 CHO
 Chinese Hamster Ovary
 CLAP
 Clathrin-Adaptor Protein
 CNS
 Central Nervous System

CO₂ Carbon dioxide

CTF Carboxyl-terminal fragment

DIV Days in vitro
Dyn Dynamin

E16 Mice embryos with 16 days of gestation

EEA1 Early endosomal antigen 1

ELISA Enzyme-Linked Immunosorbent Assay

EOAD Early-onset AD

ER Endoplamic reticulum

ERC Endocytic recycling compartment

FBS Fetal bovine serum

GFP Green Fluorescence Protein
GluR1 Glutamate receptor subunits (1)

GTP Guanosine triphosphate

GWAS Genome Wide Association Studies

HRP Horseradish peroxidase
IF Immunofluorescence

LAMP1 Lysosomal-associated membrane protein 1

LB Luria Bertani (medium)

LOAD Late-onset AD

MAP2 Microtubule-associated protein 2

MBD Myc binding domain

mRNA Messenger ribonucleic acid

MVBs Multivesicular bodies

N2a Neuro 2a

NFT's Neurofibrillary tangles

NLS Nuclear localization sequence

NTID N-terminal insert domain

PBS Phosphate buffered saline

PBST PBS-Tween 20
PM Plasma membrane
PN Primary Neurons

PNS Peripheral Nervous System

PSD-95 Postsynaptic density protein 95

PSEN1 Presenilin 1
PSEN2 Presenilin 2

RIPA Radio-Immunoprecipitation Assay

RNAi RNA-mediated interference

sAPPα Soluble APP cleaved by α-secretasesAPPβ Soluble APP cleaved by β-secretase

SDS Sodium dodecyl sulfate
SEM Standard Error of the Mean

SH3 Src homology 3

siRNA Small interference RNA

SNP Single nucleotide polymorphism

SNX4 Sorting nexin 4
Syj Synaptojanin

Tf Transferrin

TfR Transferrin receptor
TGN Trans-Golgi Network

WB Western Blot

YFP Yellow Fluorescence Protein α -CTF α -carboxyl-terminal fragment β -CTF β -carboxyl-terminal fragment

I. Introduction

1. The Nervous System and Neuron biology

The nervous system is composed by two components: the Central Nervous System (CNS) formed by brain and spinal cord; and the Peripheral Nervous System (PNS) consisting in nerves, i.e. axons of neurons extending from the brain and spinal cord to the muscles, glands and peripheral organs. The CNS comprises the basic units of the nervous system, neurons (or nerve cells), and neuroglia. Neurons can communicate with each other through the generation of electrical signals that run throughout the neuron and culminate in the release of chemical signals (neurotransmitters). This allows the interaction between nerve cells, coordinating the functions of organs and movements, thereby maintaining homeostasis throughout the body. Neuroglia are the supporting cells, not capable of electrical signaling, but with an essential role to neurons, providing them a physical and metabolic support in development and in adult brain (Purves, D., et al. 2004; Vander, A., et al. 2001).

Neurons are composed of four sections: a cell body, dendrites, an axon, and axon terminals (Figure I.1). The cell body contains the same structures like other types of cells: the nucleus, ribosomes, endoplasmic reticulum, Golgi apparatus, mitochondria, and some other vesicular structures, meaning that the genetic information and machinery necessary for protein synthesis are present here. The dendrites are the branched projections of cell body that allow neurons to have an increased surface area to receive the inputs from other neurons, enabling intercellular communication. The axon is a single long process that extends from the cell body to its target cells. In the axon initial segment (or axon hillock) the electrical event called action potential is generated and propagates to the axon terminals (or, sometimes, back along the dendrites) (Purves, D., et al. 2004; Vander, A., et al. 2001).

The axon terminals are the local where synapse, the junction between two neurons that in most of the cases occurs between axon terminal of one neuron (presynaptic neuron) and the dendrite or cell body of another neuron (postsynaptic neuron), happens. Here, neurotransmitters are released from synaptic vesicles, diffuse through the synaptic cleft from presynaptic neuron and alter the postsynaptic neuron by binding with specific membrane neurotransmitter receptors. This chemical and electrical process encoded by action potentials that occurs at synaptic contacts is called synaptic transmission, and this is the basis for neurons communication (Purves, D., et al. 2004; Vander, A., et al. 2001).

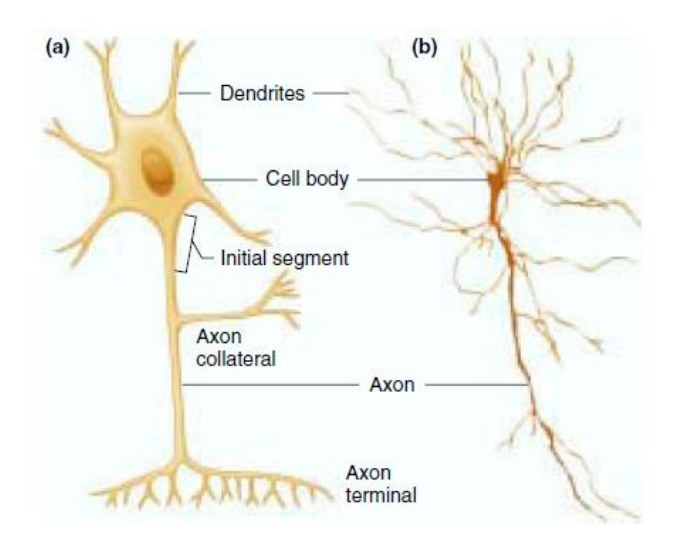


Figure I.1 – (a) Representation of a neuron with all its components: dendrites, cell body, axon and axon terminals. The axon proportions are misleading because this may be more than 5000 times longer than the cell body is wide. **(b)** Looking through a microscope the neurons can be observed like this, with a much higher complexity. The image cannot show the axon terminals because of the magnification used. Image adapted from Vander *et al.* 2001.

2. Alzheimer's disease

2.1. Brief History of Alzheimer's Disease

Dr. Alois Alzheimer, a German physician with a fascinating capacity of linking symptoms to microscopic brain changes, describes in 1907 the results of an autopsy from a female patient with progressive cognitive decline and memory loss. In this autopsy, Alzheimer noted two different histopathological features on her brain: the "peculiar substance" occurring as extracellular deposits in specific brain regions, like cortex, surrounded by dystrophic neuronal processes, now referred as amyloid plaques; and neurofibrillary tangles (NFT's) or abnormal intracellular aggregates, that are now known to be composed by aggregates of the microtubule-associated protein tau abnormally hyperphosphorylated (Gouras *et al.*, 2005; LaFerla *et al.*, 2007; O'brien and Wong, 2011). Afterwards, Glenner and Wong discovered that the "peculiar substance" in the cortex consisted of aggregates of a small peptide (4.2 kDa) with 40 or 42 amino acids known as amyloid-β-peptide (Aβ peptide) (Glenner and Wong, 1984; O'brien and Wong, 2011).

2.2. Alzheimer's Disease Pathogenesis

Alzheimer's disease (AD) is the most common cause of dementia and an age-related progressive neurodegenerative disease, affecting 10% of the population over 65 years and 50% of the population over the age of 85. It is thought that in 2040 the incidence of the disease will reach 81.1 million people in the world (Tang, 2009). AD is characterized by an impairment of memory and cognitive function. The clinical symptoms result from the deterioration of selective cognitive domains related with memory, such as hippocampus and cortex. The disease begins with a mild cognitive impairment in short-term and spatial memory, and become more severe with disease progression (LaFerla *et al.*, 2007; Zhang *et al.*, 2011; Musardo *et al.*, 2013).

It has been reported that the major neuropathological features are the neurofibrillary tangles of hyperphosphorylated tau protein and the extracellular deposits composed by A β peptides, delimited by dystrophic and degenerating neuronal processes, named amyloid plaques (Gouras *et al.*, 2005) (Figure I.2). It was speculated that amyloid plaques formation is a consequence of the progressive accumulation and aggregation of secreted A β to the extracellular space. However, the biological origin of amyloid plaques is still unknown (Gouras *et al.*, 2005; Gouras *et al.*, 2000).

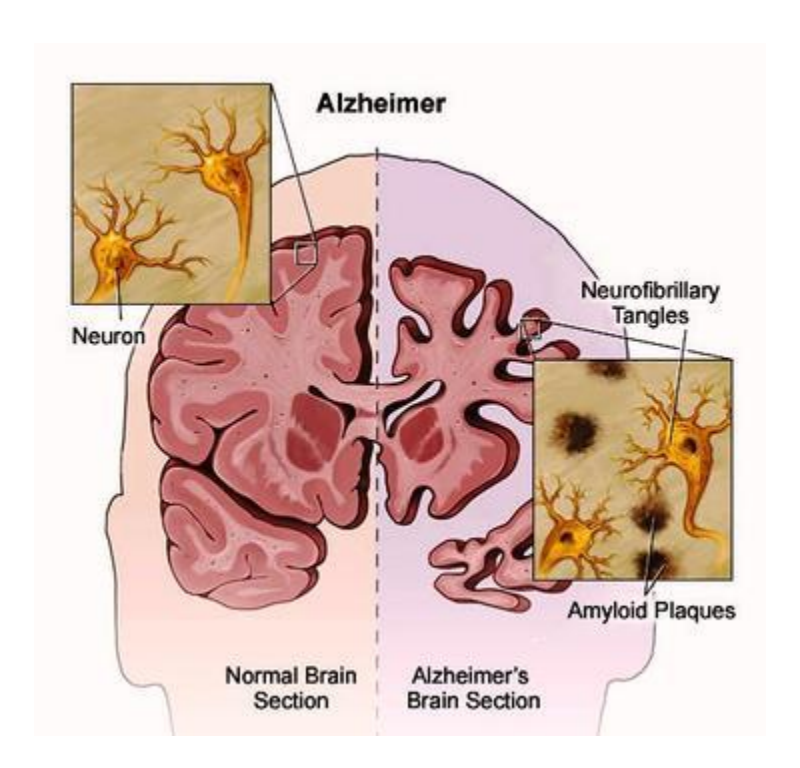


Figure I.2 – Comparison between the normal brain and the neuropathological features of the brain with AD: neurofibrillary tangles of hyperphosphorylated tau protein and the extracellular deposits of Aβ peptides (amyloid plaques). Image from: http://studentosteopathicmedicine.tumblr.com/post/21720073214/alzheimers-disease

Synaptic activity seems to have a role on Aβ secretion in mouse brains (Cirrito *et al.*, 2005; Cirrito *et al.*, 2008). This is of great importance since hippocampus and cortex, the brain areas most affected in AD, have abnormally high synaptic activity (Tampellini and Gouras, 2010).

A β peptide accumulation plays a central role in the pathogenesis of AD. Toxic effects of A β on synapses have been reported and related with synaptic loss. As such, the cognitive impairment seems to better correlate with loss of synapses, considered the earliest site of pathology, than with amyloid plaques or hyperphosphorylated tau tangles (Selkoe, 2002; Coleman and Yao, 2003; Dong *et al.*, 2007). Still, it remains poorly understood the mechanism whereby extracellular A β induces toxicity to synapses although it appears to occur via intraneuronal A β accumulation (Tampellini and Gouras, 2010).

A β peptide, specifically A β 42, was described as being enriched in multivesicular bodies (MVBs). These compartments are formed from early endosomes, and therefore are considered as late endosomes with inner vesicles formed by invaginations of the membrane. It was reported that A β 42 accumulates on MVBs on distal processes and synapses in human AD brains (Takahashi *et al.*, 2002; Gouras *et al.*, 2005; Almeida *et al.*, 2006).

It was also shown that A β 42 accumulate within neurons in AD-vulnerable brain areas (Gouras *et al.*, 2000). In 2004, it was demonstrated that A β 42 accumulation and oligomerization within neurons led to alterations in synaptic compartments (synaptic dysfunction) and in distal neurites in AD brains (Takahashi *et al.*, 2004).

It was reported that A β 42 accumulation within neurons is involved in alterations in pre- and post-synaptic compartments. The levels of the postsynaptic density protein (PSD-95), a protein involved in the recruitment and binding of glutamate receptor subunits (GluR1) to the post-synaptic region, was decreased and, as a consequence, GluR1 levels, important to post-synaptic excitation, were decreased as well. With time in culture, the severity of the alterations was increased and the number of active presynaptic compartments was reduced. Thus, it seems that first A β 42 accumulation is involved in the dysfunction, and only later in the loss, of synapses (Almeida *et al.*, 2005).

Therefore it was suggested that intracellular A β 42 accumulation can be an early pathological event in neuronal dysfunction underlying AD since it seems to appear prior to both neurofibrillary tangles and A β plaques formation (Gouras *et al.*, 2000).

Although some evidences point to a progressive accumulation of intraneuronal A β 42, that leads to the degeneration of synapses and distal processes and, as such, to a high accumulation of extracellular A β 42 that can be toxic to surrounding synapses with aging, the central question about what begins the cascade of events underlying AD, whether extracellular or intracellular A β accumulation, remains to be elucidated (Tampellini and Gouras, 2010).

2.3. Early-onset AD vs Late-onset AD

There are two types of AD, the rare form of AD, i.e. the early-onset familial AD (EOAD) with Mendelian inheritance (onset in population with less than 65 years), and the late-onset AD or sporadic AD (onset in population older than 65 years), the most common form of AD over 95% of AD cases (Bettens *et al.* 2013; Davinelli *et al.* 2011; Tang, 2009). In case of EOAD, the problem is on hereditary monogenic defects (Tang, 2009). The identified genes related with the onset of the disease were: amyloid precursor protein (APP), presenilin 1 (PSEN1) and presenilin 2 (PSEN2). The last two genes encode proteins that are components of γ -secretase, which is of major importance in APP processing (Turner *et al.*, 2003). Mutations in these genes cause an autosomal dominant form of AD leading to a higher production of A β peptide. Because of that, a central role for A β in AD was recognized (Davinelli *et al.*, 2011; Schellenberg and Montine, 2012; Bettens *et al.*, 2013).

On the other hand, several susceptibility genes were discovered to contribute to the risk for late-onset AD (LOAD). These genes were identified by Genome Wide Association Studies (GWAS), comparing different samples (persons with disease (cases) or without (controls)) for the allele frequencies of polymorphisms at or near a specific gene (Schellenberg and Montine, 2012). With these GWAS it was possible to identify a strong evidence for Bridging Integrator 1 (BIN1) as an AD risk locus (Seshadri *et al.*, 2010). The current work will focus on the role of Bin1 in AD development.

2.4. Amyloid precursor protein (APP)

A β peptide is produced by the cleavage of a larger precursor, Amyloid Precursor Protein or APP. APP is a single pass transmembrane protein with an extracellular domain at N-terminus (the bigger domain) and an intracellular domain (cytoplasmic domain) at C-terminus (O'Brien and Wong, 2011; Turner *et al.*, 2003). By alternative splicing it is possible to obtain 3 different isoforms of this protein: APP₆₉₅, APP₇₅₁ and APP₇₇₀. The isoform with 695 amino acids is mainly expressed in brain and the one that gets more attention in AD, whereas the other two isoforms are ubiquitously expressed (O'Brien and Wong, 2011; Turner *et al.*, 2003).

The physiological function of APP is not yet well defined; however it seems that it is involved in neurite growth, neuronal migration and repair via interaction with extracellular matrix proteins (Musardo *et al.*, 2013).

2.4.1. APP trafficking in neurons

Neurons are polarized cells meaning that different cellular compartments like axon and somatodendrites have specific membrane proteins and are able to perform different functions (Haass *et al.*, 2012; Horton and Ehlers, 2003). These compartments differ in the orientation of microtubules and in the presence of spines. In axons, microtubules have the plus-end distally in axon terminals, whereas in dendrites the microtubules have the plus-end pointing to nucleus or to dendrite terminals. Only dendrites have dendritic spines, specialized structures where excitatory synapses happen (Musardo *et al.*, 2013).

The microtubules orientation is of extreme importance in trafficking along the axon and dendrites. Membrane-bound organelles cargoes can be transported from cell body to axons and dendrites by the molecular motor kinesin - anterograde transport (from the minus-end to the plus-end of microtubules). On the other hand, membrane-bound organelles cargos can be transported from axon terminals and dendrites to cell body by retrograde axonal transport (from the plus-end to the minus-end of microtubules) and the molecular motor that is responsible for this trafficking is dynein (Musardo *et al.*, 2013).

In neurons, the sorting of membrane proteins can follow two different pathways. After following the secretory pathway, being synthesized in endoplasmic reticulum (ER), transported through Golgi apparatus and vesicular transport intermediates, proteins can undergo: (1) sorting in Trans-Golgi Network (TGN) into secretory vesicles targeted to axon or somatodendritic compartment in a polarized way and fusion with the membrane of this compartment; (2) sorting in TGN into secretory vesicles targeted to one compartment (axon or dendrites) in an indirect polarized way and after fusion with the membrane of this compartment, the protein is endocytosed and a polarized delivery by the endocytic pathway allow the endosomes to reach the final compartment where it fuses. This is called transcytosis (Musardo *et al.*, 2013; O'Brien and Wong, 2011; Turner *et al.*, 2003; Lasiecka and Winckler, 2011).

The sorting of APP can be carried out through the secretory and endocytic pathway. In the secretory pathway, APP tubulovesicular carriers traffic from TGN to plasma membrane of dendrites and axon (to presynaptic terminals by anterograde transport). From plasma membrane APP is endocytosed via clathrin-mediated endocytosis. From endosomes, APP can have different fates: transcytosis from axons to somatodendritic compartment; recycling back to plasma membrane; degradation through the lysosomal pathway or processing within the endosome generating Aβ peptide (Figure I.3) (Musardo *et al.*, 2013; O'Brien and Wong, 2011; Brunholz *et al.*, 2012).

Hence, APP is spread throughout neurons, in axon, dendrites and synaptic sites (pre- and postsynaptic compartments) (Turner *et al.*, 2003; Musardo *et al.*, 2013).

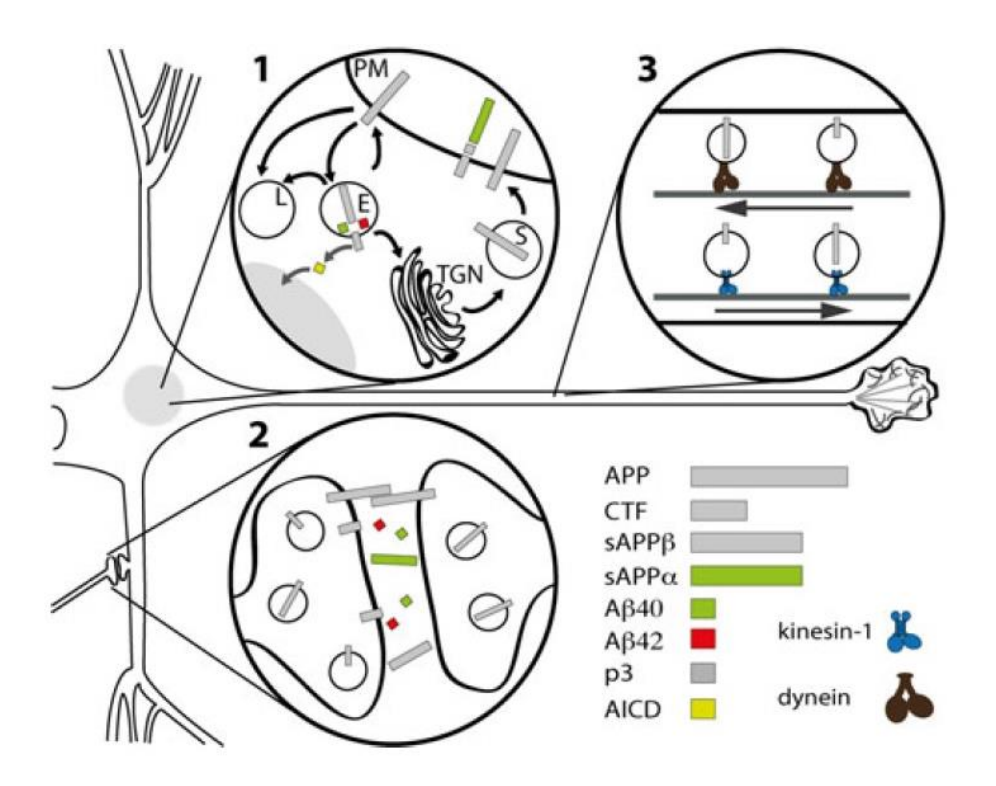


Figure I.3 - **APP trafficking in neurons.** Newly synthesized APP (*inset 1; grey*) is transported from the Trans-Golgi Network (TGN) to plasma membrane (PM) of the axon (*inset 3; kinesin anterograde transport (blue)*) and dendrites (*inset 1*) in secretory vesicles (*inset 1;* S). After binding to the plasma membrane (PM), some APP is cleaved by α-secretase generating the sAPPα fragment (*inset 1; green*), which diffuses through the extracellular space (*inset 1 and 2*), and some is reinternalized into endosomes (*inset 1;* E). In endosomes (*inset 1;* E), APP can have different fates: processing within the endosome generating Aβ40 (*small green*) or 42 (*red*) peptide and sAPPβ (*small grey*) that can be released to the extracellular space (*inset 1 and 2*); recycling back to plasma membrane (PM) (*inset 1*); follow transcytosis from axons to somatodendritic compartment (*inset 3; dynein retrograde transport (black)*) or follow degradation through the lysosomal pathway (*inset 1;* L). Image adapted from Brunholz *et al.*, 2012.

2.4.2. APP processing

The processing of APP can occur in different sites by different enzymes. There are three APP secretases involved in its processing: (1) α -secretase with the cleavage site within the A β peptide region; (2) β -secretase, which can be identified as BACE-1 (aspartyl protease β -site APP cleaving enzyme 1), with the cleavage site in the N-terminus of A β peptide; and (3) γ -secretase with the cleavage site in the C-terminus of A β peptide, within the transmembrane domain of APP (Figure I.4). The α -cleavage can occur within the plasma membrane whereas β - and γ -cleavage can occur within the TGN and endosomes (Turner *et al.*, 2003).

APP processing can be divided into two pathways: (1) the nonamyloidogenic and, (2) the amyloidogenic. In the first one, APP at cell surface is cleaved by α -secretase producing a large soluble ectodomain at N-terminus (612 amino acids), named sAPP α , that is secreted to the extracellular space. The remainder portion of APP that stays tethered to the membrane is referred as the α -carboxyl-terminal fragment (α -CTF), containing 83 amino acids (C83) that include part of A β peptide domain, precluding its formation. C83 is subsequently cleaved by the γ -secretase leading to the formation of 2 fragments, a small fragment called p3 that is released to the extracellular space and the C-terminal fragment that remains inside the cell, termed APP intracellular domain (AICD) (Figure I.4) (O'Brien and Wong, 2011; LaFerla *et al.*, 2007; Turner *et al.*, 2003).

On amyloidogenic pathway, APP at cell surface is internalized by clathrin-mediated endocytosis into endosomes containing BACE-1 and γ -secretase. The first cleavage is the β -cleavage, resulting in the release of a large soluble ectodomain at N-terminus (595 amino acids), called sAPP β , that is secreted to the extracellular space. The remainder portion of APP that stays tethered to the membrane is referred as the β -carboxyl-terminal fragment (β -CTF), containing 99 amino acids (C99) that includes at the N-terminus the first amino acid of A β peptide. C99 is subsequently cleaved by the γ -secretase leading to the formation of two fragments, A β peptide, which is released to the extracellular space or remains in endosomes; the γ -CTF is released to the cytosol, termed APP intracellular domain (AICD) (Figure I.4) (O'Brien and Wong., 2011; LaFerla *et al.*, 2007; Turner *et al.*, 2003).

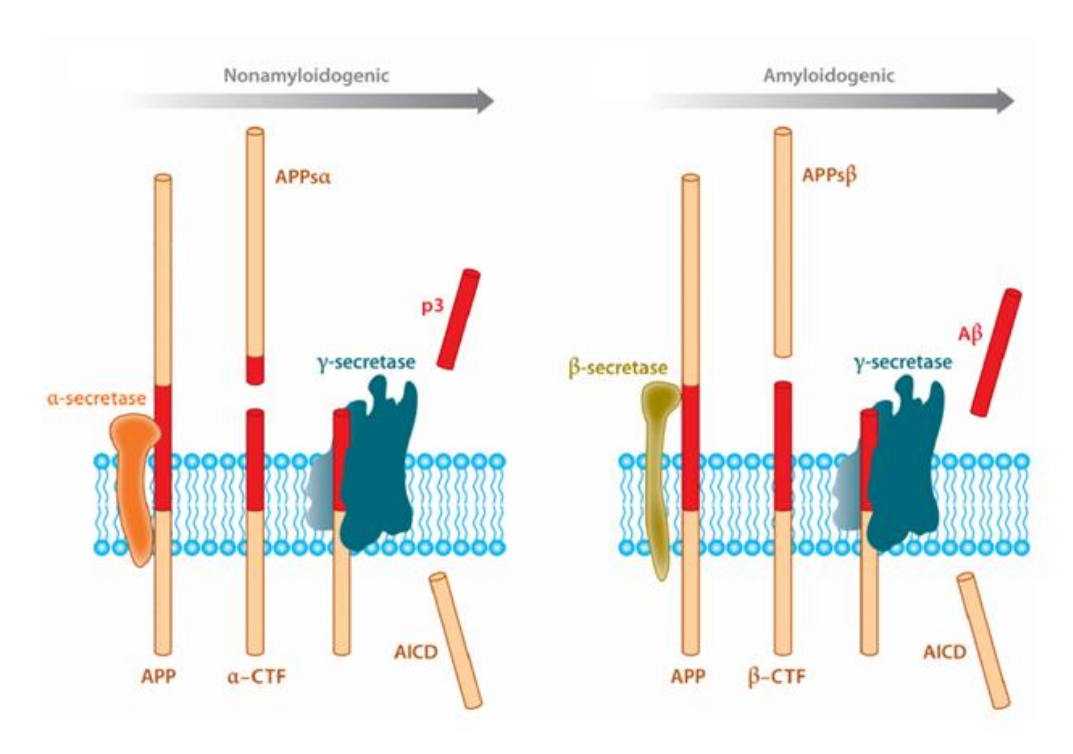


Figure I.4 – Processing of APP through the non-amyloidogenic and amyloidogenic pathway. On nonamyloidogenic pathway, APP at cell surface is cleaved by α -secretase producing sAPP α and the α -CTF, containing 83 amino acids (C83). C83 is subsequently cleaved by the γ -secretase leading to the formation of p3 and a

C-terminal fragment, named APP intracellular domain (AICD). On amyloidogenic pathway, APP at cell surface is cleaved by β -secretase, resulting in two fragments sAPP β , which is secreted to the extracellular space, and β -CTF, containing 99 amino acids (C99). C99 is subsequently cleaved by the γ -secretase leading to the formation of A β peptide that is released to the extracellular space, and C-terminal fragment, named APP intracellular domain (AICD). Image adapted from O'Brien and Wong, 2011.

A β peptide can have two different forms differing by just two amino acids, A β_{40} and A β_{42} . A β_{40} is the peptide that is most produced and less hydrophobic whereas A β_{42} is less produced (approximately 10% of A β production), more hydrophobic and toxic (susceptible to fibril formation) and the main form present in A β plaques in AD (Figure I.5) (LaFerla *et al.*, 2007).

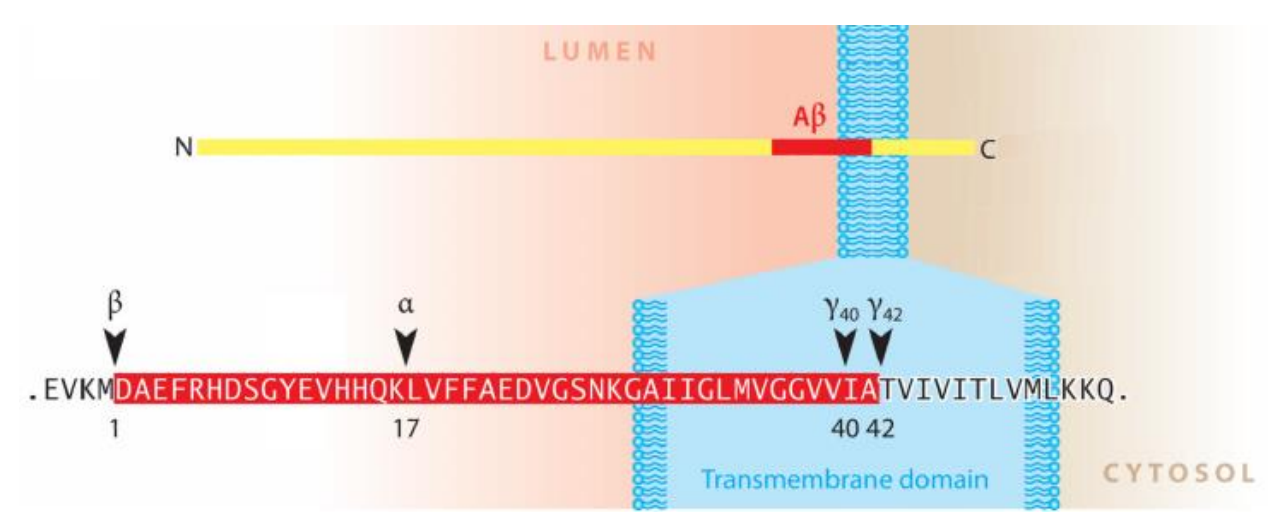


Figure I.5 – Sites of APP cleavage by the different secretases. Image adapted from O'Brien and Wong, 2011.

2.4.3. The role of APP endocytosis for AD development

As mentioned above, APP after synthesized can be delivered to cell surface. However, the presence of APP at cell surface is very short since APP is rapidly internalized through clathrin-mediated endocytosis or proteolyzed at cell surface by α -secretase. Still, it remains unclear why some APP is endocytosed and some is proteolyzed (O'brien and Wong, 2011).

In the intracellular cytoplasmic domain, APP has an amino acid domain named YENPTY that is of extreme importance for APP endocytosis and sorting, since this domain regulates clathrin-coated pit internalization (O'brien and Wong, 2011).

Some evidences have shown that alterations in the endocytosis can have a role in the development of AD. In 1994 it was demonstrated in a Chinese Hamster Ovary (CHO) cell line that

deletion of the C-terminus cytoplasmic domain of APP led to a decrease in APP internalization and, as such, to a decrease in A β production and release. This highlighted the importance of C-terminus domain of APP for protein internalization and the importance of the endocytic pathway for A β production (Koo and Squazzo, 1994).

In 2008, it was shown that, *in vivo*, the inhibition of clathrin-mediated endocytosis lowers the levels of $A\beta$ in brain interstitial fluid of living mice. About 70% of $A\beta$ released requires endocytosis and a great part of endocytosis is dependent of synaptic activity. This showed that $A\beta$ needs to follow the endocytic pathway to be produced within early endosomes, and, after this, recycled to the extracellular space (Cirrito *et al.*, 2008).

2.5. β-site APP-cleaving enzyme 1 (BACE-1)

BACE-1 is a membrane-bound aspartyl protease that is ubiquitously expressed with a higher expression in neurons, where it seems to have a role in axonal growth and brain development (Musardo *et al.*, 2013; Turner *et al.*, 2003; Ye and Cai, 2014). This enzyme is considered the most important secretase involved in Aβ generation, being the initial rate-limiting step of APP processing on amyloidogenic pathway. In brain cortex of AD patients the level/activity of BACE-1 is increased, as well as in aging (Ye and Cai, 2014; Musardo *et al.*, 2013).

BACE-1 is distributed in several compartments like ER, TGN, cell membrane and endosomes. This enzyme needs an acidic pH to have a higher efficiency on APP processing and, as such, APP cleavage by BACE-1 occurs preferentially in endosomes and TGN (Musardo *et al.*, 2013; Buggia-Prévot *et al.*, 2013; Ye and Cai, 2014; Chia *et al.*, 2013).

After synthesized in ER, BACE-1 is transported through Golgi and follows the secretory pathway until the cell surface. Here, BACE-1 is internalized by endocytosis, into early endosomes. BACE-1 can also be sorted to endosomes directly from TGN. Within endosomes BACE-1 can follow four different routes: recycle to cell surface; go directly to recycling endosomes; fuse with the TGN; or follow the lysosomal pathway (Chia *et al.*, 2013; Musardo *et al.*, 2013; Ye and Cai, 2014; Buggia-Prévot *et al.*, 2013).

Both APP and BACE-1 follow the secretory and endocytic pathways, however the exact trafficking pathways of these proteins in neurons are not yet well understood (Chia *et al.*, 2013; Musardo *et al.*, 2013).

2.5.1. The role of BACE-1 endocytosis for AD development

The intracellular trafficking of APP and BACE-1 needs to be coordinated with the occurrence of APP cleavage and Aβ generation. In cultured cell lines and primary neurons (PN), just a part of APP is cleaved in order to generate Aβ. This can be related with the distinct intracellular sorting and organelle localization of BACE-1 and APP that can vary in polarized neurons and non-neuronal cells (Buggia-Prévot *et al.*, 2014; Buggia-Prévot *et al.*, 2013).

Recently it was demonstrated that, in non-neuronal and neuronal cell lines the itinerary of cell surface internalized APP and BACE-1 diverge. BACE-1 is transported mainly from cell surface to early endosomes and then to recycling endosomes, where it recycles to plasma membrane. APP is transported from cell surface to early endosomes and then follows to late endosomes/lysosomes. Hence, the common compartments of BACE-1 and APP transport seem to be the early endosomes and not the TGN. It was proposed that the transport of BACE-1 to the recycling endosomes, passing through early endosomes, may be of great importance in the regulation of Aβ production (Chia *et al.*, 2013).

However, in hippocampal cultured neurons, it was demonstrated that from the TGN BACE-1 is trafficked to the plasma membrane and recycling endosomes while APP is sorted to the plasma membrane in different Golgi-derived vesicular carriers. The different localizations of these two proteins change upon neuronal activity, leading to the convergence of APP and BACE-1 in acidic endosomes via clathrin-mediated endocytosis. Even though it seems that clathrin mediated endocytosis is necessary for this convergence, the mechanisms that regulate the encounter of APP and BACE-1 in the same compartment are not yet well known (Das *et al.*, 2013).

In neurons BACE-1 localizes to axon and dendrites, and in brains of AD patients this enzyme seems to be accumulating at axon terminals. As mentioned above, APP follows anterograde transport through axon until it reaches axon presynaptic terminals. Thus, BACE-1 can potentially be active during this transport, mediating the $A\beta$ production and release at or near presynaptic sites. Still, the molecular mechanism by which BACE-1 is sorted to axon remains unknown (Buggia-Prévot *et al.*, 2014; Buggia-Prévot *et al.*, 2013).

3. Bridging integrator 1 (BIN1) or amphiphysin 2 (AMPH2)

As reported above, there are two major types of AD, EOAD and the LOAD, varying in the age of onset. EOAD forms are linked to the familiar history or autosomal dominant mutations in three different genes (*APP*, *PSEN-1*, and *PSEN-2*) that are associated with changes in APP metabolism and Aβ42 increased production (Lambert and Amouyel, 2011). LOAD forms or sporadic AD are not related with familiar history. Several susceptibility genes were discovered, by GWAS, to contribute to the higher

genetic risk for LOAD. Among these genes, it was possible to identify a strong evidence for BIN1 or amphiphysin 2 (AMPH2) as an AD risk locus (Seshadri *et al.*, 2010). BIN1 was identified as the second most important genetic susceptibility locus in AD. The main associated single nucleotide polymorphism (SNP) (rs744373) stands approximately 30kb upstream BIN1 gene, in the 5' BIN1 non coding region. This SNP may be related with gene regulation and involved in alterations on BIN1 expression level (Hu *et al.*, 2011; Seshadri *et al.*, 2010; Chapuis *et al.*, 2013).

It was reported that Bin1 protein level was found increased in a small study of human AD brains, (Karch *et al.*, 2012). It was also reported that, in AD human brains, the BIN1 transcript levels were increased (Chapuis *et al.*, 2013). In contrast, Bin1 protein level was found reduced in a small study with sporadic AD brains (Glennon *et al.*, 2013). More recently, it was also described that the amount of the neuronal isoform of Bin1 was reduced whereas the ubiquitous isoform of Bin1 was increased in AD brains (Holler *et al.*, 2014). Thus, it remains unclear if BIN1 gene variants associated with AD increase or decrease Bin1 at the protein level.

3.1. BIN1 gene and domain organization

The domain organization of Bin1 is similar to amphiphysin 1, containing an N-terminal BAR (<u>BIN-Amphiphysin-Rvs</u>) domain that is present in all splice isoforms. This domain has a shape similar to a banana, with the ability to sense and generate membrane curvature through binding to lipid membranes. And a C-terminal domain, Src homology 3 (SH3), also present in all splice isoforms, that binds to prolinerich motifs (Ren *et al.*, 2006).

At least 20 exons are encoded by BIN1, which are alternatively spliced generating multiple Bin1 splice isoforms. However, the major forms (brain-specific isoform, muscle-specific isoform and the ubiquitous isoform) vary in the inclusion of four exons: 6a, 10, 12 and 13 (Ren *et al.*, 2006). The exon 6a encodes a 31-residue brain-specific N-terminal insert domain (NTID) within BAR domain and it is present in some brain splice variants. The exon 13 is present in all splice variants, encoding part of the Myc binding domain (MBD). Only brain splice variants include the exon 12, containing alternative brain-specific exons (12A to -D) that encode Clathrin-AP2 binding domain (CLAP), a central insert domain able to interact with clathrin and α -adaptin/AP-2, also known as the endocytosis domain (Ren *et al.*, 2006; Tan *et al.*, 2013; Leprince *et al.*, 1997). Muscle splice variants include just two exons, exon 13 and specifically the exon 10 that encodes a nuclear localization sequence, (NLS; 15-residue domain) (Figure I.6) (Ren *et al.*, 2006; Tan *et al.*, 2013).

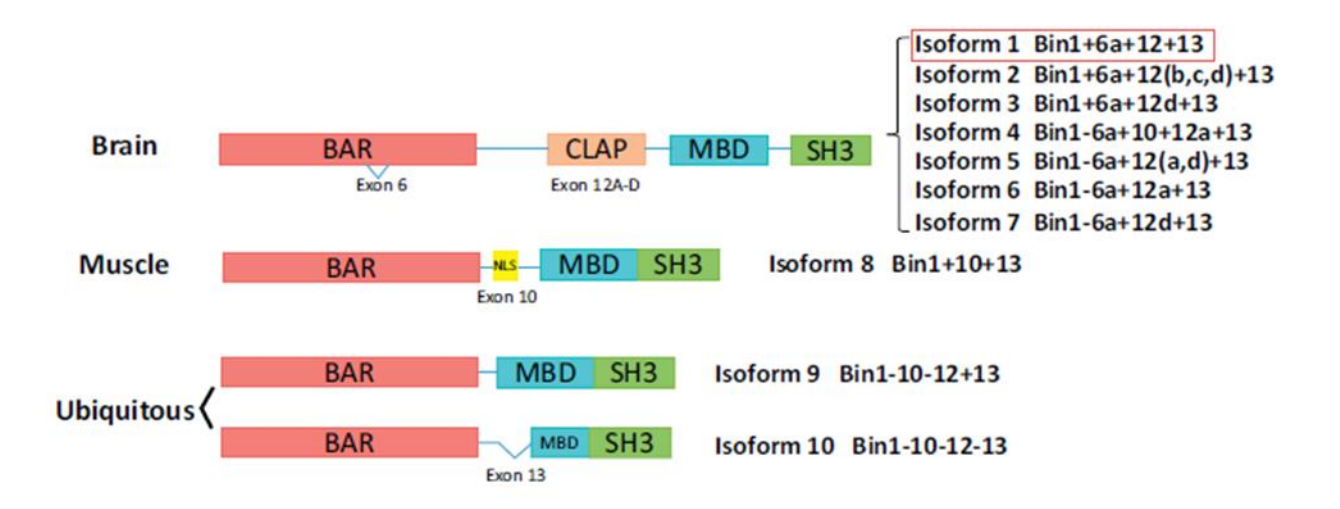


Figure I.6 – Alternative splicing isoforms of BIN1/Amphiphysin 2, with the different functional domains for each tissue specific isoform. Abbreviations: BAR, BIN1/Amphiphysin 2/Rvs; CLAP, Clathrin-AP2 binding region; MBD, Myc-binding domain; SH3, Src homology 3 domain; NLS, Nuclear localization sequence. Red box: Brain specific isoform of Bin1 studied in the current work. Image adapted from Tan *et al.*, 2013.

3.2. Bin1 cellular functions

3.2.1. The role of Bin1 in endocytosis and trafficking

It has been shown that amphiphysin family of proteins has a role on endocytosis (Leprince *et al.*, 1997; Ramjaun *et al.*, 1997). Bin1/amphiphysin 2, as a member of amphiphysin family, was identified as having a role in binding to molecules required for endocytosis, specifically clathrin-mediated endocytosis, and probably being involved in synaptic vesicle endocytosis, since it was identified as a protein enriched in nerve terminals (Leprince *et al.*, 1997; Ramjaun *et al.*, 1997; Wigge *et al.*, 1997).

Clathrin-mediated endocytosis at synapses (Figure I.7) involves several molecules and steps:

- 1) Recruitment of Adaptor Protein-2 heterotetrameric complex (AP-2) to plasma membrane, which interacts with clathrin and with amphiphysin 1 and 2 through its α -subunit, both enriched in nerve terminals;
- 2) Recruitment of clathrin by AP-2 and by the central region of amphiphysin 1 and 2 that lead to the polymerization of clathrin into a polygonal lattice that forms the matrix for coated pit;
- 3) Amphiphysin 1 interaction with: dynamin, synaptojanin and amphiphysin 2. Through its SH3 domain (C-terminal) amphiphysin 1 can interact with proline-rich domain of dynamin or with synaptojanin (a lipid phosphatase that is enriched in nerve terminals), containing a proline-rich domain similar to

dynamin that may regulate negatively the interaction with dynamin. Through its BAR domain (N-terminal) amphiphysin 1 interacts with amphiphysin 2, forming a stable heterodimer that is the main form found in brain;

- 4) Recruitment of dynamin by amphiphysin heterodimer. The interaction of both SH3 domains of heterodimer with several molecules of dynamin (GTP binding protein) in its dissociated form lead to the self-assemble of dynamin into a ring like structure on the collar of coated pit;
- 5) Vesicle fission. At nerve terminal, dynamin self-assembled on the collar of coated pit triggers the dissociation of the heterodimer and the vesicle fission, upon GTP hydrolysis (Ramjaun *et al.*, 1997; Wigge *et al.*, 1997; Wigge and McMahon, 1998).

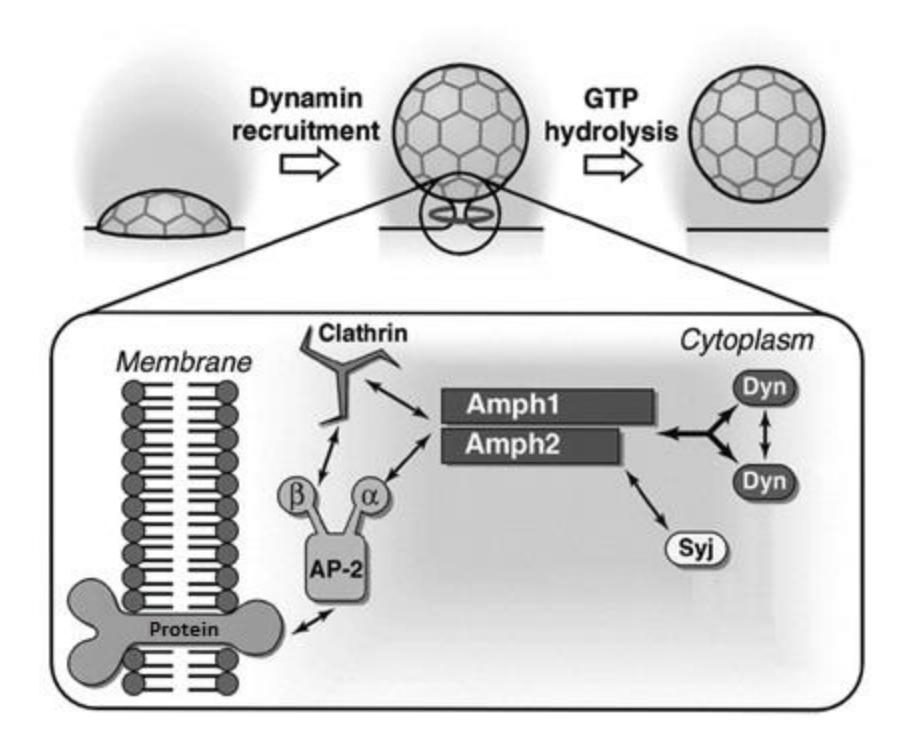


Figure I.7 – Molecular mechanisms in clathrin-mediated endocytosis. At nerve terminal, several protein-protein interactions may happen. The formation of clathrin-coated vesicles at the plasma membrane is driven by the assembly of clathrin triskelia into polygonal lattices. Clathrin is recruited to the plasma membrane by Adaptor Protein-2 heterotetrameric complex (AP-2) and amphiphysin heterodimer (Amph1/Amph2). The subsequent formation of invaginated constricted coated pit and its detachment from the plasma membrane requires various additional proteins. Amph1/Amph2 may interact with: 1) Synaptojanin (Syj), which is a negatively regulator of the interaction with Dynamin (Dyn); 2) Dyn, a GTPase crucial to vesicle fission. Dyn is targeted to the necks of endocytic coated pits where it participates in the fission reaction upon GTP hydrolyses, leading to the formation of the coated vesicle. Image adapted from Wigge and McMahon, 1998.

Several evidences for the role of amphiphysins in endocytosis have been reported. In COS-7 fibroblasts, exogenous expression of the amphiphysin 1 SH3 domain led to the blockade of transferrin uptake *in vivo*. The explanation for this event was that the interaction between amphiphysin 1 and dynamin was disturbed by the exogenous SH3 domain of amphiphysin 1. This suggest that amphiphysin 1 has a role in clathrin coated pits by recruiting dynamin (Wigge *et al.*,1997b).

In cortical neurons of knockout mice for amphiphysin 1, a great decrease in the levels of amphiphysin 2 was observed but not in the levels of amphiphysin 2 mRNA. A possible interpretation of these results can be related with previous reports showing that the stable form of amphiphysin 1 and 2 is obtained by the formation of heterodimers. Like that, the lack of amphiphysin 1 disrupted the stability of the heterodimer, and, as a consequence, the levels of amphiphysin 2 decreased (Wigge *et al.*, 1997; Di Paolo *et al.*, 2002). Knockout mice lacking amphiphysin 1 demonstrated synaptic vesicle recycling deficits and a decreased capacity of vesicles to be reused. It also demonstrates a decrease in cytosolic endocytic proteins (clathrin, AP-2 and synaptojanin) supporting the hypothesis that amphiphysin may function as an adaptor protein linking cytosolic proteins from endocytic machinery to plasma membrane. Thus, it was demonstrated that amphiphysin 1 has an important role in synaptic vesicle recycling, regulating the function of endocytic machinery at plasma membrane (Di Paolo *et al.*, 2002). Since amphiphysin 1 interacts with amphiphysin 2, the latter may have a role in the same pathway.

In addition to probably having a role in endocytosis, amphiphysin 2 seems to be important in regulating intracellular trafficking and recycling as well. In HeLa cells it was reported that the overexpression of sorting nexin 4 (SNX4), a protein adaptor, inhibits transferrin receptor endocytosis. This result was related with a possible association between amphiphysin 2 and SNX4 which the overexpression led to the sequestration of amphiphysin 2 and as such to a defect in endocytosis. It was also demonstrated that these two proteins colocalized with vesicles containing transferrin that would be recycled, which suggests that amphiphysin 2 may have a post-endocytic role regulating intracellular trafficking of the endocytic vesicle (Leprince *et al.*, 2003).

In HeLa cells, it was shown that amphiphysin 2 is important for vesicle recycling from endocytic recycling compartment (ERC) to the plasma membrane. It was demonstrated that cells knocked down for amphiphysin 2 showed defects on transferrin recycling upon a normal transferrin uptake, with increased levels of intracellular transferrin retained near nucleus, on ERC (Pant *et al.*, 2009).

3.2.2. Endocytic trafficking and AD

Endocytosis and intracellular trafficking have been implicated in AD by several experimental evidences. In 2000, it was observed that, in sporadic AD brain the volume of neuronal early endosomes as well as in the number of recycling vesicles were increased, suggesting an increase in endocytic and

recycling pathway. The early endosomal defects were found to be the earliest neuropathological alteration in sporadic AD, preceding extracellular deposition of A β (Cataldo *et al.*, 2000). It was also reported that the endocytosis of APP and its secretases can promote A β generation, within early endosomes (Cirrito *et al.*, 2008; Das *et al.*, 2013).

BIN1 was identified as a genetic risk factor for sporadic AD, and it seems to control endocytosis and intracellular trafficking/recycling. Thus, we hypothesized that, Bin1 may influence APP and BACE-1 trafficking and, as a consequence, APP processing and A β production. This may have an impact on the AD development.

4. Aims of the current work

Although AD has been widely studied, an effective treatment to this disease is still missing. The presence of amyloid plaques and neurofibrillary tangles are the major hallmarks of AD. However, prior to amyloid plaques formation, Aβ accumulates intra- and extracellularly, oligomerizes and causes synaptic dysfunction that could be related with the cognitive impairment seen in the disease patients.

Still, the cause and mechanisms of $A\beta$ accumulation in sporadic AD are not known. Defects in endocytosis and intracellular trafficking may be AD mechanisms since they have been implicated in AD. However, it is not clear how these defects contribute to the development of sporadic AD.

BIN1 was identified as a putative risk factor for late-onset AD but it is not known how it contributes to AD development. Some evidences pointed to a role in endocytosis and intracellular trafficking for Bin1. The increase or decrease in the protein level may disturb APP and BACE-1 endocytosis and trafficking, enhancing $A\beta$ generation by increasing the residence time of these proteins in a common compartment, endosomes.

Thus, the main goal of this thesis is to explore the role of Bin1 on A β accumulation through the study of the molecular pathways where this risk factor impacts A β generation and increases A β accumulation, leading to AD development. To explore this, we raised the following questions:

- 1. Does Bin1 overexpression/downregulation alter Aβ accumulation?
- 2. Does Bin1 overexpression/downregulation alter APP processing?
- 3. Does Bin1 overexpression alter APP and BACE-1 trafficking?

As an experimental model to answer these questions we will use cortical PN from embryonic E16 mouse embryos. This model is extremely advantageous because neurons present a highly complex and polarized structure, achieving axonal/dendritic differentiation and synapse formation at 12 days *in vitro* (DIV) (Pravettoni *et al.*, 2000).

The final purpose of this thesis is to provide new insights about Bin1 as a player in the development of AD and to understand a possible trafficking mechanism by which this protein leads to the accumulation of $A\beta$ in neurons.

II. Materials and methods

1. Reagents

Table II.1 – Antibodies and probes

| | IF dilution | WB dilution | Supplier | |
|--|-------------|-------------|--------------------------------|--|
| Primary antibodies | | | | |
| α-tubulin | - | 1:5000 | Millipore | |
| Αβ42 | 1:50 | - | Genetex | |
| Ankyrin G | 1:100 | - | Santa Cruz | |
| APPY188 | 1:200 | 1:1000 | Genetex | |
| Bin1 | 1:100 | 1:1000 | Millipore | |
| EEA1 | 1:50 | - | Santa Cruz | |
| GFP | - | 1:5000 | Gift M.Arpin (Institute Curie) | |
| Giantin | 1:500 | - | Curie | |
| Lamp1 | 1:500 | - | Santa Cruz | |
| Мус | 1:500 | 1:5000 | Curie | |
| TfR | 1:50 | - | Curie | |
| Secondary antibodies | | | | |
| Alexa-488 anti-mouse | 1:500 | - | Molecular probes/Invitrogen | |
| Alexa-488 anti-rabbit | 1:500 | - | Molecular probes/Invitrogen | |
| Alexa-555 anti-Goat | 1:500 | - | Molecular probes/Invitrogen | |
| Alexa-555 anti-mouse | 1:500 | - | Molecular probes/Invitrogen | |
| Alexa-555 anti-rabbit | 1:500 | - | Molecular probes/Invitrogen | |
| Alexa-647 anti-mouse | 1:500 | - | Molecular probes/Invitrogen | |
| Alexa-647 anti-rabbit | 1:500 | - | Molecular probes/Invitrogen | |
| HRP anti-mouse | - | 1:5000 | Bio-Rad | |
| HRP anti-rabbit | - | 1:5000 | Bio-Rad | |
| Probes | | | | |
| Alexa Fluor [™] 647-Conjugated Human Transferrin (1 mg/ml) | - | - | Jackson Immunoresearch Lab | |

2. DNA amplification

E.coli DH5α Transformation

Slowly thawed competent bacteria ($E.coli\ DH5\alpha$) (Life technologiesTM) on ice. Added 0.5 µg of DNA to 50µL of bacteria and mixed. Bacteria were incubated on ice 30 min and then exposed to a heat shock (an increase in temperature) at 42°C for 20 sec, inducing the formation of pores through which plasmidic DNA can enter. After, returning the cells to a lower temperature (2 min on ice) the cell wall could self-heal. Once cells had taken up the plasmid, 100-200µL Luria Bertani (LB medium) (Sigma-AldrichTM) was added and they were put to grow on shaker for 1h at 37°C. After this, the medium with bacteria was spread on LB-agar plates containing 100 µg/ mL of antibiotics depending on the antibiotic resistance of the construct used (ampicillin 50 mg/mL; kanamycin, 5 mg/mL) (VWR). Cells grew overnight at 37°C.

Plasmid DNA preparation

A single colony of transformed bacteria, grown in LB-agar plate or from a glycerol stock was picked with a sterile pipette tip. The pipette tip was deposited in 5 mL LB medium containing either ampicillin (100 μg/ mL) or kanamycin (100 μg/ mL). Bacteria were incubated for 8h at 37°C in an orbital shaker (189 rpm). After this, 5 mL starter culture was used to inoculate erlenmeyer containing 200 mL LB media supplemented with antibiotic depending on the antibiotic resistance of the construct used. The 200 mL culture was incubated overnight at 37°C in an orbital shaker (189 rpm). Plasmid DNA purification from *E.coli* cells was performed using the NZYTechTM NZYMidiprep following the protocol described in the NZYTech handbook. The precipitated DNA was dissolved in ultraPureTM DNase/RNase Free Distilled water (InvitrogenTM, Life technologies) and the DNA concentration was determined by absorbance at 260 nm, using NanoDrop 2000 UV-Vis spectrophotometer (Thermo ScientificTM).

Glycerol stocks

After transformed and grown in LB medium overnight at 37°C, *E.coli* cells in exponential phase of growth (500 μl) were added to 50% glycerol (500μl) in a cryovial (Thermo ScientificTM) and then stored at -80°C.

3. Tissue Culture

Cell lines

HeLa is a human cell line originated from a cervical cancer. It is the most commonly used human cell line that serves as a model to study cellular and molecular biology (Landry *et al.*, 2013). N2a cells are a mouse neuroblastoma cell line (Mouse Neuro 2a or N2a). This cell line, are like neural precursors that have the ability to differentiate into neurons, and are able of unlimited proliferation *in vitro* (Tremblay *et al.*, 2010). HeLa (Human cervical cancer) and N2a (Mouse neuroblastoma) cells were cultured in Dulbecco's Modified Eagle Medium (DMEM) (DMEM+GlutaMAXTM supplement, GibcoTM, Life Tecnhologies) supplemented with 10% fetal bovine serum (FBS) (Sigma-AldrichTM) and 1% Penicillin/Streptomycin (10 000 Units/ mL of penicillin; 10 000 μg/ml of streptomycin) (GibcoTM, Life technologies), in a humidified incubator at 37°C with 5% CO₂. Once the cells reached 90% confluence they were washed once with 1 mL of phosphate buffered saline (PBS pH 7.4) (GibcoTM, Life technologies) and 1mL of trypsin (Life technologies) was added to dissociate adherent cells from the dish where they were plated. After trypsin addition, cells were incubated 5 minutes at 37°C with 5% CO₂. Trypsin activity was stopped by adding 9 ml of complete media (DMEM+FBS+Pen/Strep). Cell suspension resulting from trypsinization process contained round shaped cells that were split in 1:10 to another dish (Ø 10 cm) to maintain culture. Then, they were plated in different amounts and different plates, depending on the aim of each experiment.

Mouse primary neuronal cultures

Mouse primary neuronal cultures were prepared from cerebral cortices of mice embryos with 16 days of gestation (E16). Brains were dissected in ice-cold Hanks balanced salt solution (HBSS; GibcoTM, Life Technologies) with 0.45% glucose (from 50% D-glucose stock in water) (Sigma-AldrichTM) and 0.5% HEPES 10mM (GibcoTM, Life technologies). Under magnifier, cortices were separated from brains and digested with 0.1% trypsin (Life technologies) in HBSS/Glucose/HEPES solution at 37°C for 15 min. After this, trypsin was removed and cortices were washed 3 times with HBSS/Glucose/HEPES solution to inhibit trypsin activity. To dissociate neurons from the cortices, Dulbecco's Modified Eagle Medium (DMEM) (GibcoTM, Life technologies) supplemented with 10% fetal bovine serum (FBS) and 1% Penicillin/Streptomycin was added and by pipetting up and down with a glass pipette the cortices were triturated. A centrifugation step was performed to remove the supernatant and ressuspend the pellet in DMEM/FBS/Pen/Strep solution. After counting, the cells were plated on Poly-D-lysine hydrobromide (2mg/ml) (Sigma-AldrichTM) coated plates (6-well plates) (VWR) and glass coverslips (Ø12 mm) (Menzel) on 24-well plates (VWR) diluted in complete media for PN, and incubated at 37°C with 5% CO₂. The day after, medium was substituted with NeurobasalTM medium (GibcoTM, Life technologies) containing 0.1% GlutaMAXTM supplement (GibcoTM, Life technologies), 1% Penicillin/Streptomycin and 2% B-27TM

supplement (GibcoTM, Life Technologies). All the process of dissection was always performed by Florent Ubelmann or Cláudia Almeida, and I helped them with the coating of coverslips (addition of poly-D-lysine), preparation of Neurobasal/GlutaMAX/Pen/Strep/B-27 solution, complete media for PN and HBSS/D-Glucose/HEPES solution.

Counting cells

After trypsinization and dilution in complete media, 20μ L of trypan blue (Amresco), a dye that do not colour intact cell membranes, was added to 20μ L cell suspension. 10 μ L of cells in complete media plus trypan blue were added to Neubauer Chamber (or Haemacytometer) and the cells not stained with trypan blue (viable) within the four grid squares placed on each corner of the slide were counted. After this the average of squares was determined and multiplied by the dilution factor as well as by the conversion factor for neubauer, 10^4 (cell densities $>10^4$ cells/ml).

Plating cells

Table II.2 – Number of cells per mL that were plated to perform each type of method

| Cell type | | Number of cells | Method | Plates |
|----------------|------------------------|-----------------|--------------------|---------------|
| | | per well | Method | Flates |
| Overexpression | N2a, HeLa | 50 000 | Immunofluorescence | 24-well plate |
| | NZa, HeLa | 100 000 | Western blot | 6-well plate |
| | HeLa | 70 000 | Immunofluorescence | 24-well plate |
| | (pre-permeabilization) | 70 000 | immunondorescence | |
| | PN | 50 000 | Immunofluorescence | 24-well plate |
| | FIN | 600 000 | Western blot | 6-well plate |
| Downregulation | NOo | 40 000 | Immunofluorescence | 24-well plate |
| | N2a | 80 000 | Western blot | 6-well plate |
| | PN | 50 000 | Immunofluorescence | 24-well plate |
| | | 600 000 | Western blot | 6-well plate |

Plasmid Transiently transfection

N2a cells were plated in glass coverslips inside a 24-well plate or in a 6-well plate and cultured in complete media in 5% CO₂ at 37 °C. After 24h of culture, the confluency was about 90%–95% and cells were transiently transfected with cDNA encoding mouse brain amphiphysin 2, C-terminal domain of mouse brain amphiphysin 2 in expression vector pRK5-myc (Gently ceded by C.Leprince) or the empty vector pCS2 with GFP, using LipofectamineTM 2000 (Invitrogen TM). The amounts and volumes are given on a per well basis. For each plasmid transfection, two separate mixes were prepared, one with 0.5 μ g DNA in 12.5 μ L of Opti-MEM medium and the other with 0.5 μ L LipofectamineTM 2000 in 12.5 μ L of Opti-MEM medium. Mixes were incubated for 5 min at room temperature, combined gently and incubated for another 20 min at room temperature. The cell culture media was removed from 24-well plate and 250 μ L complete growth medium without Pen/Strep was added. The mixture containing Opti-MEM, LipofectamineTM 2000 and DNA was then added to each well and incubated with the cells at 37 °C in a 5% CO₂ incubator for 24h. To better assess the level of A β , cells were incubated for 48 h before immunofluorescence assay.

HeLa cells were plated and cultured as described for N2a cells. Cells were transiently transfected with cDNA encoding: mouse brain amphiphysin 2, C-terminal domain of mouse brain amphiphysin 2 in expression vector pRK5-myc; the empty vector pCS2 with GFP; APP-monomeric Red Fluorescence Protein (APP-mRFP) (Gift from Stephan Kins) in expression vector pcDNA3.1.; or BACE-1-GFP (Gift from Stephanie Miserey Lenkei), using LipofectamineTM 2000. The plasmid transfection was performed as described for N2a cells except that after 3 hours at 37° C in a 5% CO₂, the medium was changed to complete media, with Pen/Strep.

PN were transfected at 7-12 *DIV* when the confluency was about 90%–95% and neurons are completely developed, having somatodendritic polarity and mature synapses (Pravettoni *et al.*, 2000). Cells were transiently transfected with cDNA encoding: mouse brain amphiphysin 2, C-terminal domain of mouse brain amphiphysin 2 in expression vector pRK5-myc or the empty vector pCS2 with GFP using LipofectamineTM 2000 as described for N2a cells.

siRNA transfection

N2a cells and PN were transfected with 10nM of siRNA specific for BIN1 (20uM) (GGA UCU UCG GAC CCU AUC UGt t) and non-targeting control siRNA (10uM) (UUC UCC GAA CGU GUC ACG UTT ACG UGA CAC GUU CGG AGA ATT) (Life Technologies). The amounts and volumes are given on a per well basis. For each siRNA transfection, two separate mixes were prepared, one with 0.25 μ L siRNA against BIN1/ 0.5 μ L non-targeting siRNA in 25 μ L of Opti-MEM medium and the other with 0.8 μ L

LipofectamineTM RNAiMAX transfection reagent (InvitrogenTM, Life technologies) in 25 μL of Opti-MEM medium. Mixes were incubated for 5 min at room temperature and then combined gently and incubated for another 20 min at room temperature. The cell culture media was removed from 24-well plate and 450 μL complete growth medium without Pen/Strep was added. The mixture containing Opti-MEM, LipofectamineTM 2000 and siRNA was then added to each well and incubated with the cells at 37 °C in a 5% CO₂ incubator for 72 h.

4. Fluorescence microscopy

Standard Immunofluorescence

HeLa and N2a cells, after 24 hours of transfection, were washed in phosphate buffered saline (PBS 1X) and fixed in 4% (v/v) paraformaldehyde (Sigma-AldrichTM) in PBS for 20 minutes at room temperature. Thereafter, cells were washed 2 times in PBS (1X) and permeabilized in 0.1% saponin (Sigma-AldrichTM) in PBS 1X for 1 hour at room temperature. Cells were then blocked in 2% FBS in PBS 1X for 1 hour at room temperature. After blocking, cells were incubated for 1 hour at room temperature with primary antibodies in blocking solution. Cells were then washed three times with PBS 1X to remove the excess of primary antibody. Appropriate secondary antibodies diluted in blocking solution were used for 1 hour at room temperature. After washing three times with PBS 1X, coverslips were mounted on slides with Fluoromount-G (SouthernBiotech).

PN immunofluorescence assays were performed as described for N2a and HeLa cells, except the fixation step that was performed in 4% (v/v) paraformaldehyde plus 4% sucrose (Fisher Chemical) diluted in PBS for 20 minutes at room temperature and the blocking step that was done in 2% FBS plus 1% BSA in PBS 1X for 1 hour at room temperature.

Immunofluorescence and pre-permeabilization

HeLa cells, after 24 hours of transfection, were washed in PBS 1X and were pre-permeabilized. As previously reported (Chapuis *et al.*, 2013), cells were incubated for 3 minutes at room temperature in 0.01% saponin (Sigma-AldrichTM) in PBS 1X and after this were permeabilized with 0.25% (v/v) Triton X-100 (Acros Organics) in PBS 1X for 10 min. Thereafter cells were washed 2 times in PBS (1X) and fixed in 4% (v/v) paraformaldehyde for 20 minutes. Then cells were washed in PBS 1X 3 times and were blocked in 1% (w/v) Bovine serum albumin (BSA)(NZYTechTM) in PBS 1X for 1 hour at room temperature. After blocking, the procedure was the same as described in *Standard immunofluorescence*.

Immunofluorescence and Aβ staining

Immunofluorescence assays in N2a cells and PN with the aim of measuring A β 42 were performed as described in *Standard immunofluorescence* with the exception that, after blocking, cells were incubated with primary antibodies in blocking solution overnight at 4°C.

Transferrin uptake

The day after transfection, HeLa cells were placed with DMEM without FBS (starvation) at 37°C for 1h, to improve the uptake of transferrin. Then, cells were placed with Alexa Fluor TM 647-conjugated Human transferrin (Jackson Immunoresearch Lab) (2µl to 500µl DMEM/FBS) for 3 min in DMEM/FBS medium, at 37°C. After this, cells were washed 2 times with PBS 1X and fixed with 4% (v/v) paraformaldehyde for 20 min and washed 3 times with PBS 1X.

Single cell quantitative analysis

Images were acquired on a Leica DMRA2 upright microscope, equipped with a CoolSNAP HQ CCD camera, using the a63x 1.4NA Oil immersion objetive, FITC (519 nm) + CY5 (665 nm) + TRITC (576 nm) fluorescence filtersets and DIC optics, controlled with the MetaMorph V7.5.1/software.

Images were analyzed with Fiji software. To assess the average fluorescence on cell lines, cells were outlined using 'polygon selection' tool. First, the average fluorescence of a region of the background was measured and after this, the average fluorescence of a cell region was quantified with 'Measure' function. The average fluorescence of the background was then subtracted to the average cellular fluorescence. The results were presented in percentage of the average fluorescence of cells expressing GFP or siRNA Control (100%, control).

To assess the average fluorescence on PN, cell body, 2 dendrites and the axon were outlined in FITC channel using 'polygon selection' tool. After this, with 'clear outside' tool it was possible to have just the sections delimitated, without any processes background. Then, using 'Threshold' tool each region was delimitated and selected using 'wand tool'. The selections made on the FITC channel were transferred with 'ROI Manager' tool, to Cy5 or TRITC channel. The average fluorescence of each region was quantified with the 'Measure' tool. The average fluorescence of a region of the background was measured as well and after this, the average fluorescence of the background was subtracted to the average cellular fluorescence measured of each region. The results were presented in percentage of the average fluorescence of cells expressing GFP or siRNA Control (100%, control).

Bin1 colocalization with different organelle markers was analyzed using JaCoP object-based colocalization (plug-in of ImageJ/Fiji). Briefly, epifluorescence images of single cells were analyzed upon background subtraction and threshold to segment Bin1 and organelle objects. Nearest-neighbour distance approach by merging green and red channel centroids was automatically measured by JaCoP. Objects colocalized when the distance between centroids was less than 4 pixels (optical resolution). A colocalization index was obtained by dividing the number of colocalized objects over the total number of Bin1 objects. Fluorescence intensity profile was measured along the line in the merged panels (grey line) (A.U.) using software Fiji.

5. Immunobloting

Preparation of cell lysates

N2a cells and PN after 24h or 72h of DNA or siRNA transfection, respectively, were placed on ice and washed with ice-cold phosphate buffered saline (PBS 1X). Lysis buffer or RIPA buffer (Radio-Immunoprecipitation Assay) was added to cells to enable a rapid and efficient cell *lysis* (75 μ l). RIPA buffer was composed by 50nM Tris-HCl pH 7.4 (Sigma-AldrichTM), 1% NP-40 (Sigma-AldrichTM), 0.25% sodium deoxycholate (Sigma-AldrichTM), 150mM NaCl (NZYTechTM), 1mM EGTA (Sigma-AldrichTM) supplemented with protease inhibitor cocktail (Roche Diagnostics). After RIPA buffer addition, cells were lysed by scraping with a rubber policeman to ensure the complete rupture of cell membranes. Lysates were placed on ice for 15 min and after this were centrifuged for 10 min at 12 000 x g at 4°C. Supernatants were used in the same day on Western blot assays or snap frozen in liquid nitrogen and stored at -80°C.

Western Blot

Proteins from cell lysates were denaturated by the addition of sample buffer (Tris 0.25M pH 6.8, 40% glycerol (Sigma-AldrichTM), 8% sodium dodecyl sulfate (SDS) (Sigma-AldrichTM), Bromophenol blue 0.015% (w/v) (GE Healthcare) and 10% β-mercaptoethanol (Sigma-AldrichTM)) and by heating to 95°C for 5 min. Cells were separated by using Tris-Glycine SDS-PAGE (running buffer: 25 mM Tris, 192 mM glycine (NZYTechTM) and 0.1% (w/v) SDS) at 120 V for 2-3h, using BioRad Mini-PROTEANTM. Electrophoretic transfer (transfer buffer: 150mM glycine, 20mM Tris, 0.037% SDS, 20% (v/v) ethanol 96% (VWR)) to nitrocellulose membranes (0.1mm) (GE Healthcare Life sciences) was performed at 10 V for 1h, using BoltTM Mini Blot Module . Percentage of acrylamide (NZYTechTM) gels varied between 10 or 15% according to the molecular weight of proteins being analysed.

After transfer, membranes were blocked in PBS containing 0.1% (v/v) Tween 20 (PBST) (Sigma-Aldrich[™]) and 5% (w/v) non-fat dry milk for 30 min at room temperature, in order to proteins from milk bind to the membrane in all places where the target proteins have not bound, preventing non-specific antibody binding to the membrane after antibody addition. Incubation with primary antibody diluted in 1% (w/v) nonfat dry milk in PBST was done for 1h at room temperature or overnight at 4°C, always under stirring. Then membranes were rinsed three times with PBST, during 5 min, to remove the non-specifically bound primary antibody. Membranes were incubated with secondary antibody, conjugated to the reporter enzyme Horseradish peroxidase (HRP), in 1% (w/v) diluted in PBST, for 1h at room temperature. Membranes were further rinsed three times with PBST, during 5 min, to remove the non-specifically bound secondary antibody. To detect target proteins, membranes were incubated with equal amounts of luminol and peroxide solution, for 1 min, in a process called enhanced chemiluminescent (AmershamTM ECLTM Prime Western Blotting Detection Reagent, GE Healthcare). Horseradish peroxidase catalyzes the oxidation of luminol, emitting light in the same proportion of protein quantity. The protein immunoreactive bands were visualized by ChemiDoc XRS+ system that offers fast and sensitive chemiluminescence detection. Exposure times varied depending on the target proteins. Analysis of protein band intensities was performed using Image Lab TM software (Bio-Rad) and the band intensities of the proteins of interest were normalized to the corresponding band intensity for α-tubulin.

6. Statistical analysis

Experiments done with sets of neurons prepared from sibling embryos from different mothers were considered independent experiments. Experiments done with cells plated in different days were considered independent experiments. Statistical comparisons of independent experiments were made using t-test or ANOVA with the automated Turkey-Cramer post-hoc tests for multiple comparisons, with significance placed at p < 0.05. Data is presented as mean \pm SEM (standard error of the mean).

III. Results

1. Characterization of Bin1 localization in cell lines and primary neurons

1.1. Distribution of endogenous Bin1 in HeLa cells, N2a cells and primary neurons

In order to characterize the endogenous Bin1 distribution we performed an immunofluorescence assay with non-neuronal (HeLa cells) and neuronal cells (PN and N2a cells).

HeLa cells, N2a and PN were immunolabeled with mouse anti-all Bin1 isoforms and fluorochrome-conjugated secondary antibody anti-mouse. Bin1 fluorescence was distributed broadly in HeLa (Figure III.1a), N2a cells (Figure III.1b), 12 *DIV* PN (Figure III.1c) and 21 *DIV* PN (Figure III.1d) consistent with a cytosolic and membrane associated localization, as previously described in HeLa cells (Leprince *et al.*,2003), in a different type of neuroblastoma cell line (Glennon *et al.*, 2013) and in PN (Di Paolo *et al.*, 2002). In mature neurons (21 *DIV*) Bin1 could be found enriched in puncta (Figure III.1d, arrowheads) consistent with the previously demonstrated localization in pre-synaptic puncta (Di Paolo *et al.*, 2002).

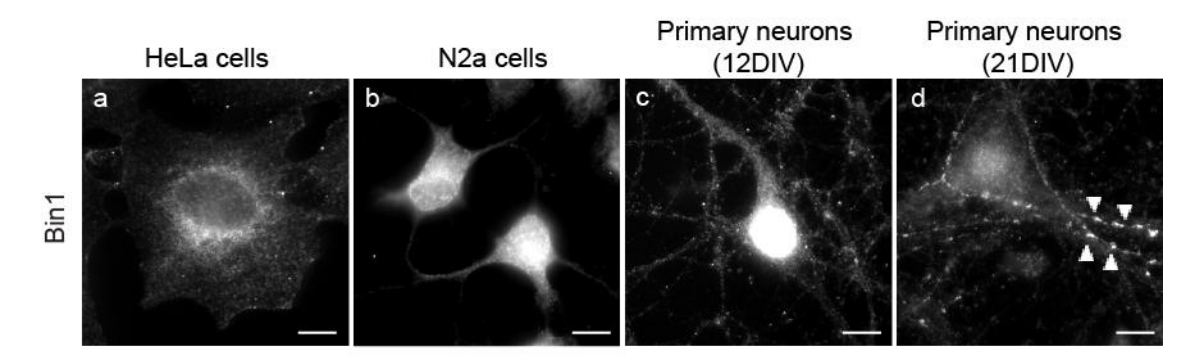


Figure III.1 – Intracellular distribution of endogenous Bin1. Endogenous Bin1 detected by immunolabeling of HeLa cells, N2a cells and PN with anti-Bin1 antibody and Alexa488 anti-mouse secondary. Epifluorescence microscopy images of endogenous Bin1 in HeLa cells (a) (n = 1), N2a cells (b) (n = 2), 12 DIV PN (c) (n = 3) distribution throughout plasma membrane and cytoplasm and 21 DIV PN (d, arrowheads) showed an enriched presynaptic puncta (n = 3). Scale bars, $10\mu m$.

1.2. Distribution of exogenous Bin1 in HeLa cells, N2a cells and primary neurons

Next we investigated the cellular distribution of the neuronal isoform of Bin1 (myc-Bin1) and of its c-terminal domain (myc-Bin1 c-ter) (Figure III.2).

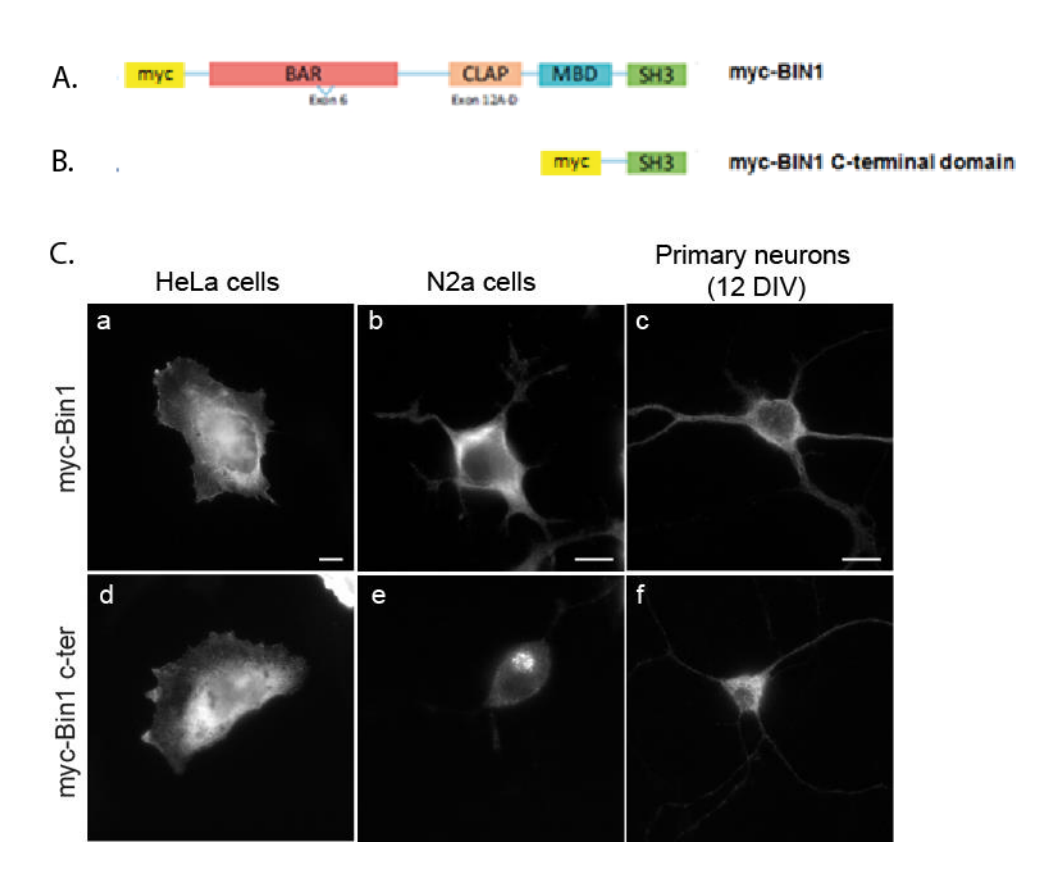


Figure III.2 – Intracellular distribution of exogenous Bin1 and of Bin1 c-terminal domain. A. and B. Scheme of plasmid encoding myc-BIN1, brain-specific isoform with myc tag at N-terminal and of plasmid encoding myc-BIN1 c-ter, the C-terminal region of myc-BIN1, containing only the SH3 domain. Abbreviations: BAR, BIN1/Amphiphysin 2/Rvs; CLAP, Clathrin-AP2 binding region; MBD, Myc-binding domain; SH3, Src homology 3 domain. Image adapted from Tan *et al.*, 2013. **C.** Representative epifluorescence images of HeLa cells (a,d), N2a cells (b,e) and 12 DIV PN (c,f) transiently transfected with myc-BIN1 (a,b,c) and myc-BIN1 c-ter (d,e,f). Upon 24h cells were immunolabeled with anti-myc. myc-Bin1 shows an uniform cellular distribution throughout HeLa cells (a,d) (n = 3), N2a cells (b) (n = 3) and 12 DIV PN (c,f) (n = 3). myc-Bin1 c-ter domain shows a perinuclear concentration consistent in N2a cells (e). Images were processed with software Fiji. Scale bars, 10µm.

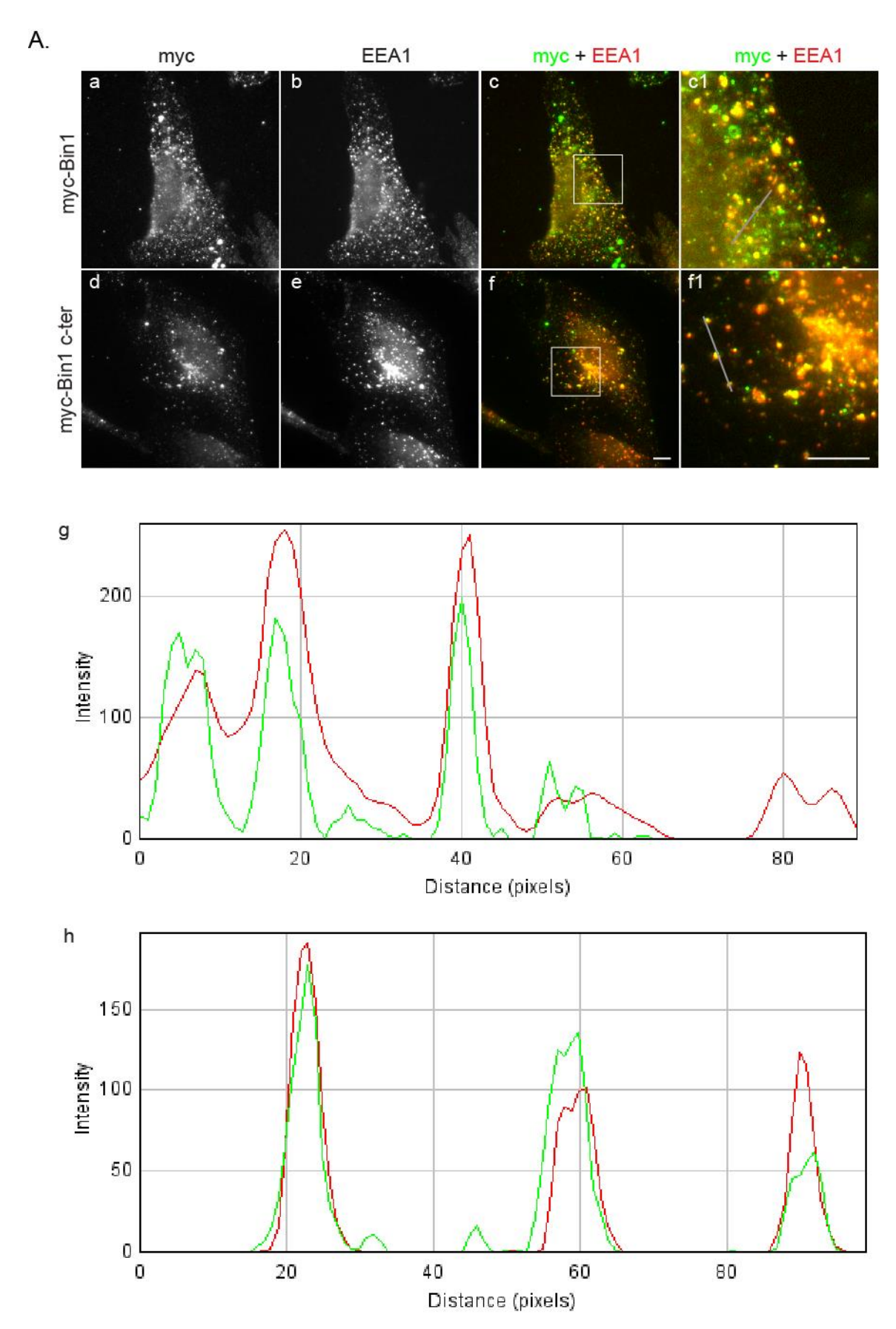
HeLa cells, N2a cells and PN were transiently transfected with plasmids encoding myc-BIN1 and myc-BIN1 c-ter. To detect myc-Bin1 and myc-Bin1 c-ter we performed immunofluorescence with anti-myc primary antibody. Representative images of HeLa cells, N2a cells, and PN expressing myc-Bin1 and myc-Bin1 c-ter are shown in Figure III.2 a-f.

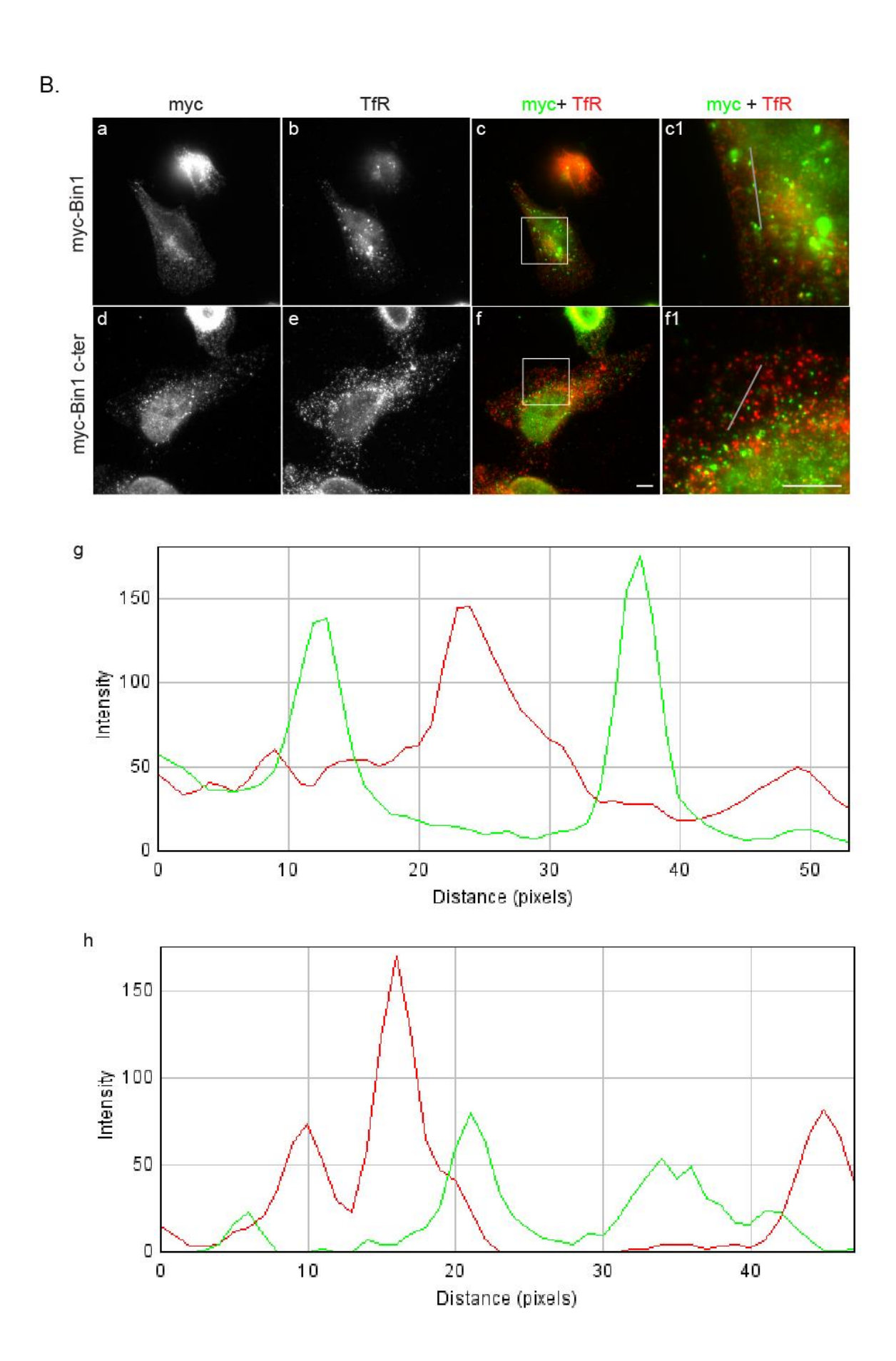
In all panels myc signal shows an uniform cellular distribution similar to endogenous Bin1 (Figure III.1). This uniform distribution of overexpressed Bin1 has been previously reported for HeLa cells and for endogenous Bin1 in PN (Leprince *et al.*, 2003; Di Paolo *et al.*, 2002). In N2a cells, myc-Bin1 c-ter was enriched in the Golgi region (Figure III.2e) suggesting that in these cells the overexpressed c-terminal domain of Bin1 is enriched in perinuclear membrane compartments. In PN we did not observe Bin1 concentration in pre-synaptic puncta probably due to the excess of cytosolic protein or to PN maturation.

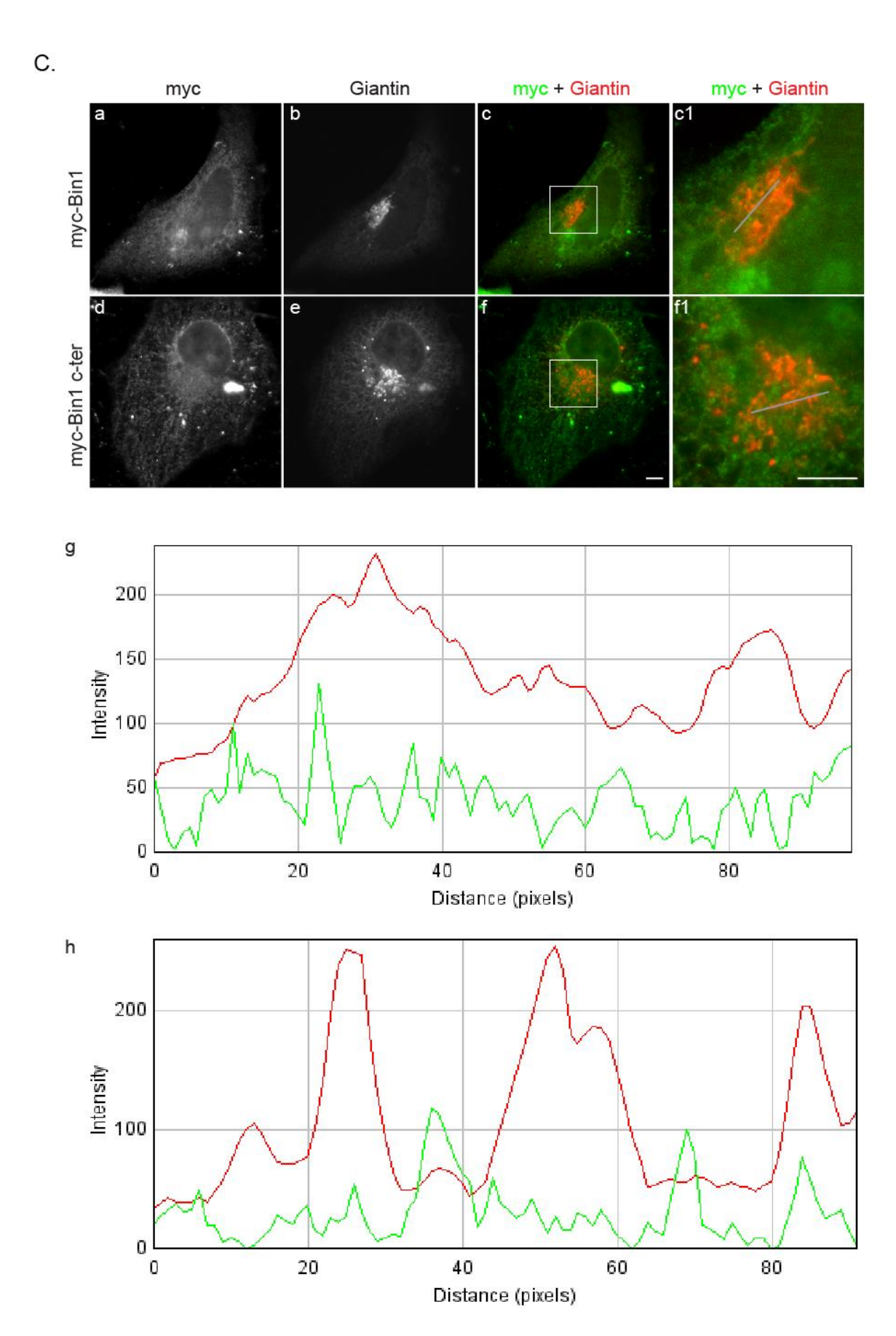
1.3. Subcellular distribution of exogenous Bin1 in HeLa cells

Myc-Bin1 has been previously reported to localize to early endosomes after pre-extraction of the cytosol in HeLa cells (Chapuis *et al.*, 2013; Leprince *et al.*, 2003). To confirm this we expressed myc-BIN1 as well as myc-BIN1 c-ter in HeLa cells and did a pre-extraction by permeabilizing live cells with low concentration of detergent. After fixation, HeLa cells were stained for myc expression with anti-myc and for organelle-specific markers: anti-EEA1, anti-TfR and anti-Giantin primary antibodies to label early endosomes, recycling endosomes and the Golgi apparatus, respectively. These proteins are highly enriched in specific organelles. Thus, by comparing their cellular distribution with that of Bin1, we will get insight onto Bin1 subcellular localization. Early endosomal antigen 1 (EEA1) is a polypeptide required for early endosome fusion (Lawe *et al.*, 2000). Transferrin receptor (TfR) is a protein enriched in recycling endosomes due to its function in binding transferrin (an iron-binding protein) at cell surface. Both transferrin and transferrin receptor enter, by clathrin-mediated endocytosis, inside cell and are trafficked to early endosomes to deliver iron. After this both proteins can be directed to recycling endosomes and further go to cell surface (slow recycling route) or recycle directly from early endosomes to cell surface (fast recycling route) (Mayle *et al.*, 2012). Giantin is a conserved protein localized to the Golgi complex as an integral component of the Golgi membrane (Linstedt and Hauri, 1993).

As shown in Figure III.3, myc, EEA1 and TfR staining exhibited a punctate vesicular distribution and Giantin staining appears consistent with the morphology of the Golgi apparatus. Both myc-Bin1 and myc-Bin1-c-ter puncta often colocalized with EEA1 (Figure III.3A (c1, g) and (f1, h), respectively) but not with TfR (Figure III.3B (c1, g) and (f1, h), respectively) or Giantin (Figure III.3C (c1, g) and (f1, h), respectively). Our observations confirmed the preferential localization of membrane associated Bin1 to early endosomes (Figure III.3D) (Leprince *et al.*, 2003).







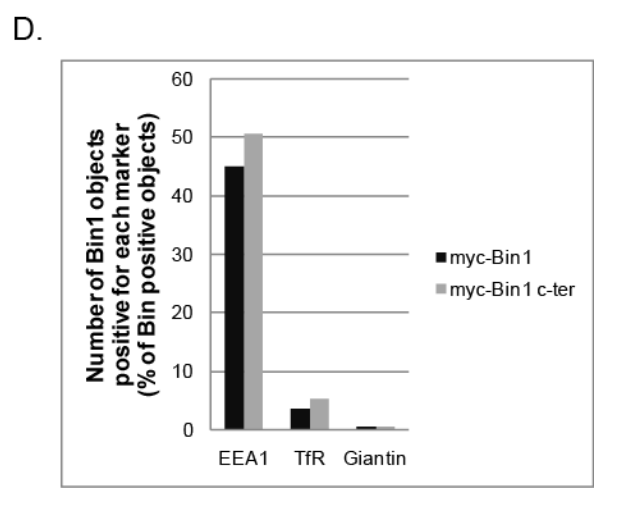
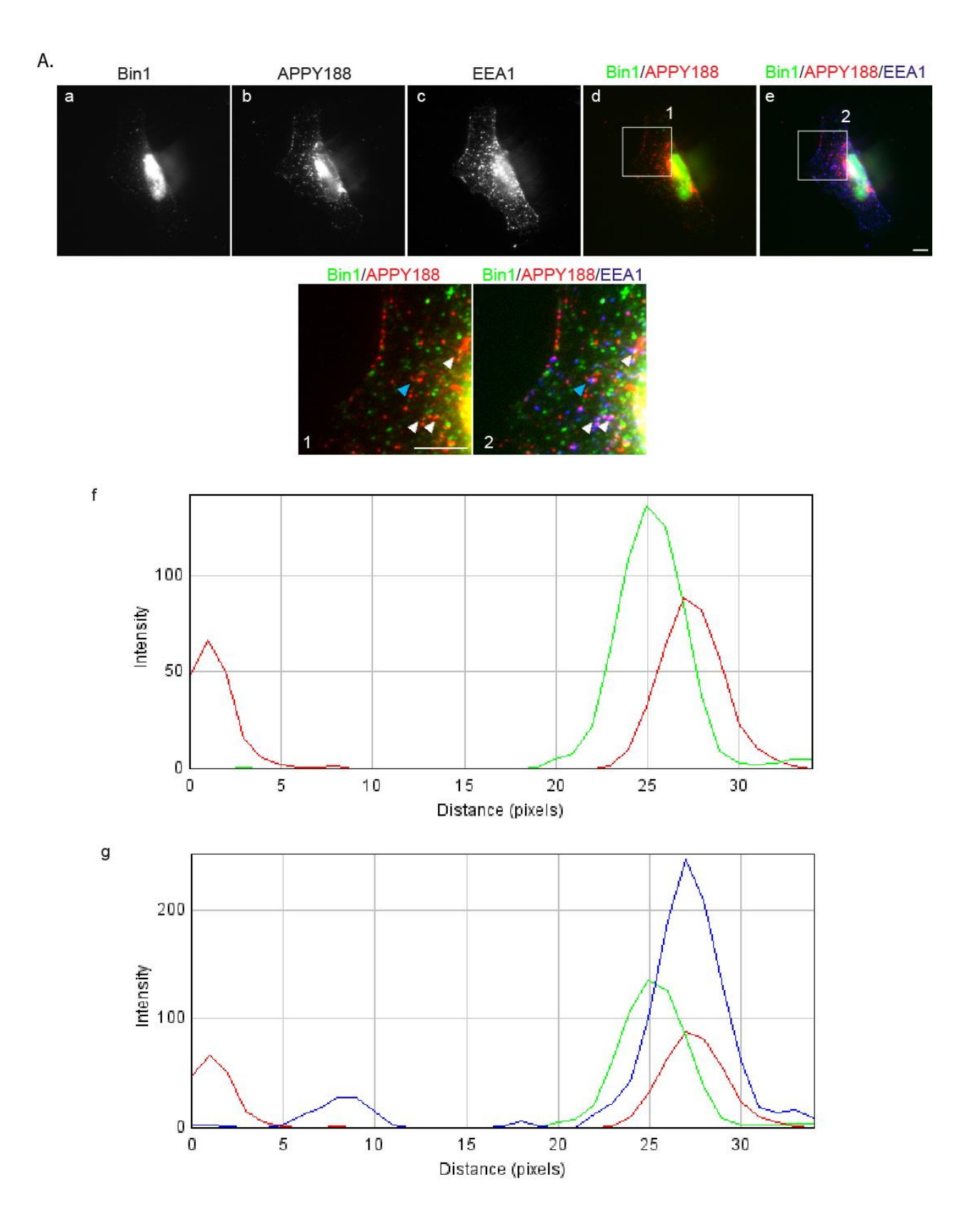


Figure III.3 - Subcellular distribution of exogenous Bin1. Representative epifluorescence images of HeLa cells transfected with myc-BIN1 and myc-BIN1 c-ter, fixed upon 24h, and immunolabeled with different subcellular markers. A. Cells were labeled with anti-myc (a,d) and co-immunostained with anti-EEA1 (b,e). Merged image of Bin1 and Bin1 c-ter (green) with EEA1 (red) (c and f, respectively). White boxes indicate regions magnified in (c1,f1) where colocalization with EEA1 is evident. Fluorescence intensity profile was measured along the line in the merged panels (grey line) (A.U.) to evaluate colocalization between myc-Bin1 (green line) and EEA1 (red line) (g) or myc-Bin1 c-ter (green line) and EEA1 (red line) (h); B. Cells were labeled with anti-myc (a,d) and co-immunostained with anti-TfR (b,e). Merged image of Bin1 and Bin1 c-ter (green) with TfR (red) (c and f, respectively). White boxes indicate regions magnified in (c1,f1) where colocalization with TfR is not evident. Fluorescence intensity profile was measured along the line in the merged panels (grey line) (A.U.) to evaluate colocalization between myc-Bin1 (green line) and TfR (red line) (g) or myc-Bin1 c-ter (green line) and TfR (red line) (h); C. Cells were labeled with anti-myc (a,d) and co-immunostained with anti-Giantin (b,e). Merged image of Bin1 and Bin1 c-ter (green) with Giantin (red) (c and f, respectively). White boxes indicate regions magnified in (c1,f1) where colocalization with Giantin is not evident. Fluorescence intensity profile was measured along the line in the merged panels (grey line) (A.U.) to evaluate colocalization between myc-Bin1 (green line) and Giantin (red line) (g) or myc-Bin1 c-ter (green line) and Giantin (red line) (h); D. Number of Bin1 objects positive for EEA1 show preferential localization of membrane associated Bin1 to early endosomes, (n = 2). Images were processed with Fiji software. Colocalization appears in yellow. Scale bars, 10µm.

Since exogenous Bin1 localized to early endosomes, we next investigated if endogenous Bin1, APP and BACE-1 also localized to early endosomes, in HeLa cells. Upon pre-extraction we detected APP with anti-APPY188 that recognizes APP c-terminal, BACE-1-GFP was detected by GFP fluorescence, endogenous Bin1 was detected with anti-Bin1, and early endosomes with anti-EEA1 (Figure III.4).

As we can observe in Figure III.4, Bin1 colocalizes with APP (Figure III.4A. (d, *inset 1)*; f) and with BACE-1 (Figure III.4B. (d, *inset 1)*; f) in a subset of vesicles. A pool of vesicles positive for APP and Bin1 was also positive for EEA1 (Figure III.4A. (e, *inset 2)*; g). A pool of vesicles positive for BACE-1 and Bin1 was also positive for EEA1 (Figure III.4B. (e, *inset 2)*; g).

Thus, we can speculate that early endosomes may be the common compartment for Bin1, APP and BACE-1 in HeLa cells, like previously proposed (Chia *et al.*, 2013).



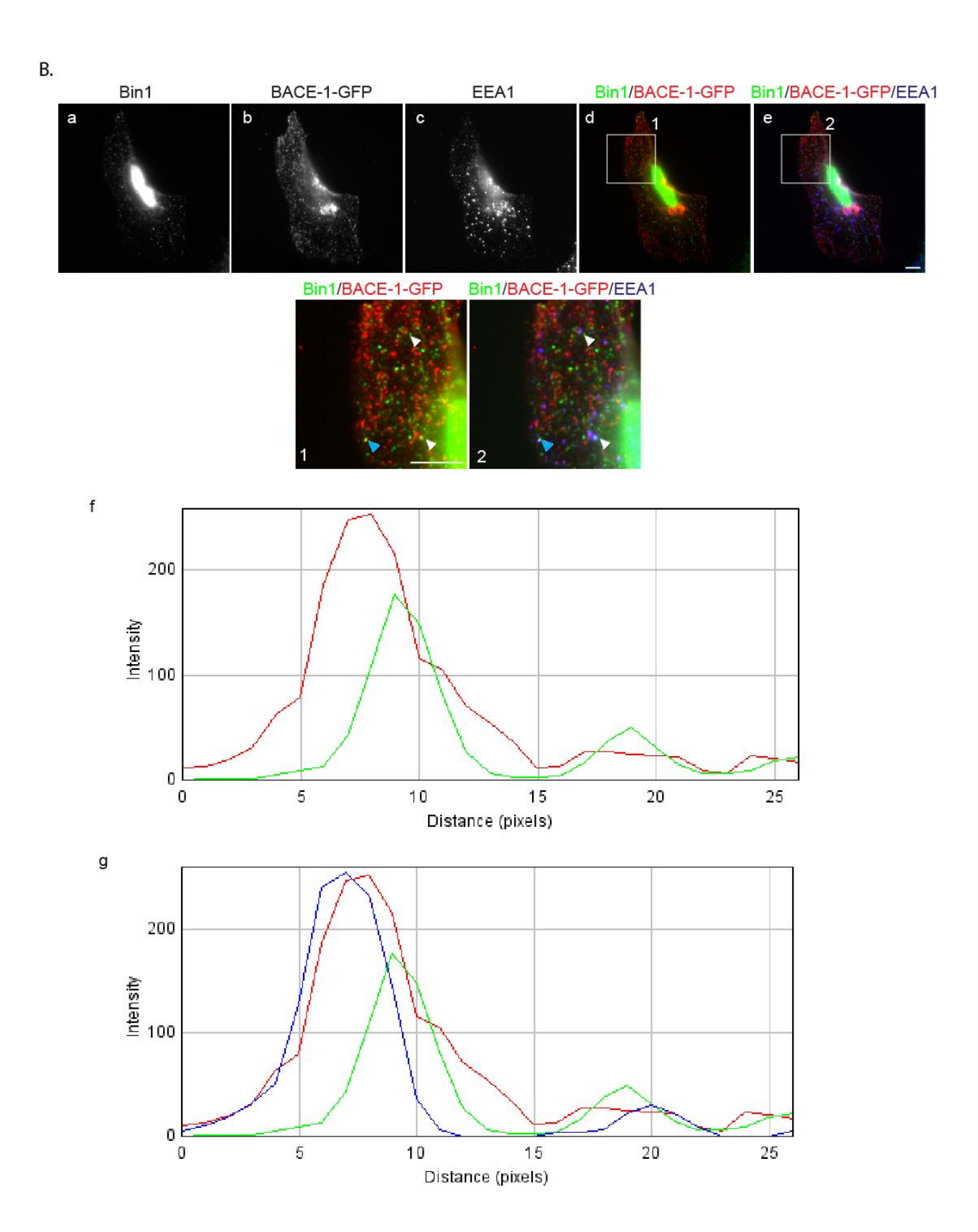


Figure III.4 - A pool of Bin1 can be found associated with APP and BACE-1 in early endosomes. HeLa cells were transiently transfected with BACE-1-GFP for 24h. Representative epifluorescence images of HeLa cells immunostained with: A. anti-Bin1 (a) anti-APPY188 (b) and anti-EEA1 (c). A pool of vesicles positive for Bin1 (green) and APP (red) was observed (d, inset 1, arrowheads). Fluorescence intensity profile was measured along the blue arrowhead in the merged panels (A.U.) (d, inset 1) to evaluate colocalization between Bin1 (green line) and APP (red line) (f). Some early endosomes labeled by EEA1 (blue) are positive for APP (red) and Bin1 (green) (e, inset 2, arrowheads). Fluorescence intensity profile was measured along the blue arrowhead in the merged panels (A.U.) (e, inset 2) to evaluate colocalization between Bin1 (green line), APP (red line) and EEA1 (blue line) (g); B. anti-Bin1 (a), GFP fluorescence (BACE-1-GFP) (b) and anti-EEA1 (c). A pool of vesicles positive for Bin1 (green) and BACE-1 (red) was observed (d, inset 1, arrowheads). Fluorescence intensity profile was measured along the blue arrowhead in the merged panels (A.U.) (d, inset 1) to evaluate colocalization between Bin1 (green line) and BACE-1 (red line) (f). Some vesicles are positive for BACE-1 (green), Bin1 (red) and EEA1 (blue) (e, inset 2, arrowheads). Fluorescence intensity profile was measured along the blue arrowhead in the merged panels (A.U.) (e, inset 2) to evaluate colocalization between Bin1 (green line), BACE-1 (red line) and EEA1 (blue line) (g), (n = 1). White boxes indicate regions magnified in panels 1 and 2. Images were processed with Fiji software. Colocalization appears in yellow (double staining) or white (triple staining). Scale bars, 10µm.

1.4. Subcellular distribution of endogenous Bin1 in primary neurons

To assess the subcellular localization of Bin1 in PN (17 - 21 *DIV*) we performed an immunofluorescence assay with organelle markers. PN were stained for Bin1 and EEA1, Lysosomal-associated membrane protein 1 (LAMP1), or Giantin primary antibodies to label dendritic early endosomes, late endosomes, and Golgi apparatus, respectively (Figure III.5 A-C). As we can observe in Figure III.5, endogenous Bin1 shows some colocalization with EEA1 in the cell body (Figure III.5A (c and c1)). Colocalization was not evident with EEA1 in dendrites neither with LAMP1 or Giantin (Figure III.5B. and C).

It was previously reported that Bin1 was present in the axon initial segment (Butler *et al.*, 1997). Axon initial segments have a cortical cytomatrix containing a neuron-specific isoform of ankyrin 3, ankyrinG (AnkG) (Butler *et al.*, 1997). To confirm the presence of Bin1 in this neuronal structure we stained PN for AnkG. However, as we can observe in Figure III.5D (c and c1), with the anti-Bin1 used we did not detect endogenous Bin1 enriched in AnkG positive axonal initial segment.

Taken together, these results suggest that endogenous Bin1 is mainly present in early endosomes at neuronal cell bodies.

Next we investigated if we could detect APP and A β 42 with Bin1, in PN. PN were stained for Bin1, APP and A β 42 (Figure III.5E and F). No significant colocalization was observed between Bin1 and APP or with A β 42. The lack of colocalization of Bin1 with APP and A β 42 can be explained by previous reports

showing that: 1) Aβ42 has an intracellular distribution in neurons throughout dendrites and axon and is enriched in MVBs (Takahashi *et al.*, 2002; Almeida *et al.*, 2006); 2) APP at steady state is mostly enriched at the Golgi complex and post-Golgi vesicles and much less at early endosomes (Guo *et al.*, 2012), where Bin1 seems to localize. Taken together, these results suggest that a pool of endogenous Bin1 is present in early endosomes at neuronal cell bodies.

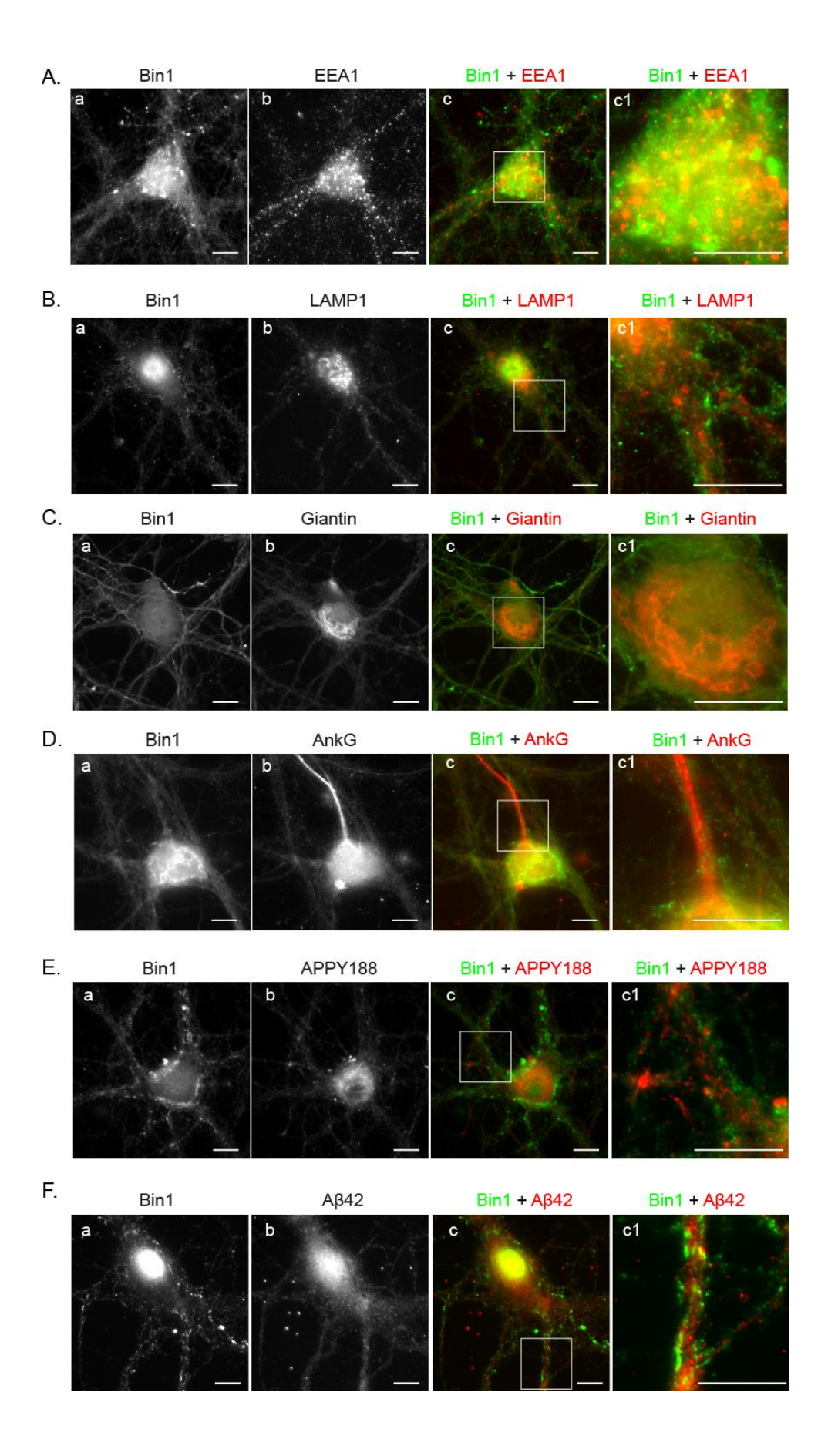


Figure III.5 - Subcellular endogenous Bin1 distribution and colocalization with organelle markers in primary neurons. Representative epifluorescence images of PN (17 - 21 DIV) immunostained with: **A.** anti-Bin1 (a) and anti-EEA1 (b). A partial colocalization of endogenous Bin1 with EEA1 was observed in the cell body (c); **B.** anti-Bin1 (a) and anti-LAMP1 (b); **C.** anti-Bin1 (a) and anti-Giantin (b); **D.** anti-Bin1 (a) and anti-AnkG (b); **E.** anti-Bin1 (a) and anti-APPY188 (b); **F.** anti-Bin1 (a) and anti-Aβ42 (b) (n = 3). All (c) panels are merged images of (a, green) and (b, red), white boxes indicate regions magnified in panels c1. Images were processed with Fiji software. Colocalization appears in yellow. Scale bars, 10μm.

2. Role of Bin1 in APP processing and Aβ42 accumulation

2.1. Effect of Bin1 overexpression on Aβ42 accumulation and APP processing in N2a cells

BIN1 gene was identified as the second most important genetic susceptibility locus in LOAD according to the Alzgene database (http://www.alzgene.org/). It was previously shown that Bin1 has a role in endocytosis (Wigge et~al., 1997; Di Paolo et~al., 2002; Ramjaun et~al., 1997) and that the amyloidogenic processing of APP requires the endocytosis of APP (Cirrito et~al., 2008; Koo and Squazzo, 1994). To determine if Bin1 has a role in A β 42 accumulation we overexpressed myc-Bin1, myc-Bin1 c-ter or GFP, used as control, in N2a cells. Upon 48h of expression we fixed and immunostained the cells with anti-myc and anti-A β 42 (Figure III.6A). In Figure III.6A we can observe the characteristic punctate pattern of A β 42 immunofluorescence in all conditions; interestingly the intensity of A β 42 immunofluorescence was higher in myc-Bin1 (Figure III.6A. (e)) than myc-Bin1 c-ter (Figure III.6A. (f)) expressing cells. Indeed, quantification of A β 42 fluorescence indicates that Bin1 increased A β 42 accumulation by nearly 2.5 fold and Bin1 c-ter alone increased A β 42 by 80%, compared with GFP-control cells. These results indicate that Bin1 overexpression increases A β 42 levels (figure III.6B).

On the amyloidogenic pathway, APP cleavage by β -secretase (BACE-1) results in the formation of β -CTF that is subsequently cleaved by the γ -secretase, leading to the formation of A β peptide (O'Brien and Wong, 2011). To investigate whether the processing of APP is altered by Bin1 we overexpressed myc-Bin1 and myc-Bin1 c-ter in N2a cells and we analyzed the levels of APP and APP CTFs by western blot (Figure III.6C). Myc-Bin1 and myc-Bin1 c-ter overexpression altered the level of APP in the cell lysate. Myc-Bin1 increased APP level by 31% while myc-Bin1 c-ter decreased APP level by 10 % compared to GFP expressing cells (Figure III.6D). APP CTFs were not altered in cells overexpressing myc-Bin1 but increased by 49% in cells overexpressing myc-Bin1 c-ter (Figure III.6D). As a result, the ratio of APP CTFs over APP decreased by 28% in cells overexpressing myc-Bin1 and increased by 66% in cells overexpressing myc-Bin1 c-ter (Figure III.6D). This preliminary result suggests that, in N2a cells, Bin1 controls A β 42 levels by increasing APP levels and not its processing rate. The c-terminal domain of Bin1 alone does not seem to be sufficient to alter APP levels but, on the other hand, it seems to be sufficient to control APP processing.

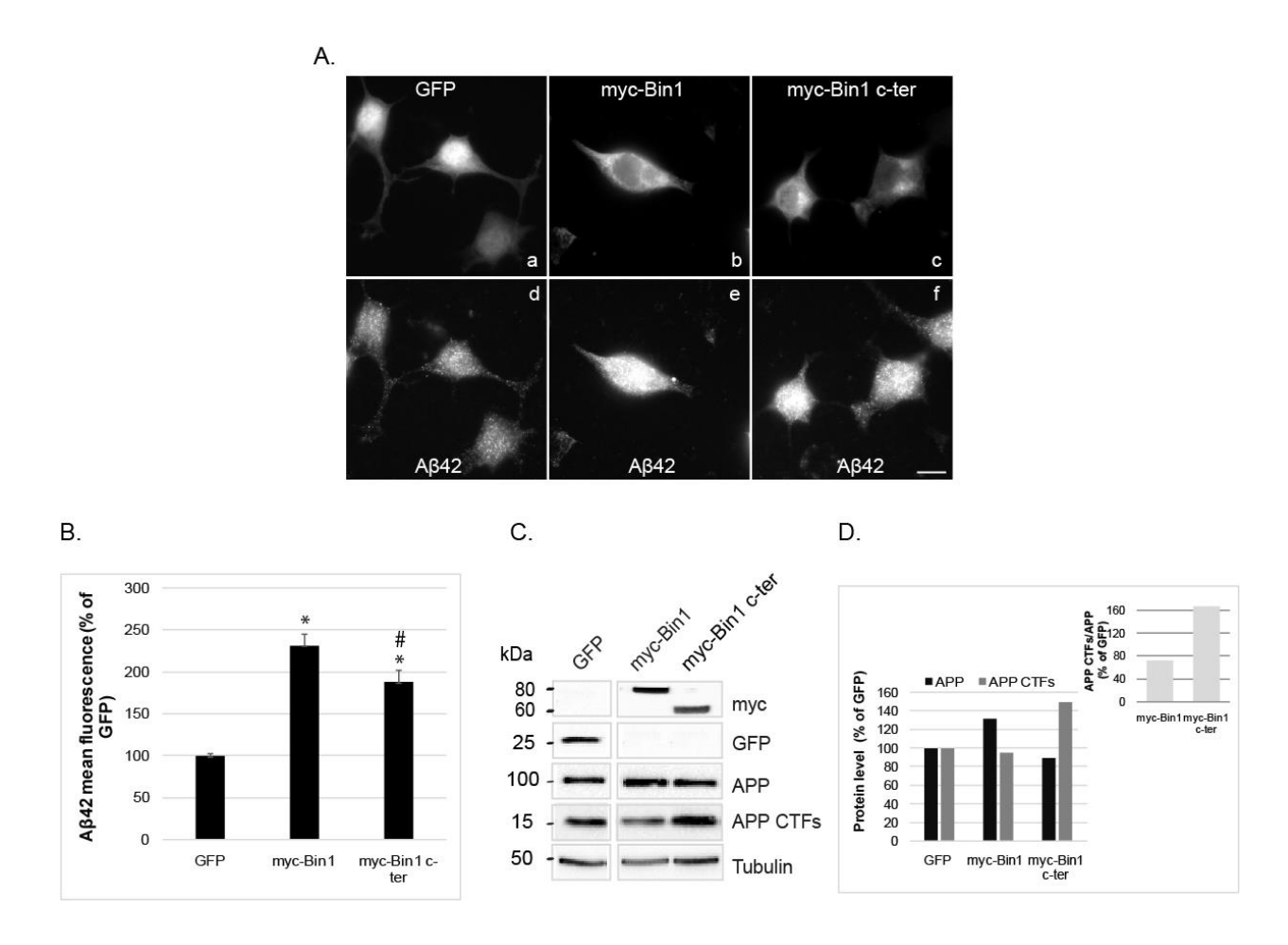


Figure III.6 – Bin1 overexpression impacts Aβ42 accumulation and APP processing in N2a cells. N2a cells were transiently transfected with GFP, myc-BIN1 and myc-BIN1 c-ter for 48h. **A.** Representative epifluorescence images of GFP-expressing N2a cells (a); myc-Bin1-expressing cells immunostained with anti-myc (b); myc-Bin1 c-ter-expressing cells immunostained with anti-myc (c); In the three conditions cells were co-immunostained with anti-Aβ42 (d-f). A punctate pattern of Aβ42 immunofluorescence was observed in GFP, myc-Bin1 and myc-Bin1 c-ter expressing cells. Scale bars, 10 μm. **B.** Quantification of Aβ42 mean fluorescence in GFP-, myc-Bin1- and myc-Bin1 c-ter-expressing cells (115, 76 and 79 cells respectively; n = 3) using software Fiji. Results shown were normalized to Aβ42 mean fluorescence in GFP-expressing cells. Aβ42 levels were increased in cells overexpressing myc-Bin1 (231.9 ± 13.7 %) and in cells overexpressing myc-Bin1 c-ter (187.9 ± 14.6 %). Error bars indicate SEM. * p < 0.01 vs GFP; # p < 0.01 vs myc-Bin1. **C.** Western Blot analysis of cell lysates from N2a cells overexpressing GFP, myc-Bin1 and myc-Bin1 c-ter with antibodies against GFP, myc, APP and α-tubulin. **D.** Quantification of band intensities of APP and APP CTFs of the western blot shown in C, normalized by α-tubulin. The ratio of APP CTFs over APP is also shown (*inserted graph*). The levels of APP and APP CTFs were normalized to the levels measured in GFP-expressing cells. APP CTFs/ APP ratio decreased by 28% in cells overexpressing myc-Bin1 and increased by 66% in cells overexpressing myc-Bin1 c-ter in this preliminary experiment (n = 1).

2.2. Bin1 overexpression, APP processing and Aβ42 accumulation in primary neurons

We have seen that the overexpression of myc-Bin1 and myc-Bin1 c-ter increased A β 42 levels on N2a cells. To assess if this happens in neurons, we overexpressed myc-Bin1, myc-Bin1 c-ter or GFP in 12 *DIV* PN (Figure III.7). Upon 48h of expression we fixed and immunostained the cells with anti-A β 42 (Figure III.7A). In Figure III.7A, we show the A β 42 immunofluorescence in cell bodies, dendrites and axons, identified based on the characteristic neuronal morphology highlighted by the GFP fluorescence or by the myc signal. Similarly to N2a cells, cell bodies of neurons overexpressing myc-Bin1 and myc-Bin1 c-ter had higher levels of A β 42 fluorescence as compared to control. The biggest increased in A β 42 fluorescence was observed in axons of neurons overexpressing myc-Bin1 (32%) and myc-Bin1 c-ter (46%), when compared with GFP-control axons (Figure III.7B.). This higher increase in A β 42 expression in axons is consistent with Bin1 pre-synaptic localization (Di Paolo *et al.*, 2002; Ramjaun *et al.*, 1997). Since Bin1 and Bin1 c-ter similarly changed A β 42 accumulation, it is likely that the c-terminal domain of Bin1 is sufficient to alter A β 42 levels in PN. Together, the results obtained in N2a cells and in PN indicate that Bin1 regulates A β 42 accumulation.

Next we investigated the impact of overexpression of myc-Bin1 and myc-Bin1 c-ter in processing of APP in 12 *DIV* PN. For that, we measured the levels of APP and APP CTFs by western blot and we calculated the ratio of APP CTFs over APP (Figure III.7C and D). Myc-Bin1 and myc-Bin1 c-ter overexpression altered the level of APP in neurons. Myc-Bin1 increased APP level by nearly 4.5 fold and myc-Bin1 c-ter by 4 fold compared to GFP expressing cells (Figure III.7D). APP CTFs levels increased by 13% in cells overexpressing myc-Bin1 and by 28% in cells overexpressing myc-Bin1 c-ter (Figure III.7D). As a result, we can observe a decrease by 74% of APP CTFs/APP ration in cells overexpressing myc-Bin1 and 69% of APP CTFs/APP ration in cells overexpressing myc-Bin1 c-ter (Figure III.7D). This preliminary experiment is consistent with the fact that Bin1, via its c-terminal domain, has a major effect on APP levels and a smaller effect in APP processing, thus potentially explaining the increased Aβ42 levels shown in Figure III.7A.

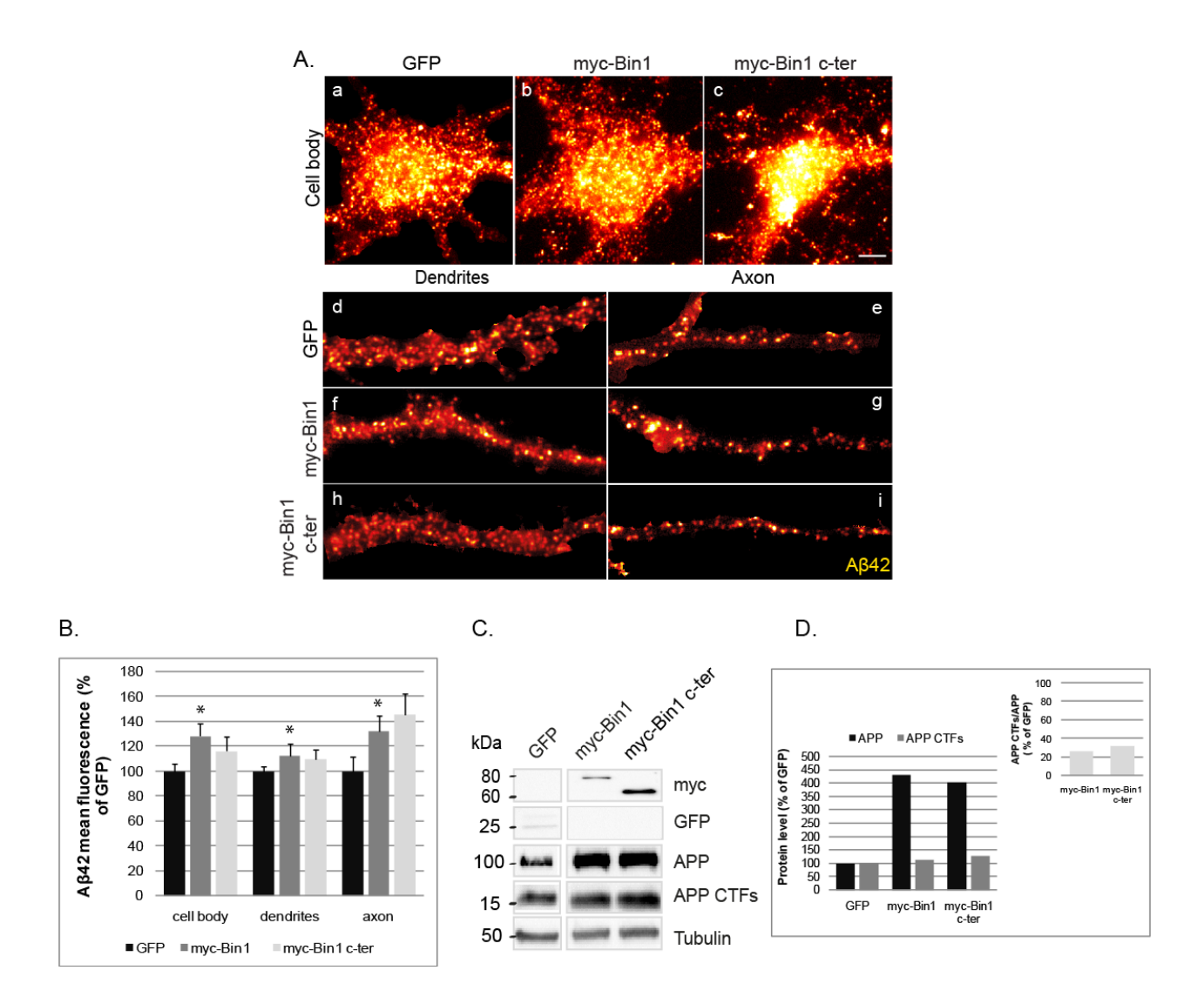


Figure III.7 - Myc-Bin1 and myc-Bin1 c-ter overexpression increase Aβ42 accumulation and alter APP processing in primary neurons. PN were transiently transfected with GFP, myc-BIN1 and myc-BIN1 c-ter for 48h. A. Representative epifluorescence images of 12 DIV PN cell bodies, dendrites and axons expressing: GFP (a, d, e); myc-Bin1 (b, f, g); myc-Bin1 c-ter (c, h, i) not shown; In the three condition cells were immunostained with anti-Aβ42 (a-i). A punctate pattern of Aβ42 immunofluorescence was observed in the GFP, myc-Bin1 and myc-Bin1 c-ter expressing cells. Scale bars, 10μm. B. Quantification of Aβ42 mean fluorescence in GFP-, myc-Bin1- and myc-Bin1 c-ter- expressing cells (52, 34 and 10 cells respectively; n = 3) using software Fiji. Results shown were normalized to Aβ42 mean fluorescence in GFP-expressing cells. In cells overexpressing myc-Bin1 and myc-Bin1 c-ter, Aβ42 levels were increased (128.2 ± 10.4 %) and (116.2 ± 11.6 %), respectively, in cell body; (112.3 ± 9.5 %) and (109.3 ± 8.0 %), respectively, in dendrites; (131.8 ± 12.7 %) and (145.7 ± 16.3 %), respectively, in axon, compared with GFP-control PN. Error bars indicate SEM. * p < 0.01 vs GFP. C. Western blot analysis of cell lysates from 12 DIV PN overexpressing GFP, myc-Bin1 and myc-Bin1 c-ter with antibodies against GFP, myc, APP and α-tubulin. D. Quantification of band intensities of APP and APP CTFs normalized by total α-tubulin. The ratio of APP CTFs over APP is also shown (*inserted graph*). The levels of APP and APP CTFs were normalized to the levels measured in

GFP-expressing cells. APP CTFs/APP ratio decreased by 74% in cells overexpressing myc-Bin1 and 69% in cells overexpressing myc-Bin1 c-ter (n = 1).

2.3. The effect of Bin1 downregulation on Aβ42 accumulation in N2a cells

Double-stranded RNA-mediated interference (RNAi) is a method that is known to provide the knockdown expression of a target gene and an important tool for gene-specific therapeutic activities that target the mRNAs of disease-related genes (Agrawal *et al.*, 2003). To confirm the results of Bin1 overexpression on A β 42 accumulation, the opposite experiment was performed in which endogenous Bin1 expression was knocked down by Bin1 siRNA treatment of N2a cells for 72 h.

Quantitative immunoblotting was used to evaluate the efficiency of Bin1 downregulation in N2a cells treated with Bin1 siRNA. Bin1 western blot revealed multiple bands; three bands around 75 kDa are shown in Figure III.8A. Bin1 has several isoforms as a result of alternative splicing. In neurons mainly two isoforms have been described, a neuronal isoform at 80 kDa (isoform 1, Figure III.8A) and Bin ubiquitous isoform at 60 kDa (isoform 9, Figure III.8A) (Holler *et al.*, 2014). The upper band is likely non-specific since its intensity was not altered by the Bin1 siRNA treatment. The other two bands most likely correspond to the neuronal and the ubiquitous isoform since they virtually disappear upon Bin1 siRNA treatment (Figure III.8A). Bin1 knockdown cells showed a decrease of Bin1 neuronal isoform (80 kDa) of 83% and of Bin1 ubiquitous isoform (60 kDa) of 66% compared to non-targeting siRNA control (Figure III.8B). This level of Bin1 depletion confirms the downregulation efficiency of the treatment with Bin1 siRNA.

Next, we assessed the impact of Bin1 knockdown on A β 42 accumulation by immunofluorescence with anti-A β 42 (Figure III.8C) and anti-Bin1 (not shown). As shown in Figure III.8C, we can observe that the punctate pattern of A β 42 immunofluorescence is brighter in siRNA Bin1-treated N2a cells compared with siRNA control-treated N2a cells. We did not observe a decrease in Bin1 immunofluorescence upon treatment with siRNA (data not shown). On average, A β 42 fluorescence increased significantly by 35% in siRNA Bin1-treated N2a cells compared with siRNA control-treated N2a cells (Figure III.8D).

Overall these results suggest a correlation between the increase of A β 42 expression levels and the downregulation of Bin1.

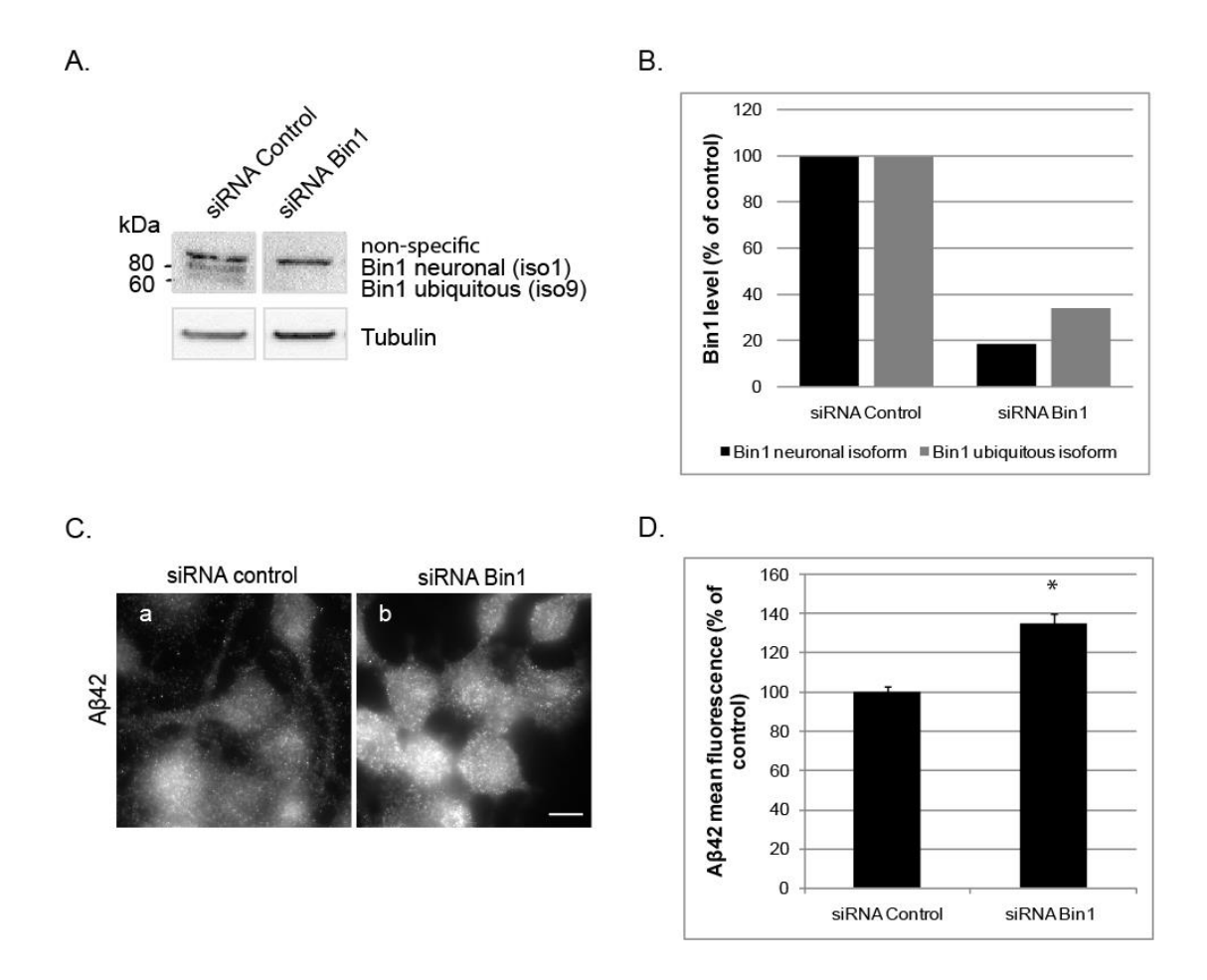


Figure III.8 - Bin1 downregulation increases Aβ42 accumulation in N2a cells. N2a cells were transiently transfected with non-targeting siRNA control and siRNA against Bin1 for 72h. **A.** Western Blot analysis of cell lysates from N2a cells transfected with siRNA against Bin1 and non-targeting siRNA control with antibodies against Bin1 and α-tubulin. **B.** Quantification of band intensities of total Bin1 neuronal and ubiquitous isoforms, normalized by total α-tubulin. The levels of Bin1 neuronal and ubiquitous isoforms were normalized to the levels measured in non-targeting siRNA control cells. Bin1 neuronal and ubiquitous isoform decreased by 83% and 66% comparing to control cells (n = 1). **C.** Representative epifluorescence images of N2a cells treated with siRNA control (a) and siRNA Bin1 (b); cells were immunostained with anti-Aβ42 (a,b). The punctate pattern of Aβ42 immunofluorescence was observed increased in Bin1 siRNA treated cells compared to control siRNA treated cells. Images were processed with Fiji software. Scale bars, 10μm. **D.** Quantification of Aβ42 mean fluorescence in control and Bin1 siRNA treated cells (202 and 165 cells, respectively; n = 3) using software Fiji. Aβ42 mean fluorescence increased in Bin1 siRNA treated cells (134.9 ± 4.9 %) compared to in control siRNA treated cells. Error bars indicate SEM. * p < 0.01 vs siRNA control. Results were normalized to Aβ42 mean fluorescence in non-targeting siRNA control cells.

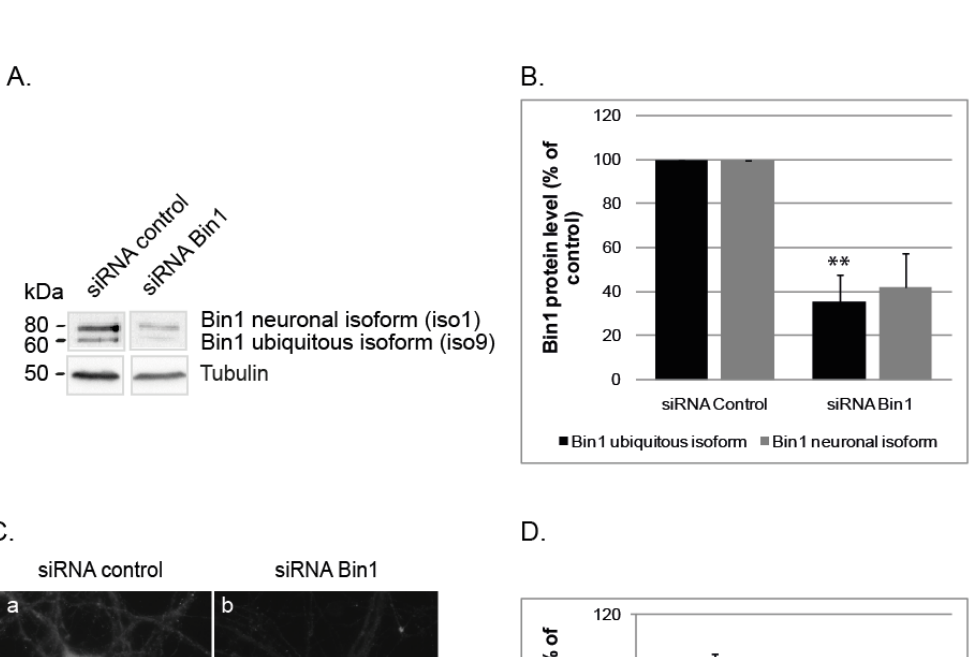
2.4. Bin1 downregulation, APP processing and Aβ42 accumulation in primary neurons

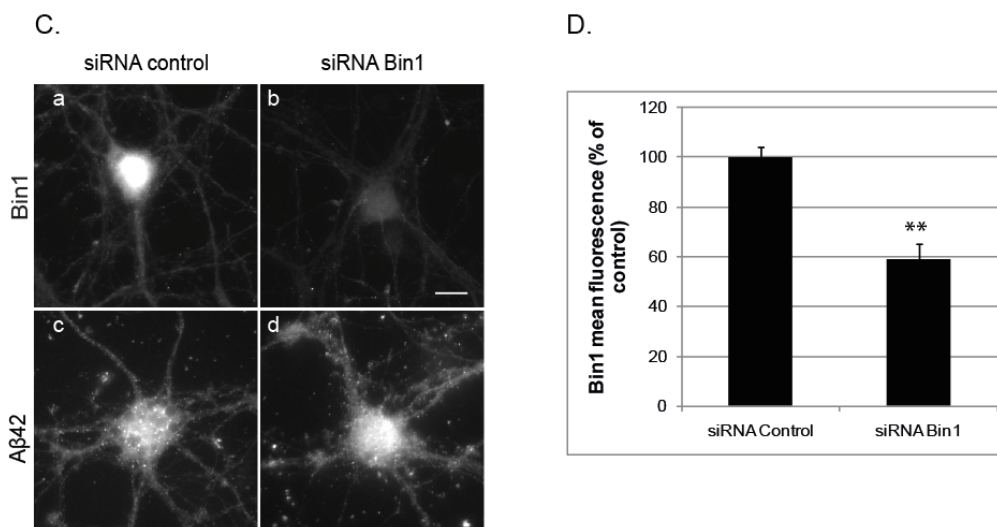
To assess the effect of Bin1 downregulation on Aβ42 accumulation and APP processing in neurons, we treated PN with Bin1 siRNA and control siRNA for 72 h. Quantitative immunoblotting was used to evaluate the efficiency of Bin1 downregulation (Figure III.9A). Western blot with anti-Bin1 showed a two bands pattern for Bin1, corresponding to Bin1 neuronal (iso1; 80 kDa) and ubiquitous (iso9; 60 kDa) spliced isoforms as described for N2a cells (Figure III.8) and previously reported (Holler *et al.*, 2014). Bin1 knockdown caused a decrease of protein level in PN treated with siRNA against Bin1 compared to a non-targeting siRNA control. Bin1 neuronal isoform decreased by 58% and Bin1 ubiquitous isoform protein level decreased by 65% compared to non-targeting siRNA control (Figure III.9A and B).The evident decrease of Bin1 protein confirms the downregulation efficiency in PN.

The levels of Bin1 and A β 42 were analyzed by immunofluorescence upon Bin1 siRNA treatment (Figure III.9C). As shown in Figure III.9C., fluorescence microscopy revealed that knockdown expression of Bin1 reduces the level of Bin1 staining, compared to a siRNA control (Figure III.9C (a,b)). Indeed, Bin1 mean fluorescence decreased by 42% in the cell body of Bin1 knockdown cells comparing to siRNA control, (Figure III.9D). In Figure III.9C (c,d) we can detect that the characteristic punctate pattern of A β 42 immunofluorescence was brighter in Bin1 knockdown cells compared to control. Indeed, A β 42 fluorescence increased by 25% in the cell body of Bin1 knockdown comparing to non-targeting siRNA control cells (Figure III.9E). These results indicate a correlation between the increase of A β 42 levels with decrease of Bin1 levels in PN.

To investigate whether knockdown of Bin1 affects APP processing we measured the levels of APP, APP CTFs and the ratio of APP CTFs over APP in PN, by western blot (Figure III.9F and G). In Bin1 knockdown cells there was a tendency for a decrease in the level of APP in cell lysate. In contrast, we observed a significant increase in the level of CTFs of 47%, compared to non-targeted siRNA control cells (Figure III.9G). As a result, we can observe an increase of 89% in the APP CTFs/APP ratio in Bin1 knockdown cells compared to non-targeted siRNA control cells (Figure III.9G, *inserted graph*).

These data suggests that Bin1 downregulation mainly increases APP processing thus explaining the increase in Aβ42 levels.





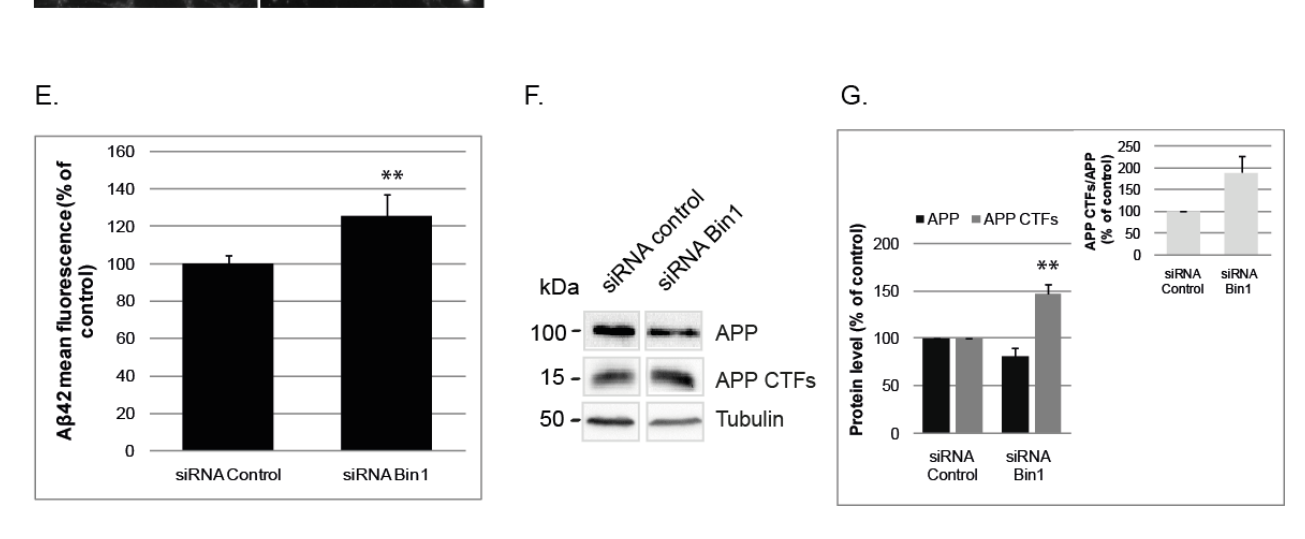


Figure III.9 - Bin1 downregulation increases Aβ42 accumulation and alters APP processing in primary neurons. Primary neurons 12 DIV were transiently transfected with non-targeting siRNA control and siRNA against Bin1 for 72h. A. Western Blot analysis of cell lysates from PN transfected with siRNA against Bin1 and non-targeting siRNA control with antibodies against Bin1 and α-tubulin. B. Quantification of band intensities of Bin1 neuronal and ubiquitous isoform normalized by total α-tubulin. The levels of Bin1 neuronal and ubiquitous isoform were normalized to the levels measured in non-targeting siRNA control cells. Bin1 neuronal and ubiquitous isoform decreased by 58% and 65%, respectively (n = 3). ** p < 0.05 vs siRNA control. **C.** Representative epifluorescence images of knockdown with siRNA control (a) and siRNA Bin1 (b); Cells were immunostained with anti-Bin1 (a,b) and anti-Aβ42 (c,d). Bin1 knockdown cells showed a decrease in Bin1 fluorescence (a,b). The punctate pattern of Aβ42 immunofluorescence was observed increased in the control and Bin1 knockdown cells (c,d). D. Quantification of Bin1 mean fluorescence in the cell bodies of siRNA control and Bin1 knockdown cells (35 and 40 cells, respectively; n = 3) using software Fiji. Results shown were normalized to Bin1 mean fluorescence in control cells. Bin1 levels were decreased (58.8 ± 6.3 %) compared to control cells. ** p < 0.05 vs siRNA control. E. Quantification of Aβ42 mean fluorescence in non-targeting siRNA control and Bin1 knockdown cells (31 and 27 cells, respectively; n = 3) using software Fiji. Results shown were normalized to Aβ42 mean fluorescence in control cells. Aβ42 levels were increased in Bin1 knockdown cells (125.5 ± 11.5 %) compared to control cells. Error bars indicate SEM. ** p < 0.05 vs siRNA control. F. Western blot analysis of cell lysates from 12 DIV PN knockdown with non-targeting siRNA control and siRNA against Bin1 with antibodies against APP and α-tubulin. G. Quantification of band intensities of APP and APP CTFs normalized by total α-tubulin. The ratio of APP CTFs over APP is also shown. The levels of APP, APP CTFs and APP CTFs/APP were normalized to the levels measured in non-targeting siRNA control cells. Bin1 knockdown cells showed an increase by 47 % in APP CTFs compared to non-targeted siRNA control cells. ** p < 0.05 vs siRNA control. APP CTFs/ APP ratio increase by 89% in Bin1 knockdown cells compared to non-targeted siRNA control cells (n = 3). Scale bars, 10 μ m.

3. Role of Bin1 in APP and BACE-1 distribution

3.1. Bin1 overexpression effect on APP distribution

After synthesis in the ER, APP matures at the TGN and traffics through the secretory pathway to the plasma membrane. Upon endocytosis or directly from the TGN (at least in HeLa cells) APP is delivered to endosomes, where it can be processed or eventually be degraded in lysosomes. In spite of APP complex intracellular itineraries its steady-state distribution includes the Golgi complex and endosomes (Caporaso *et al.*, 1994; Haass *et al.*, 1992).

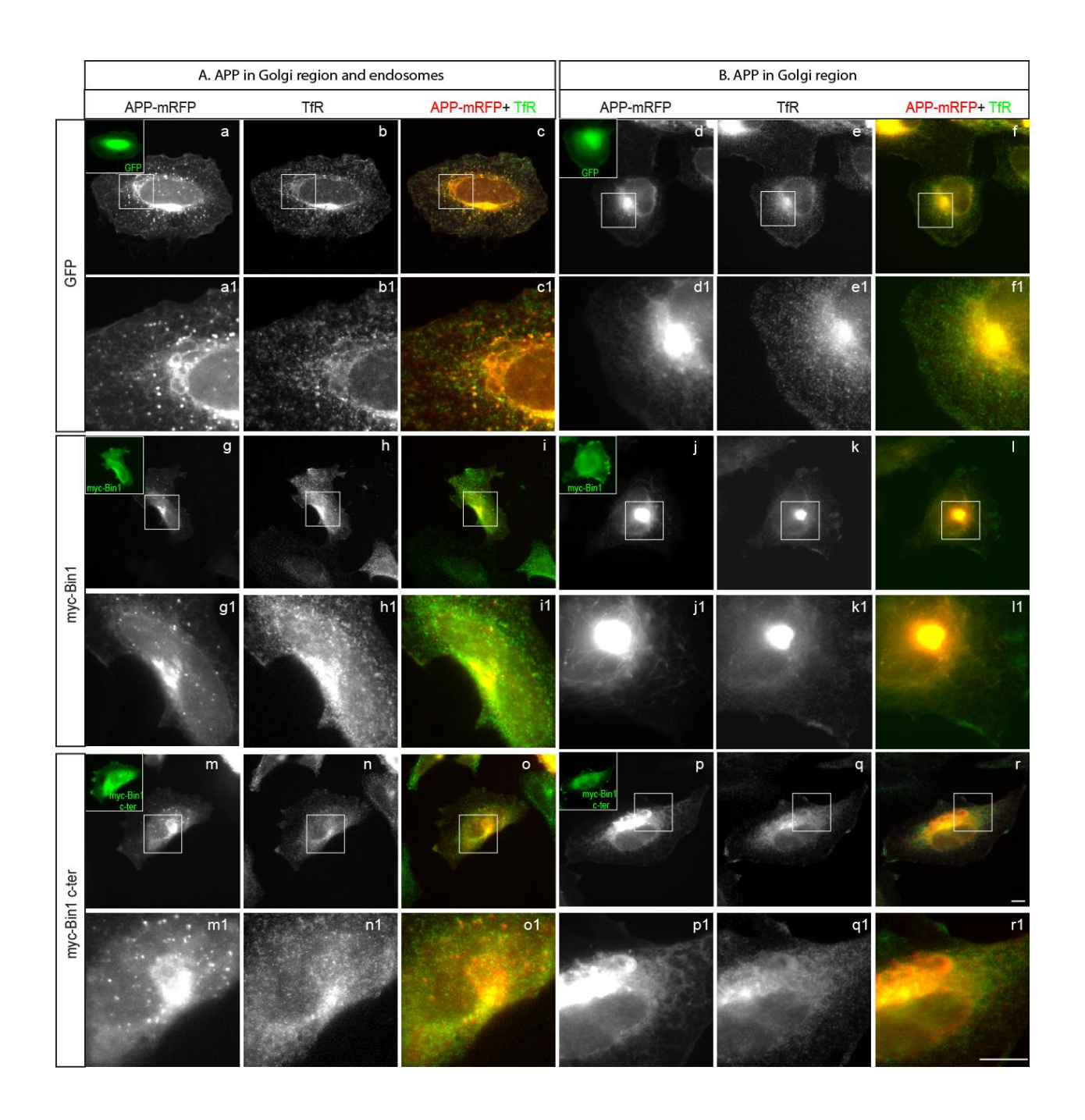
In order to identify the role of Bin1 as a regulator of APP trafficking we studied the impact of overexpressing Bin1 on APP steady-state distribution.

We decided to first study the distribution of APP tagged with APP-mRFP since it has a distribution similar to endogenous APP although its presence in endosomes is more prominent. Upon 24h of co-

expression with myc-Bin1, myc-Bin1 c-ter or GFP (control) cells were fixed and immunostained with antimyc to label Bin1 and Bin1 c-ter and with anti-TfR to label recycling endosomes (Figure III.10).

As we can notice in Figure III.10, the overexpression of myc-Bin1 and myc-Bin1 c-ter altered APP-mRFP distribution. In GFP-expressing cells, two different distributions of APP-mRFP were observed: 1) APP was enriched in the Golgi region and in recycling endosomes, identified by the presence of TfR (Figure III.10A. (a-c)); 2) APP mainly localized to the Golgi region (Figure III.10B. (d-f)).

Bin1 and Bin1-c ter overexpression increased the number of cells with APP enriched in the Golgi region (Figure III.10B. (j - r) and C.). The Bin1 c-ter effect on APP distribution was less pronounced. Bin1 similarly affected the distribution of TfR. In addition, often cells overexpressing Bin1 showed the presence of tubules likely emanating from the Golgi (Figure III.10B. (j, p)). Bin1 has a BAR domain and the capacity of inducing membrane tubules (Meunier *et al.*, 2009). We can propose that, in HeLa cells, Bin1 could be functioning at early endosomes to enhance recycling to the TGN by facilitating the formation of endosomal recycling tubular carriers. The tubulating potential of Bin1 could have a role in APP intracellular trafficking and distribution throughout HeLa cells.



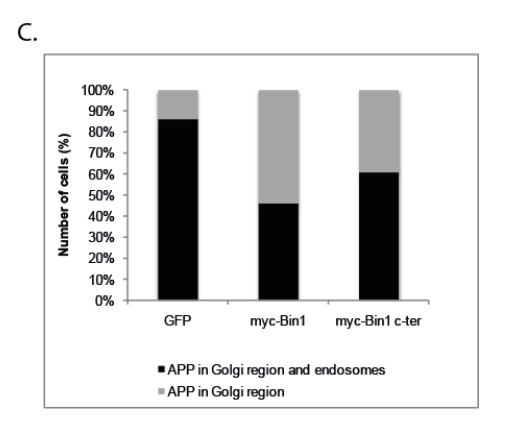
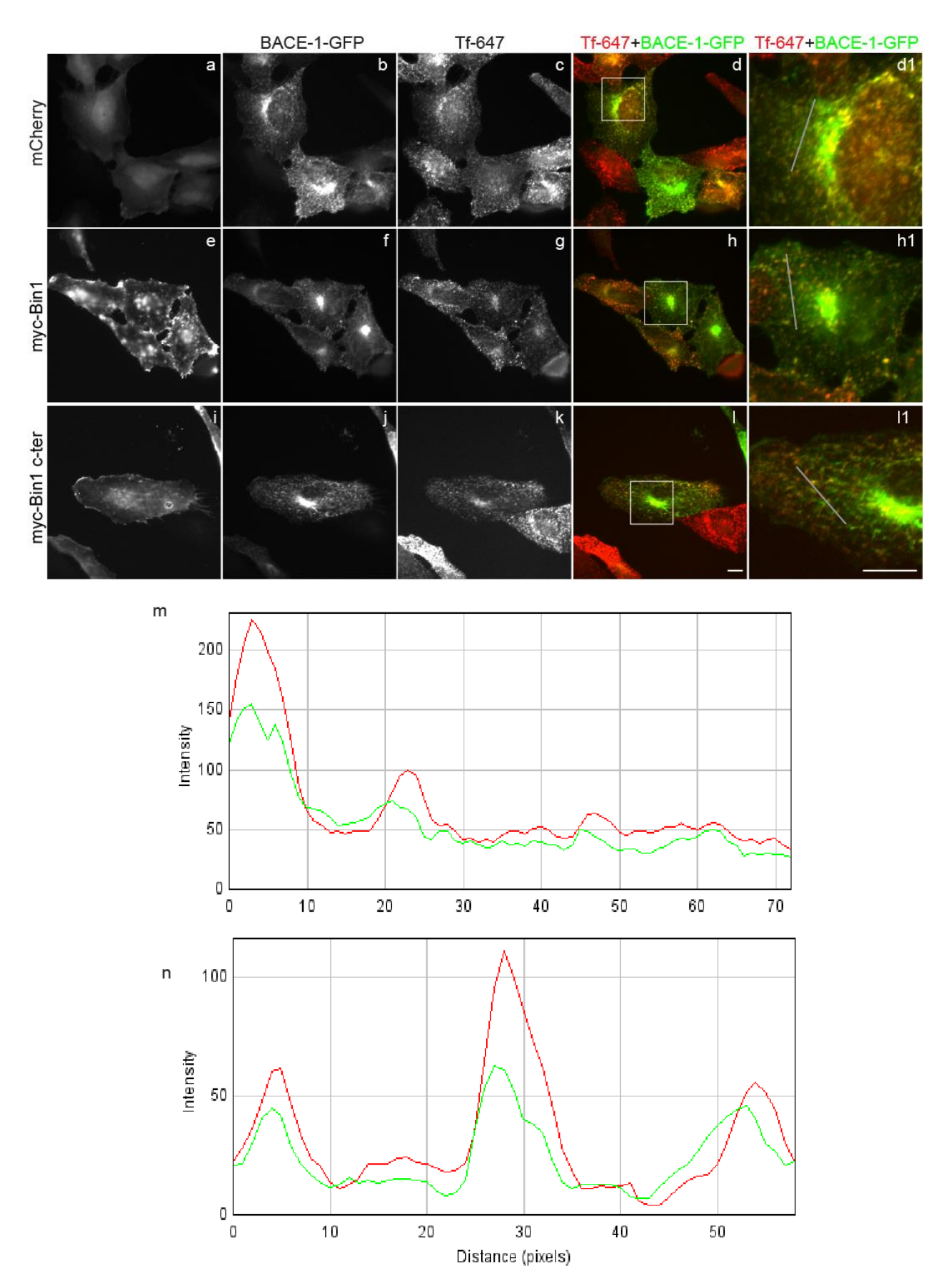


Figure III.10 – Myc-Bin1 and myc-Bin1 c-ter overexpression has an effect on APP distribution. HeLa cells were transiently transfected with GFP, myc-BIN1, myc-BIN1 c-ter and APP-mRFP for 24h. Representative epifluorescence images of HeLa cells expressing APP-mRFP (a, d, g, j, m, p) and GFP (*inset* in panel a and d; green); myc-Bin1 immunostained with anti-myc (*inset* in panel g and j; green); myc-Bin1 c-ter immunostained with anti-myc (*inset* in panel m and p; green). In the three conditions cells were co-immunostained with anti-TfR (b, h, n, e, k, q). The two different phenotypes observed for APP distribution are shown: (A) APP localized to Golgi region and endosomes or (B) APP localized to Golgi region only. Cells overexpressing myc-Bin1 and myc-Bin1 c-ter showed APP tubules (B. (j,p)) that seem to retain both APP and TfR, depleting APP and TfR in endosomes (B.(i, l, o,r)). GFP expressing cells showed colocalization between APP and TfR in endosomes and Golgi region (A. (c, f)) (n = 1). Images were acquired on epifluorescence microscope and processed using Fiji software. White boxes indicated magnified regions shown in panels a1- r1. Colocalization appears in yellow. Scale bar, 10μm.C. Quantification of the number of cells expressing GFP, myc-Bin1 and myc-Bin1 c-ter that contain APP-mRFP in Golgi region and endosomes or just in Golgi region. Results are shown in percentage of total number of cells analyzed (n=1, 57 cells were analyzed).

3.2. Effect of Bin1 overexpression on BACE-1 distribution

It was reported that BACE-1 distribution is spread throughout HeLa cells but with a higher concentration near perinuclear region, in the perinuclear recycling endosome also known as ERC. Although some studies reported that BACE-1 may recycle from early endosomes to TGN (Wahle *et al.*, 2005), it was shown that the staining pattern of BACE-1, at steady state, extensively overlaps with early and recycling endosome markers and less with Golgi or TGN markers (Chia *et al.*, 2013). To determine the effect of Bin1 overexpression on the intracellular distribution of BACE-1 we examined the steady-state distribution of BACE-1-GFP upon overexpression of myc-Bin1, myc-Bin1 c-ter, and mCherry (monomeric red fluorescent protein), as control, upon 24h of expression in HeLa cells. The recycling endosomes were labeled by Transferrin-647 (Tf-647) uptake. Upon transferrin uptake, BACE-1-GFP colocalized significantly with Tf-647 in control, myc-Bin1 and myc-Bin1 c-ter overexpressing cells. As we can observe in Figure III.11, overexpression of myc-Bin1 and myc-Bin1 c-ter did not alter distribution of BACE-1-GFP as strongly as we observed for APP-mRFP. In this preliminary experiment the levels of BACE-1-GFP and Tf-647 seemed slightly higher in the ERC than in peripheral recycling endosomes, where the fluorescence intensity profiles of mCherry, myc-Bin1 and myc-Bin1 c-ter expressing cells (Figure III.11 (m,n,o), respectively) to evaluate colocalization between Tf-647 and BACE-1-GFP were similar.

It was suggested that BACE-1 and TfR have a similar intracellular trafficking pathway (Chia *et al.*, 2013). Since transferrin is an iron-binding protein that has the ability to bind to TfR and recycle between plasma membrane and recycling endosomes (Mayle *et al.*, 2012) and it is increased in the perinuclear ERC, we can propose that, in HeLa cells, Bin1 could have a role in regulating BACE-1 recycling.



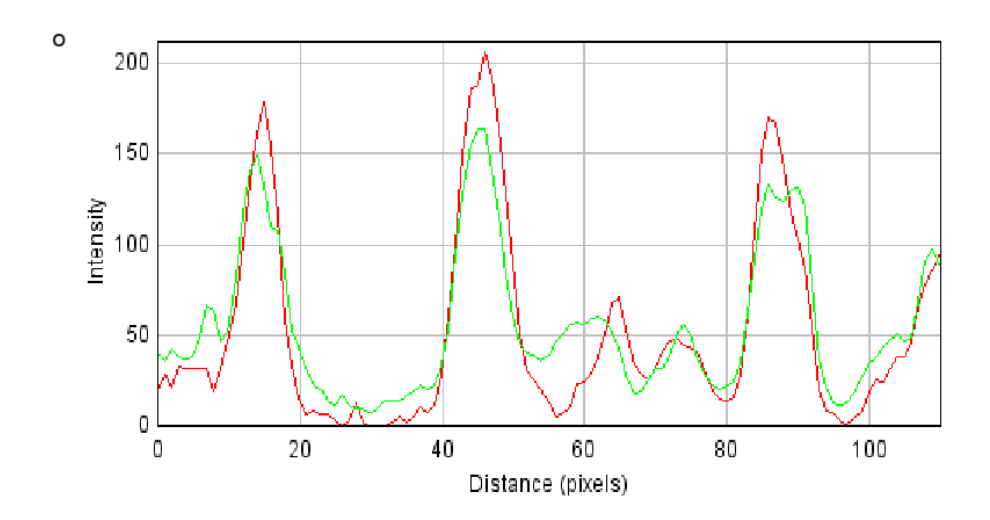


Figure III.11 – Myc-Bin1 and myc-Bin1 c-ter overexpression has an effect on BACE-1 distribution. HeLa cells were transiently transfected with mCherry, BACE-1-GFP, myc-BIN1 and myc-BIN1 c-ter. Representative images of HeLa cells expressing: mCherry (a); BACE-1-GFP (b, f, j); myc-Bin1 immunostained with anti-myc (e) and myc-Bin1 c-ter immunostained with anti-myc (i). In the three conditions recycling endosomes were labeled with Tf-647 (c, g, k). Merged images of BACE-1-GFP (green) and Tf-647 (red) in mCherry (d), myc-Bin1 (h) and myc-Bin1 c-ter (l) cells. White boxes indicate magnified region shown in d1, h1, I1. Fluorescence intensity profiles of mCherry (m), myc-Bin1 (n) and myc-Bin1 c-ter (o) were measured along the grey line in the merged panels (A.U.) (d1, h1, l1) to evaluate colocalization between BACE-1-GFP (green line) and Tf-647 (red line) in peripheral endosomes, (n = 1). Images were acquired with epifluorescence microscope and processed using Fiji software. Colocalization appears in yellow. Scale bars, 10µm.

IV. Discussion

In this work we explored the contribution of Bin1 to the development of AD.

First, we characterized the intracellular endogenous and exogenous protein distribution in neuronal (PN and N2a cells) and non-neuronal cells (HeLa cells) (Figure III.1 and III.2). In this study, we found that endogenous and exogenous Bin1 seem to be localized to the plasma membrane and cytoplasm although, in N2a cells, Bin1 c-ter seems to be also associated with membrane compartments. An interesting fact was that, in mature neurons (21 DIV) we observed Bin1 enriched in puncta consistent with the previously demonstrated pre-synaptic localization (Di Paolo et al., 2002). Next, we characterized the subcellular distribution of exogenous and endogenous Bin1 using different organelle markers in HeLa cells (Figure III.3 and III.4) and PN (Figure III.5). In HeLa cells, we improved the visualization of membrane compartments, by pre-permeabilizing the cells with a low concentration of detergent to remove the cytosol. It was shown that Bin1 and Bin1 c-ter exhibit the same distribution as the early endosome marker (EEA1), localizing preferentially to early endosomes, as previously reported (Leprince et al., 2003). A pool of these early endosomes contained APP and BACE-1 were also positive for EEA1. This finding pointed to early endosomes being the common compartment where APP and BACE-1 can interact, like previously reported (Chia et al., 2013). In PN, endogenous Bin1 presented no colocalization with A\(\beta 42\), APP, AnkG, LAMP1, or Giantin in cell body and dendrites, but colocalizes with early endosome marker (EEA1). However, EEA1 colocalizes with Bin1 just in cell body, not in dendrites which can be explained by the fact that Bin1 is mainly localized to the axon (Di Paolo et al., 2002; Ramjaun et al., 1997).

Second, it has been reported by GWAS that some variants in the BIN1 gene increased the risk for sporadic AD. The main associated SNP (rs744373) stands approximately 30kb upstream BIN1 gene, in the 5' BIN1 non coding region, which may be involved with a change in BIN1 expression level (Hu et al., 2011; Seshadri et al., 2010). It has been shown that Bin1 has a role in synaptic vesicle endocytosis, in clathrin-mediated endocytosis and endocytic recycling (Wigge et al., 1997; Di Paolo et al., 2002; Ramjaun et al., 1997) and that the amyloidogenic processing of APP requires the endocytosis of APP (Cirrito et al., 2008; Koo and Squazzo, 1994). We tried to understand the role of an increased Bin1 expression in APP processing and Aβ42 accumulation in N2a cells (Figure III.6) and PN (Figure III.7). In these cells it was seen an increase in A642 mean fluorescence with the increased expression of myc-Bin1 and c-ter. We also found that in N2a cells Bin1 controls A\(\beta\) levels probably by increasing APP levels and not its processing rate. The c-terminal domain of Bin1 alone does not seem to be sufficient to alter APP levels but, it is sufficient to increase APP processing. In PN, cells overexpressing myc-Bin1 and myc-Bin1 c-ter demonstrated an increase in Aβ42 mean fluorescence, mainly in axons. This higher increase in Aβ42 expression in axon is consistent with the enrichment of Bin1 in presynaptic puncta (Di Paolo et al., 2002; Ramjaun et al., 1997). The increase in the levels of APP and the decrease observed in APP CTFs/APP ratio upon Bin1 and Bin1 c-ter overexpression indicates that Bin1, via its c-terminal domain, has a major effect on APP levels and a smaller effect in APP processing, thus potentially explaining the increase in A β 42 levels. These results in neurons are somewhat different from the ones obtained in N2a cells, suggesting that complex morphology and trafficking of neurons has an impact on the mechanisms involved in A β generation. We have shown that the increased expression of Bin1 correlates with an increase in APP CTFs formation and A β 42 accumulation. To confirm the results obtained by the overexpression, we performed the inverse experiment, decreasing the Bin1 protein level by treatment with siRNA against Bin1 in N2a cells (Figure III.8) and PN (Figure III.9). In N2a cells and PN, the knockdown was highly efficient for both isoforms, neuronal and ubiquitous. In both cell types it was observed an increased A β 42 levels in Bin1 knockdown cells. Since we observed an increase in A β 42, we tried to understand if the APP processing was also altered with the downregulation of Bin1. Our data showed an increase in APP processing in PN depleted for Bin1. These results led us to propose that both excess and lack of Bin1 affect the generation of A β 42, probably by altering APP levels when Bin1 is in excess and by increasing APP processing when Bin1 is depleted. Overall this data suggest that Bin1 regulates A β 42 generation by regulation of APP processing through the amyloidogenic pathway.

Third, since Bin1 may regulate endocytic trafficking we investigated if in HeLa cells, overexpression of Bin1 could alter APP and BACE-1 cellular distribution to endosomes. Two different patterns of exogenous APP distribution were observed (Figure III.10). In control cells, APP was mainly localized to endosomes and Golgi region but, cells overexpressing exogenous Bin1, demonstrated less APP distributed throughout cells in endosomes, more in the Golgi region and also the formation of APP tubules. It was previously shown that Bin1 overexpression in HeLa cells leads to the formation of tubules, considered as traffic intermediates. This demonstrated that Bin1 could regulate APP trafficking via its tubulating potential (Meunier *et al.*, 2009). A similar alteration in distribution was observed for TfR, with APP colocalizing with TfR in tubules in the Golgi region. This is consistent with Bin1 enhancing the recycling of APP to the ERC or to the TGN, that localize to the Golgi region. Since APP has not been described to recycle to the ERC it is likely that APP is accumulating in the TGN when Bin1 is overexpressed. These results suggest that the overexpression of Bin1 alter the trafficking of APP but further experiments are necessary to clarify exactly how.

Fourth, we found that Bin1 had a lesser impact on the distribution of BACE-1 between early Tf endosomes and Tf labeled ERC (Figure III.11). The increased expression of Bin1 seems to slightly increase the proportion of BACE-1 in the Golgi region vs. the peripheral early Tf endosomes compared to control cells. These results are in agreement with recent data on the similar intracellular trafficking pathway of BACE-1 and TfR (Chia et al., 2013). Although some studies reported that BACE-1 may recycle from early endosomes to TGN (Wahle et al., 2005), it was shown that the distribution of BACE-1, at steady state, extensively overlaps with early and recycling endosome markers and less with Golgi or TGN markers (Chia et al., 2013). Given these results, we can speculate that BACE-1 and Tf are subjected to an increased recycling to the ERC or to the TGN in cells with a higher level of Bin1.

As such, the endocytic uptake of membrane proteins like APP and BACE-1 may probably remain unchanged, but a defect in recycling of these proteins may happen. Thus, the accumulation of A β 42 can be explained by a defect in APP and/or BACE-1 recycling, leading to the retention of these proteins in acidic endosomes or in the TGN. This retention increases the time that APP is exposed to BACE-1 activity and, as such, an increase in A β 42 production may occur (Figure III.7 and III.8). Indeed, increased A β 42 production has been described, when BACE-1 and APP localize to acidic recycling endosomes in PN (Das *et al.*, 2013) and when recycling of APP to the TGN is enhanced in Hela cells (Burgos *et al.*, 2010). To clarify the function of Bin1 in A β accumulation our next step will be to perform similar experiments in PN.

In conclusion our main findings are that the deregulation of Bin1 expression, the increased or decreased expression, increased A β 42 production and APP processing. Bin1 could be regulating APP and BACE-1 trafficking since it can associate with early endosomes. Indeed, Bin1 could be regulating the recycling of APP and BACE-1 since APP and BACE-1 distribution was biased toward the Golgi region, where they could meet at the TGN or the ERC. However, the specific intracellular trafficking mechanisms that are involved in the A β 42 production are not yet well understood.

We found that either increasing or decreasing Bin1 is relevant for A β 42 accumulation and the development of AD. Therefore, identifying the molecular pathways downstream of Bin1 is essential to develop relevant therapeutic approaches.

V. Future perspectives

In our study we found important clues about the role of Bin1 in Aβ42 accumulation through the use of an *in vitro* model of cortical PN. However, further investigations are necessary to clarify the exact mechanism by which Bin1 leads to Aβ42 intracellular accumulation. For that, it is necessary to study APP and BACE-1 trafficking upon Bin1 knockdown or overexpression. First, the identification of subcellular localization of endogenous APP and BACE-1-GFP after overexpression or downregulation of Bin1 will be necessary in neuronal cells. To do this, we will perform a pre-extraction assay and we will use specific antibodies to detect APP and organelle markers, such as EEA1 (early endosomes), TfR (recycling endosomes), and LAMP1 (late endosomes), to see in which compartment APP and BACE-1-GFP localize. Next, we will express APP-RFP and BACE-1-GFP in neurons overexpressed/downregulated for Bin1. The trafficking of these proteins in neurons will be followed by live cell imaging. The endosomes will be labeled for EEA1, TfR or Lamp1 to localize the sites where these two proteins co-localize. To identify if these proteins are present in dendrites, neurons will be immunolabelled for microtubule-associated protein 2 (MAP2).

It will be interesting to evaluate as well the levels of A β 42 extracellular upon overexpression or downregulation of Bin1. To analyze secreted A β 42 an Enzyme-Linked Immunosorbent Assay (ELISA) will be performed with the medium where neurons were cultured.

Since it was previously demonstrated that intracellular A β 42 accumulation leads to synaptic dysfunction due to alterations in the levels of PSD-95 and GluR1 (Almeida *et al.*, 2005), it will be remarkable to address if the increased A β 42 accumulation caused by the overexpression or downregulation of Bin1 leads to the same dysfunction. For this we will monitor the level of post-synaptic proteins in neurons, like PSD-95 and GluR1 like previously done (Almeida *et al.*, 2005)

Finally, it will be crucial to perform immunohistochemistry experiments using brain slices from post-mortem human brains with AD to assess the levels of Bin1 and Aβ42.

VI. References

Agrawal, N., Dasaradhi, P. V. N., Mohmmed, A., Malhotra, P., Bhatnagar, R. K., and Mukherjee, S. K. (2003). RNA Interference: Biology, Mechanism, and Applications, *67*(4), 657–685.

Almeida, C.G., Tampellini, D., Takahashi, R.H., Greengard, P., Lin, M.T., Snyder, E.M., and Gouras, G.K. (2005). Beta-amyloid accumulation in APP mutant neurons reduces PSD-95 and GluR1 in synapses. *Neurobiology of Disease 20*, 187–198.

Almeida, C.G., Takahashi, R.H., and Gouras, G.K. (2006). Beta-amyloid accumulation impairs multivesicular body sorting by inhibiting the ubiquitin-proteasome system. *J. Neurosci. Off. J. Soc. Neurosci.* 26, 4277–4288.

Bettens, K., Sleegers, K., and Van Broeckhoven, C. (2013). Genetic insights in Alzheimer's disease. *The Lancet Neurology*, *12* (1), 92–104.

Brunholz, S., Sisodia, S., Lorenzo, A., Deyts, C., Kins, S., and Morfini, G. (2012). Axonal transport of APP and the spatial regulation of APP cleavage and function in neuronal cells. *Experimental Brain Research* 217, 353–364.

Buggia-Prévot, V., Fernandez, C. G., Udayar, V., Vetrivel, K. S., Elie, A., Roseman, J., Sasse, V. A., Lefkow, M., Meckler, X., Bhattacharyya, S., George, M., Kar, S., Bindokas, V. P., Parent, A. T., Rajendran, L., Band, H., Vassar, R., and Thinakaran, G. (2013). A function for EHD family proteins in unidirectional retrograde dendritic transport of BACE1 and alzheimer's disease Abeta production. *Cell Reports*, *5*(6), 1552–1563.

Buggia-Prévot, V., Fernandez, C. G., Riordan, S., Vetrivel, K. S., Roseman, J., Waters, J., Bindokas, V.P., Vassar, R., and Thinakaran, G. (2014). Axonal BACE1 dynamics and targeting in hippocampal neurons: a role for Rab11 GTPase. *Molecular Neurodegeneration*, *9*(1), 1.

Burgos, P. V, Mardones, G. A., Rojas, A. L., daSilva, L. L. P., Prabhu, Y., Hurley, J. H., and Bonifacino, J. S. (2010). Sorting of the Alzheimer's disease amyloid precursor protein mediated by the AP-4 complex. *Developmental Cell*, *18*(3), 425–36.

Butler, M. H., David, C., Ochoa, G., Freyberg, Z., Daniell, L., Grabs, D., and De Camilli, P. (1997). Amphiphysin II (SH3P9; BIN1), a Member of the Amphiphysin/Rvs Family, Is Concentrated in the Cortical Cytomatrix of Axon Initial Segments and Nodes of Ranvier in Brain and around T Tubules in Skeletal Muscle, *137*(6), 1355–1367.

Caporaso, G.L., Takei, K., Gandy, S.E., Matteoli, M., Mundigl, O., Greengard, P., and De Camilli, P. (1994). Morphologic and biochemical analysis of the intracellular trafficking of the Alzheimer beta/A4 amyloid precursor protein. *Journal of Neuroscience*. 14, 3122–3138.

Cataldo, A.M., Peterhoff, C.M., Troncoso, J.C., Gomez-Isla, T., Hyman, B.T., and Nixon, R.A. (2000). Endocytic pathway abnormalities precede amyloid beta deposition in sporadic Alzheimer's disease and Down syndrome: differential effects of APOE genotype and presentilin mutations. *American Journal of Pathology 157*, 277–286.

Chapuis, J., Hansmannel, F., Gistelinck, M., Mounier, A., Van Cauwenberghe, C., Kolen, K. V, and Lambert, J. C. (2013). Increased expression of BIN1 mediates Alzheimer genetic risk by modulating tau pathology. *Molecular Psychiatry*, *18*(11), 1225–34.

Chia, P. Z. C., Toh, W. H., Sharples, R., Gasnereau, I., Hill, A. F., and Gleeson, P. A. (2013). Intracellular itinerary of internalised β -secretase, BACE1, and its potential impact on β -amyloid peptide biogenesis. *Traffic*, *14*(9), 997–1013.

Cirrito, J. R., Yamada, K. A, Finn, M. B., Sloviter, R. S., Bales, K. R., May, P. C., Schoepp, D. D., Paul, S. M., Mennerick, S., and Holtzman, D. M. (2005). Synaptic activity regulates interstitial fluid amyloid-beta levels in vivo. *Neuron*, *48*(6), 913–22.

Cirrito, J. R., Kang, J., Lee, J., Stewart, F. R., Verges, D. K., Silverio, L. M., Bu, G., Mennerick, S., and Holtzman, D. M. (2008). Endocytosis is required for synaptic activity-dependent release of amyloid-beta in vivo. *NIH Public Access*, *58*(1), 42–51.

Coleman, P. D. and Yao, P. J. (2003). Synaptic slaughter in Alzheimer's disease. *Neurobiology of Aging* 24, 1023–1027.

Das, U., Scott, D.A., Ganguly, A., Koo, E.H., Tang, Y., and Roy, S. (2013). Activity-induced convergence of APP and BACE-1 in Acidic Microdomains via an Endocytosis-Dependent Pathway. *Neuron*, 79, 447-460.

Davinelli, S., Intrieri, M., Russo, C., Di Costanzo, A., Zella, D., Bosco, P., and Scapagnini, G. (2011). The "Alzheimer's disease signature": potential perspectives for novel biomarkers. *Immunity & Ageing*, 8 (1), 7.

Di Paolo, G., Sankaranarayanan, S., Wenk, M. R., Daniell, L., Perucco, E., Caldarone, B. J., and De Camilli, P. (2002). Decreased synaptic vesicle recycling efficiency and cognitive deficits in amphiphysin 1 knockout mice. *Neuron*, 33(5), 789–804.

Dong, H., Martin, M. V., Chambers, S., and Csernansky, J. G. (2007). Spatial relationship between synapse loss and beta-amyloid deposition in Tg2576 mice. *Journal of Comparative Neurology*. 500, 311–321.

Glenner, G.G., and Wong, C.W. (1984). Alzheimer's disease: initial report of the purification and characterization of a novel cerebrovascular amyloid protein. Biochemical and Biophysical *Research Communications* 120, 885–890.

Glennon, E. B. C., Whitehouse, I. J., Miners, J. S., Kehoe, P. G., Love, S., Kellett, K. A. B., and Hooper, N. M. (2013). BIN1 Is Decreased in Sporadic but Not Familial Alzheimer's Disease or in Aging. *PLoS ONE*, 8(10).

Gouras, G. K., Tsai, J., Naslund, J., Vincent, B., Edgar, M., Checler, F., Greenfield, J. P., Haroutunian, V., Buxbaum, J. D., Xu, H., Greengard, P., and Relkin, N. R. (2000). Intraneuronal Abeta42 accumulation in human brain. *American Journal of Pathology*. 156, 15–20.

Gouras, G. K., Almeida, C. G., and Takahashi, R. H. (2005). Intraneuronal Aβ accumulation and origin of plaques in Alzheimer's disease. *Neurobiology of Aging*, 26, 1235-1244.

Guo, Q., Li, H., Gaddam, S. S. K., Justice, N. J., Robertson, C. S., and Zheng, H. (2012). Amyloid precursor protein revisited: neuron-specific expression and highly stable nature of soluble derivatives. *The Journal of Biological Chemistry*, 287(4), 2437–45.

Haass, C., Koo, E.H., Mellon, A., Hung, A.Y., and Selkoe, D.J. (1992). Targeting of cell-surface beta-amyloid precursor protein to lysosomes: alternative processing into amyloid-bearing fragments. *Nature* 357, 500–503.

Haass, C., Kaether, C., Thinakaran, G., and Sisodia, S. (2012). Trafficking and proteolytic processing of APP. *Cold Spring Harbor Perspectives in Medicine*, *2*(5).

Holler, C.J., Davis, P.R., Beckett, T.L., Platt, T.L., Webb, R.L., Head, E., and Murphy, M.P. (2014). Bridging Integrator 1 (BIN1) Protein Expression Increases in the Alzheimer's Disease Brain and Correlates with Neurofibrillary Tangle Pathology. *J. Alzheimers Dis.* JAD.

Horton, A. C. and Ehlers, M. D. (2003). Neuronal Polarity and Trafficking. Neuron, 40, 277–295.

Hu, X., Pickering, E., Liu, Y. C., Hall, S., Fournier, H., Katz, E., Dechairo, B., John, S., Eerdewegh, P. V., and Soares, H. (2011). Meta-Analysis for Genome-Wide Association Study Identifies Multiple Variants at the BIN1 Locus Associated with Late-Onset Alzheimer's Disease, *6*(2), 1–9.

Karch, C.M., Jeng, A.T., Nowotny, P., Cady, J., Cruchaga, C., and Goate, A.M. (2012). Expression of Novel Alzheimer's Disease Risk Genes in Control and Alzheimer's Disease Brains. *PLoS ONE* 7, e50976.

Koo, E.H. and Squazzo, S.L. (1994). Evidence that production and release of amyloid beta-protein involves the endocytic pathway. *Journal of Biological Chemistry*, *269*: 17386-17389.

LaFerla, F. M., Green, K. N., and Oddo, S. (2007). Intracellular amyloid-β in Alzheimer's disease. *Nature Reviews*, *Neuroscience*, 8, 499-509.

Lambert, J.C., and Amouyel, P. (2011). Genetics of Alzheimer's disease: new evidences for an old hypothesis? *Current Opinion in Genetics and Development 21*, 295–301.

Landry, J. J. M., Pyl, P. T., Rausch, T., Zichner, T., Tekkedil, M. M., Stütz, A. M., and Steinmetz, L. M. (2013). The genomic and transcriptomic landscape of a HeLa cell line. *G3 (Bethesda, Md.)*, *3*(8), 1213–24.

Lasiecka, Z. M. and Winckler, B. (2011). Mechanisms of polarized membrane trafficking in neurons -- focusing in on endosomes. *Molecular and Cellular Neurosciences*, *48*(4), 278–87.

Lawe, D. C., Patki, V., Heller-Harrison, R., Lambright, D., Corvera, S. (2000). The FYVE Domain of Early Endosome Antigen 1 Is Required for Both Phosphatidylinositol 3-Phosphate and Rab5 Binding. CRITICAL ROLE OF THIS DUAL INTERACTION FOR ENDOSOMAL LOCALIZATION. *Journal of Biological Chemistry*, 275(5), 3699–3705.

Leprince, C., Romero, F., Cussac, D., Vayssiere, B., Berger, R., Tavitian, a, and Camonis, J. H. (1997). A new member of the amphiphysin family connecting endocytosis and signal transduction pathways. *The Journal of Biological Chemistry*, 272(24), 15101–15105.

Leprince, C., Le Scolan, E., Meunier, B., Fraisier, V., Brandon, N., De Gunzburg, J., and Camonis, J. (2003). Sorting nexin 4 and amphiphysin 2, a new partnership between endocytosis and intracellular trafficking. *Journal of Cell Science*, *116* (10), 1937–48.

Linstedt, A. D. and Hauri, H. (1993). Giantin, a Novel conserved Golgi Membrane Protein Containing a Cytoplasmic Domain of at Least 350 kDa. *Molecular Biology of the cell, 4:* 679-693.

Mayle, K. M., Le, A. M., and Kamei, D. T. (2012). The intracellular trafficking pathway of transferrin. *Biochimica et Biophysica Acta*, *1820*(3), 264–81.

Meunier, B., Quaranta, M., Daviet, L., Hatzoglou, A., and Leprince, C. (2009). The membrane-tubulating potential of amphiphysin 2/BIN1 is dependent on the microtubule-binding cytoplasmic linker protein 170 (CLIP-170). *European Journal of Cell Biology*, 88(2), 91–102.

Musardo, S., Saraceno, C., Pelucchi, S., and Marcello, E. (2013). Trafficking in neurons: searching for new targets for Alzheimer's disease future therapies. *European Journal of Pharmacology*, 719(1-3), 84–106.

O'Brien, R. J. and Wong, P. C. (2011). Amyloid Precursor Protein Processing and Alzheimer's disease. *Annual Review of Neuroscience*, 34, 185-204.

Pant, S., Sharma, M., Patel, K., Caplan, S., Carr, C. M., and Grant, B. D. (2009). AMPH-1/Amphiphysin/BIN1 functions with RME-1/Ehd1 in endocytic recycling. *Nature Cell Biology*, *11*(12), 1399–410.

Pravettoni, E., Bacci, A., Coco, S., Forbicini, P., Matteoli, M., and Verderio, C. (2000). Different localizations and functions of L-type and N-type calcium channels during development of hippocampal neurons. *Development Biology* 227, 581–594.

Purves, D., *et al.* (2004). Studying the Nervous Systems of Humans and other Animals. *In* Neuroscience. Third Edition, pp 21-31, Sinauer Associates, Inc. Sunderland, Massachusetts U.S.A.

Ramjaun, A. R., Micheva, K. D., Bouchelet, I., and McPherson, P. S. (1997). Identification and characterization of a nerve terminal-enriched amphiphysin isoform. *The Journal of Biological Chemistry*, 272(26), 16700–16706.

Ren, G., Vajjhala, P., Lee, J.S., Winsor, B., and Munn, A.L. (2006). The BAR Domain Proteins: Molding Membranes in Fission, Fusion, and Phagy. *Microbiology and Molecular Biology Reviews 70*, 37–120.

Schellenberg, G. D. and Montine, T. J. (2012). The genetics and neuropathology of Alzheimer's disease. *Acta Neuropathologica*, *124* (3), 305–323.

Selkoe, D. J. (2002). Alzheimer's disease is a synaptic failure. Science 298, 789-791.

Seshadri, S., Fitzpatrick, A.L., Ikram, M.A., De Stefano, A.L. *et al.* (2010). Genome-wide analysis of genetic loci associated with Alzheimer disease. *JAMA* 303:1832–1840

Takahashi, R.H., Milner, T.A., Li, F., Nam, E.E., Edgar, M.A., Yamaguchi, H., Beal, M.F., Xu, H., Greengard, P., and Gouras, G.K. (2002). Intraneuronal Alzheimer A?42 Accumulates in Multivesicular Bodies and Is Associated with Synaptic Pathology. *American Journal of Pathology 161*, 1869–1879.

Takahashi, R. H., Almeida, C. G., Kearney, P. F., Yu, F., Lin, M. T., Milner, T. A., and Gouras, G. K. (2004). Oligomerization of Alzheimer's beta-amyloid within processes and synapses of cultured neurons and brain. *Journal of Neuroscience*. 24, 3592–3599.

Tampellini, D. and Gouras, G. K. (2010). Synapses, synaptic activity and intraneuronal abeta in Alzheimer's disease. *Frontiers in Aging Neuroscience*, *2* (13), 1–5.

Tan, M.S., Yu, J.T., and Tan, L. (2013). Bridging integrator 1 (BIN1): form, function, and Alzheimer's disease. *Trends Molecular Medicine* 19, 594–603.

Tang, B. L. (2009). Neuronal protein trafficking associated with Alzheimer disease. *Cell Adhesion & Migration*, *3*(1), 118–128.

Tremblay, R. G., Sikorska, M., Sandhu, J. K., Lanthier, P., Ribecco-Lutkiewicz, M., and Bani-Yaghoub, M. (2010). Differentiation of mouse Neuro 2A cells into dopamine neurons. *Journal of Neuroscience Methods*, *186*(1), 60–7.

Turner, P. R., O'Connor, K., Tate, W. P., and Abraham, W. C. (2003). Roles of amyloid precursor protein and its fragments in regulating neural activity, plasticity and memory. *Progress in Neurobiology* (Vol. 70, pp. 1–32).

Vander, A., *et al.* (2001). Neural Control Mechanisms. *In* Human Physiology: The mechanism of body function. Eight Edition, pp 186-193, The McGraw-Hill Companies, Inc.

Wahle, T., Prager, K., Raffler, N., Haass, C., Famulok, M., and Walter, J. (2005). GGA proteins regulate retrograde transport of BACE1 from endosomes to the trans-Golgi network. *Molecular and Cellular Neurosciences*, 29(3), 453–61.

Wigge, P., Köhler, K., Vallis, Y., Doyle, C. a, Owen, D., Hunt, S. P., & McMahon, H. T. (1997). Amphiphysin heterodimers: potential role in clathrin-mediated endocytosis. *Molecular Biology of the Cell*, 8(10), 2003–2015.

Wigge, P., Vallis, Y., and McMahon, H.T. (1997b). Inhibition of receptor-mediated endocytosis by the amphiphysin SH3 domain. *Current. Biology.* 7, 554–560.

Wigge, P., and McMahon, H.T. (1998). The amphiphysin family of proteins and their role in endocytosis at the synapse. *Trends Neuroscience*. *21*, 339–344.

Ye, X. and Cai, Q. (2014). Snapin-mediated BACE1 retrograde transport is essential for its degradation in lysosomes and regulation of APP processing in neurons. *Cell Reports*, *6*(1), 24–31.

Zhang, Y., Thompson, R., and Zhang, H., Xu, H. (2011). APP processing in Alzheimer's disease. *Molecular Brain*, 4(1), 3.